

Transdimensional Transformation based Markov Chain Monte Carlo

Moumita Das and Sourabh Bhattacharya¹

¹Moumita Das is a PhD student and Sourabh Bhattacharya is an Associate Professor in Interdisciplinary Statistical Research Unit, Indian Statistical Institute, 203, B. T. Road, Kolkata 700108. Corresponding e-mail: sourabh@isical.ac.in.

Abstract

Variable dimensional problems, where not only the parameters, but also the number of parameters are random variables, pose serious challenge to Bayesians. Although in principle the Reversible Jump Markov Chain Monte Carlo (RJMCMC) methodology is a response to such challenges, the dimension-hopping strategies need not be always convenient for practical implementation, particularly because efficient “move-types” having reasonable acceptance rates are often difficult to devise.

In this article, we propose and develop a novel and general dimension-hopping MCMC methodology that can update all the parameters as well as the number of parameters simultaneously using simple deterministic transformations of some low-dimensional (often one-dimensional) random variable. This methodology, which has been inspired by Transformation based MCMC (TMCMC) of Dutta & Bhattacharya (2014), facilitates great speed in terms of computation time and provides reasonable acceptance rates and mixing properties. Quite importantly, our approach provides a natural way to automate the move-types in variable dimensional problems. We refer to this methodology as Transdimensional Transformation based Markov Chain Monte Carlo (TTMCMC). Comparisons with RJMCMC in gamma and normal mixture examples demonstrate far superior performance of TTMCMC in terms of mixing, acceptance rate, computational speed and automation. Furthermore, we demonstrate good performance of TTMCMC in multivariate normal mixtures, even for dimension as large as 20. To our knowledge, there exists no application of RJMCMC for such high-dimensional mixtures.

As by-products of our effort on the development of TTMCMC, we propose a novel methodology to summarize the posterior distributions of the mixture densities, providing a way to obtain the mode of the posterior distribution of the densities and the associated highest posterior density credible regions. Based on our method we also propose a criterion to assess convergence of variable-dimensional algorithms. These methods of summarization and convergence assessment are applicable to general problems, not just to mixtures.

Keywords: Block update; Jacobian; Mixture; Move type; RJMCMC; TTCCMC.

Contents

1	Introduction	5
1.1	Overview of contributions and organisation of this paper	7
2	A brief overview of the key idea of TMCMC	8
2.1	Notation	9
2.2	Examples of transformations on two-dimensional state-space using single ϵ . . .	10
2.3	The general form of the TMCMC algorithm	11
3	TTMCMC for updating the dimension and the parameters in a single block using deterministic transformations of a single random variable	12
3.1	Illustration of the key idea of TTMCMC with a simple example	12
3.2	General TTMCMC algorithm for jumping one dimension at a time	17
3.2.1	Observations regarding Algorithm 3.1	19
3.3	Structured dependence within the moves	20
4	Jumping more than one dimensions at a time	21
5	TTMCMC: towards automation	23
5.1	Reasonably high acceptance rate	25
5.2	Good mixing properties in high-dimensional and multimodal cases	25
5.3	Applicability to all variable dimensional problems	26
5.4	Default TTMCMC algorithm and its tuning	26
6	Simulation studies with mixtures of gamma distributions with unknown number of components	27
6.1	Prior structure	27
6.2	Label switching	28
6.3	Posterior summary	28

6.4	Convergence diagnostics	29
6.5	General TTMC MC strategy for our experiments	29
6.6	An RJMC MC algorithm based on random walk proposals	30
6.7	First simulation study with data generated from a one-component gamma mixture	31
6.7.1	Comparison with the results obtained by Wiper et al. (2001)	32
6.8	Second simulation study with data generated from a two-component gamma mixture	35
6.8.1	Comparison with the results obtained by Wiper et al. (2001)	38
6.9	Third simulation study with data generated from a three-component gamma mixture	38
6.9.1	Comparison with the results obtained by Wiper et al. (2001)	38
6.10	Fourth simulation study with data generated from a four-component gamma mixture	41
6.10.1	Comparison with the results obtained by Wiper et al. (2001)	41
7	Comparison of TTMC MC and RJMC MC in the normal mixture set up with unknown number of components	41
7.1	Normal mixture	44
7.2	Prior structure	44
7.3	Enzyme data	45
7.4	Acidity data	46
7.5	Galaxy data	49
7.6	Comparison of TTMC MC with random walk RJMC MC with respect to the three real data sets	55
7.7	Relevance of autocorrelation plots for convergence diagnosis in variable dimensions	55

7.8	Comparison between TTMC MC and RJMC MC when the prior of Richardson and Green (1997) is considered	55
8	TTMC MC for multivariate normal mixtures	56
8.1	Prior structure	56
8.2	TTMC MC strategy for multivariate situations	57
8.3	Simulation experiment with $p = 3$	57
8.4	Simulation experiment with $p = 10$	58
8.5	Simulation experiment with $p = 20$	61
9	Conclusion	64
S-1	Detailed balance for Algorithm 3.1 of DB	70
S-1.1	Detailed balance for the simple example illustrated in Section 3.1 of DB	70
S-1.2	Proof of detailed balance for the general TTMC MC algorithm	72
S-2	Irreducibility and aperiodicity of TTMC MC	73
S-3	General TTMC MC algorithm for jumping m dimensions	73
S-4	Proof of detailed balance for General TTMC MC algorithm for jumping m dimensions	76
S-5	Jumping more than one dimensions at a time when there several sets of parameters are related	77
S-6	Brief discussion on label switching	83
S-7	Summarization of the posterior distribution of mixture densities	84
S-7.1	Empirical definition of central density function	85
S-7.2	Construction of desired credible regions of densities	86
S-7.3	Construction of desired HPD regions of densities	86

S-8	TTMCMC convergence diagnostics for the mixture problem	86
S-8.1	Difficulties of convergence assessment in variable dimensional problems	86
S-8.2	A new convergence diagnostic method for mixtures with known or unknown number of components	87
S-9	Further simulation studies with the gamma mixtures with different data sizes	88
S-9.1	1-component mixture	88
S-9.2	2-component mixture	89
S-9.3	3-component mixture	89
S-9.4	4-component mixture	89
S-10	Comparison between additive TTMCMC and random walk RJMCMC in normal mixtures with respect to the three real data sets	90
S-10.1	Comparison in enzyme data	90
S-10.2	Comparison in acidity data	90
S-10.3	Comparison in galaxy data	92
S-10.4	Comparison of the autocorrelations associated with additive TTMCMC and random walk RJMCMC in the three real data examples	93
S-11	Comparisons between additive TTMCMC and RJMCMC with respect to the prior structure and the algorithm of Richardson and Green (1997) in the galaxy data con- text	93
S-11.1	Prior structure	96
S-11.2	Results of additive TTMCMC with RG's prior when β is updated using additive TTMCMC	96
S-11.3	Results of additive TTMCMC with RG's prior when β is fixed	100

1. INTRODUCTION

Markov chain Monte Carlo (MCMC) is known to have revolutionized Bayesian computation. In modern times, it is often required to analyze high-dimensional, complex data, and the Bayesian paradigm, with the MCMC machinery, provides an ideal package to the statistical scientist for the purpose. As is to be anticipated, to simulate from complex Bayesian posteriors, development of quite sophisticated MCMC methods were necessary, and various approaches based on component-wise and joint updating of the parameters, such as the adaptive direction sampling (Gilks, Roberts & George (1994)), the multiple-try Metropolis method (Liu, Liang & Wong (2000)), the auxiliary variable approach (Storvik (2011)), parallel MCMC methods (Martino, Elvira, Luengo, Corander & Louzada (2016)), have emerged in response to the needs of the modern Bayesian.

However, the above methods are appropriate when the number of parameters is known in advance. When one of the unknown parameters is the number of parameters itself, then none of the traditional MCMC methods are applicable, irrespective of how sophisticated they are. Indeed, simultaneous inference on both model and parameter space is an issue that is fundamental to modern statistical practice (Sisson (2005)). Examples of such problems arise in mixture analysis where the parameters associated with the mixture components as well as the number of mixture components are unknown (see, for example, Richardson & Green (1997)); in change point analysis where the locations and the number of change points are unknown (see, for example, Green (1995)); in variable selection problems where the number of covariates and the associated coefficients are unknown (Dellaportas, Forster & Ntzoufras (2002), Dellaportas & Forster (1999)); in spline smoothing where the location and the number of knots are unknown (see Denison, Mallick & Smith (1998) for instance); in continuous wavelet representation of unknown functions with a finite, but unknown number of wavelet basis functions and the corresponding parameters (Chu, Clyde & Liang (2009)); in autoregressive time series models where the order of the autoregression and the associated parameters are unknown (Vermaak, Andrieu, Doucet & Godsill (2004)); in factor analysis where the dimension of the latent factor loading matrix and the associated parameters are unknown (Lopes & West (2004)); in spatial point processes where the locations and the number

of points are random (see Møller & Waagepetersen (2004)); to name only a few.

A general MCMC strategy which can explore variable dimensional spaces by jumping between different dimensions has been proposed by Green (1995), and is well-known as Reversible Jump MCMC (RJMCMC). The versatility of the methodology is well-reflected in the large varieties of variable-dimensional problems to which it has been applied; indeed, all the aforementioned examples make use of RJMCMC. However, one difficulty is frequently encountered when designing reversible jump algorithms is the construction of efficient proposals. Typically, dimension jumping moves in reversible jump samplers exhibit much lower acceptance rate than in fixed-dimensional moves. Al-Awadhi & Jennison (2004) observed that models with multimodal distributions yield particularly low acceptance rates. There have been many attempts of creating automatic RJMCMC samplers which also maintain high acceptance rates; see, for example, Brooks, Giudici & Roberts (2003), Robert (2003), Green (2003), Godsill (2003), Robert & Casella (2004), Sisson (2005), Fan & Sisson (2011) and the references therein. However, in spite of the commendable attempts, these ideas are perhaps relevant in quite specific models with several restrictive assumptions; see Robert & Casella (2004), Sisson (2005), Fan & Sisson (2011).

The issues discussed above point towards the need to develop general and natural move types that can change dimensions as well as update the other (within model) parameters simultaneously, while maintaining reasonable acceptance rates and mixing properties. In this regard, the transformation based MCMC (TMCMC) approach of Dutta & Bhattacharya (2014) in the fixed dimensional set-up provides the necessary motivation. The key concept of TMCMC is to propose a move-type from a set of available move-types, simulate a single, one-dimensional random variable from some arbitrary distribution and propose simple deterministic transformations to all the parameters using the one-dimensional random variable, within the proposed move-type. In this article we show that the same concept of deterministic transformations of a single random variable can be exploited to construct, for any general variable dimensional problem, a generic and effective dimension-hopping sampler which can change dimensions and update all the parameters of the proposed model in a single block while maintaining reasonable acceptance rates and mixing properties. We refer to this general variable dimensional MCMC sampler as Transdimensional

Transformation based Markov Chain Monte Carlo (TTMCMC).

1.1 Overview of contributions and organisation of this paper

Before a formal introduction of TTMCMC, it is necessary to provide a brief overview of the basic concept of TCMCMC. We do this in Section 2.

We introduce TTMCMC in Section 3, and in Section 4 we extend our proposed methodology to more general situations where one wishes to jump more than one dimension at a time. That TTMCMC thus developed closely qualifies as an automatic variable dimensional sampler, is argued in Section 5.

Although our proposed sampler is quite general and readily applicable to all transdimensional sampling frameworks, for the purpose of illustration and comparison with RJMCMC we restrict ourselves to gamma and normal mixture problems with unknown number of components. In this regard, in Section 6 we first conduct four simulation experiments with gamma mixtures with true number of components being 1, 2, 3 and 4, respectively. In Section 7 we provide details regarding applications of our methods to analyse three well-studied real data sets, namely, the enzyme, acidity and the galaxy data (see Richardson & Green (1997), for instance). In Section 8 we demonstrate the application of TTMCMC in mixtures of multivariate normal densities. In particular, we consider three simulation studies for dimensions 3, 10 and 20.

We show that the simplest possible TTMCMC algorithm, which is based on additive transformations, puts up excellent performance in all the examples, even in all the multivariate scenarios, providing ample support to our claim of automation. Also interestingly, the TTMCMC applications are able to capture very precise information regarding the number of mixture components, for both simulated and real data sets. None of the previous methods (see Richardson & Green (1997) and the references therein) were able to capture so precise information as TTMCMC. Moreover, there possibly does not exist any RJMCMC algorithm that works for multivariate mixtures with dimension as high as 20. Hence, from the high-dimensional perspective, TTMCMC is clearly far ahead of RJMCMC.

For the gamma mixtures and the normal mixtures associated with the real data applications we

compare additive TTMC MC with the closest RJMC MC analogue of additive TTMC MC, based on random walk proposals. This RJMC MC algorithm seems to be the more natural, intuitive and computationally far simpler alternative to the random walk-motivated “automatic generic transdimensional RJMC MC sampler” proposed in Green (2003). Indeed, the approach of Green (2003) is appropriate only when a small set of models is considered in the variable-dimensional problem, and as such not a viable option for our normal mixtures with maximum of 30 components; see Section 6.6 for details.

Unfortunately, the random walk RJMC MC algorithm analogue of additive TTMC MC fails to produce satisfactory results in a way that even convergence is not assured in any of the examples. In particular, with the same scales of additive TTMC MC, random walk RJMC MC yields extremely poor acceptance rate in general. Moreover, the RJMC MC-based posterior of the number of components tends to assign higher posterior probabilities to implausibly large values, clearly indicating lack of convergence. We argue that the same issue persists with general RJMC MC algorithms. This suggests that complex and difficult-to-implement algorithms with extremely large convergence time are required for RJMC MC to yield sensible results, and that there is no default choice of such algorithms. On the other hand, the potentiality of additive TTMC MC in conjunction with the results of our experiments demonstrate that additive TTMC MC is close to qualifying as the default variable-dimensional algorithm, even for large dimensions.

We summarize our work and make concluding remarks in Section 9. Additional details are provided in the supplement Das & Bhattacharya (2015a), whose sections have the prefix “S-” when referred to in this paper.

2. A BRIEF OVERVIEW OF THE KEY IDEA OF TMC MC

In order to obtain a valid algorithm based on transformations, Dutta & Bhattacharya (2014) design appropriate move types so that detailed balance and irreducibility hold. We first illustrate the basic idea of transformation based moves with a simple example. Given that we are in the current state x , we may propose the “forward move” $x' = x + \epsilon$, where $\epsilon > 0$ is a simulation from some arbitrary density $\varrho(\cdot)$ which is supported on the positive part of the real line. To move back to x from x' ,

we need to apply the “backward transformation” $x' - \epsilon$. In general, given ϵ and the current state x , we shall denote the forward transformation by $T(x, \epsilon)$, and the backward transformation by $T^b(x, \epsilon)$. For fixed ϵ the forward and backward transformations must be one-to-one and onto, and must satisfy $T^b(T(x, \epsilon), \epsilon) = x = T(T^b(x, \epsilon), \epsilon)$; see Dutta & Bhattacharya (2014) for a detailed discussion regarding these.

The simple idea discussed above has been generalized to the multi-dimensional situation by Dutta & Bhattacharya (2014). Remarkably, for any dimension, the moves can be constructed by simple deterministic transformations of the one-dimensional random variable ϵ , which is simulated from any arbitrary distribution on some relevant support. We provide some examples of such moves in the next section after introducing some necessary notation borrowed from Dutta & Bhattacharya (2014).

2.1 Notation

Suppose that \mathcal{X} is a k -dimensional space of the form $\mathcal{X} = \prod_{i=1}^k \mathcal{X}_i$ so that $T = (T_1, \dots, T_k)$ where each $T_i : \mathcal{X}_i \times \mathcal{D} \rightarrow \mathcal{X}_i$, for some set \mathcal{D} , are the component-wise transformations. Let $\mathbf{z} = (z_1, \dots, z_k)$ be a vector of indicator variables, where, for $i = 1, \dots, k$, $z_i = 1$ and $z_i = -1$ indicate, respectively, application of forward transformation and backward transformation to x_i , and let $z_i = 0$ denote no change to x_i . This “no change” step is sufficient to ensure irreducibility of TMCMC in non-additive transformations; see Dutta & Bhattacharya (2014). Given any such indicator vector \mathbf{z} , let us define $T_{\mathbf{z}} = (g_{1,z_1}, g_{2,z_2}, \dots, g_{k,z_k})$ where

$$g_{i,z_i} = \begin{cases} T_i^b & \text{if } z_i = -1 \\ x_i & \text{if } z_i = 0 \\ T_i & \text{if } z_i = 1. \end{cases}$$

Corresponding to any given \mathbf{z} , we also define the following ‘conjugate’ vector $\mathbf{z}^c = (z_1^c, z_2^c, \dots, z_k^c)$, where

$$z_i^c = -z_i.$$

With this definition of \mathbf{z}^c , $T_{\mathbf{z}^c}$ can be interpreted as the conjugate of $T_{\mathbf{z}}$.

Since 3^k values of \mathbf{z} are possible, it is clear that T , via \mathbf{z} , induces 3^k many types of ‘moves’ of the forms $\{T_{z_i}; i = 1, \dots, 3^k\}$ on the state-space. Suppose now that there is a subset \mathcal{Y} of \mathcal{D} such that the sets $T_{z_i}(\mathbf{x}, \mathcal{Y})$ and $T_{z_j}(\mathbf{x}, \mathcal{Y})$ are disjoint for every $z_i \neq z_j$. In fact, \mathcal{Y} denotes the support of the distribution $\varrho(\cdot)$ from which ϵ is simulated. This mutual exclusiveness is required to satisfy the detailed balance property; see Dutta & Bhattacharya (2014) for the details. Thus, although \mathcal{D} denotes the actual range of values that ϵ can assume in principle, for implementation of TMCMC we must restrict the support of ϵ to \mathcal{Y} .

2.2 Examples of transformations on two-dimensional state-space using single ϵ

Although for the sake of illustration we provide below examples pertaining to two-dimensional cases it is important to remark at the outset that these examples can be easily generalized to any dimension; see Dutta & Bhattacharya (2014).

1. *Additive transformation:* Suppose $\mathcal{X} = \mathcal{D} = \mathbb{R}^2$. With two positive scale parameters a_1 and a_2 , we can then consider the following additive transformation: $T_{(1,1)}(\mathbf{x}, \epsilon) = (x_1 + a_1\epsilon, x_2 + a_2\epsilon)$, $T_{(-1,1)}(\mathbf{x}, \epsilon) = (x_1 - a_1\epsilon, x_2 + a_2\epsilon)$, $T_{(1,-1)}(\mathbf{x}, \epsilon) = (x_1 + a_1\epsilon, x_2 - a_2\epsilon)$ and $T_{(-1,-1)}(\mathbf{x}, \epsilon) = (x_1 - a_1\epsilon, x_2 - a_2\epsilon)$. We set $\mathcal{Y} = (0, \infty)$.
2. *Multiplicative transformation:* Suppose $\mathcal{X} = \mathcal{D} = \mathbb{R}^2$. Then we may consider the following multiplicative transformation: $T_{(1,1)}(\mathbf{x}, \epsilon) = (x_1\epsilon, x_2\epsilon)$, $T_{(-1,1)}(\mathbf{x}, \epsilon) = (x_1/\epsilon, x_2\epsilon)$, $T_{(1,-1)}(\mathbf{x}, \epsilon) = (x_1\epsilon, x_2/\epsilon)$, $T_{(-1,-1)}(\mathbf{x}, \epsilon) = (x_1/\epsilon, x_2/\epsilon)$, $T_{(1,0)}(\mathbf{x}, \epsilon) = (x_1\epsilon, x_2)$, $T_{(1,0)}(\mathbf{x}, \epsilon) = (x_1\epsilon, x_2)$, $T_{(-1,0)}(\mathbf{x}, \epsilon) = (x_1/\epsilon, x_2)$, $T_{(0,1)}(\mathbf{x}, \epsilon) = (x_1, x_2\epsilon)$, $T_{(0,-1)}(\mathbf{x}, \epsilon) = (x_1, x_2/\epsilon)$, $T_{(0,0)}(\mathbf{x}, \epsilon) = (x_1, x_2)$. We choose $\mathcal{Y} = \{(-1, 1) - \{0\}\}$.
3. *Additive-multiplicative transformation:* It is possible to combine additive and multiplicative transformations, but here we need at least two ϵ 's, one for the additive, and another for the multiplicative transformation. For instance, if $\mathcal{X} = \mathcal{D} = \mathbb{R}^2$, then we may consider the following moves: $T_{(1,1)}(\mathbf{x}, \epsilon_1, \epsilon_2) = (x_1 + \epsilon_1, x_2\epsilon_2)$, $T_{(-1,1)}(\mathbf{x}, \epsilon_1, \epsilon_2) = (x_1 - \epsilon_1, x_2\epsilon_2)$, $T_{(1,-1)}(\mathbf{x}, \epsilon_1, \epsilon_2) = (x_1 + \epsilon_1, x_2/\epsilon_2)$, $T_{(-1,-1)}(\mathbf{x}, \epsilon_1, \epsilon_2) = (x_1 - \epsilon_1, x_2/\epsilon_2)$, $T_{(1,0)}(\mathbf{x}, \epsilon_1, \epsilon_2) = (x_1 + \epsilon_1, x_2)$, $T_{(-1,0)}(\mathbf{x}, \epsilon_1, \epsilon_2) = (x_1 - \epsilon_1, x_2)$, $T_{(0,1)}(\mathbf{x}, \epsilon_1, \epsilon_2) = (x_1, x_2\epsilon_2)$, $T_{(0,-1)}(\mathbf{x}, \epsilon_1, \epsilon_2) =$

$(x_1, x_2/\epsilon_2)$, $T_{(0,0)}(\mathbf{x}, \epsilon_1, \epsilon_2) = (x_1, x_2)$. We let $\mathcal{Y} = (0, \infty) \times \{(-1, 1) - \{0\}\}$. Although this example uses two ϵ 's for two dimensions, it is important to note that for any dimension higher than two, at most two ϵ 's will be required for validity of additive-multiplicative TMCMC, one for the additive part and another for the multiplicative part, irrespective of the dimensionality. Thus, the minimum effective dimensionality of additive TMCMC and multiplicative TMCMC is 1, while that of additive-multiplicative TMCMC in this setting is 2, for any dimensionality greater than one.

The key observation underlying the above examples is that it is always possible to construct valid transformations in high-dimensional spaces using combinations of appropriate transformations on one-dimensional spaces. These transformations and the underlying principle remain valid even in TTMCMC.

2.3 The general form of the TMCMC algorithm

For a k (≥ 1)-dimensional target distribution, with current state $\mathbf{x} = (x_1, \dots, x_k)$, Dutta & Bhattacharya (2014) apply forward and backward transformations to x_i with probabilities p_i and q_i , respectively and keep x_i unchanged with probability $1 - p_i - q_i$, for $i = 1, \dots, k$. Thus, \mathbf{z} can now be interpreted as a random vector such that for $i = 1, \dots, k$, $z_i \in \{-1, 0, 1\}$ with probabilities $q_i, 1 - p_i - q_i, p_i$, respectively. Thus, we simulate $z_i \sim \text{Multinomial}(1; p_i, q_i, 1 - p_i - q_i)$ independently for $i = 1, \dots, k$, draw $\epsilon \sim \varrho(\cdot)$, and form the proposed move $\mathbf{x} \mapsto \mathbf{x}' = T_{\mathbf{z}}(\mathbf{x}, \epsilon)$, which is accepted with probability

$$\alpha(\mathbf{x}, \epsilon) = \min \left(1, \frac{P(\mathbf{z}^c)}{P(\mathbf{z})} \frac{\pi(\mathbf{x}')}{\pi(\mathbf{x})} \left| \frac{\partial(T_{\mathbf{z}}(\mathbf{x}, \epsilon), \epsilon)}{\partial(\mathbf{x}, \epsilon)} \right| \right), \quad (2.1)$$

where

$$\frac{P(\mathbf{z}^c)}{P(\mathbf{z})} = \prod_{\{i_1: z_{i_1} = -1\}} \frac{p_{i_1}}{q_{i_1}} \prod_{\{i_2: z_{i_2} = 1\}} \frac{q_{i_2}}{p_{i_2}}.$$

Note that the acceptance ratio is *always* independent of the proposal density ϱ .

The redundant move-type $\mathbf{x} \mapsto \mathbf{x}$ has positive probability of occurrence, and hence Dutta & Bhattacharya (2014) suggest rejection of this move whenever it appears. That is, sampling of \mathbf{z}

is to be continued until at least one $z_i \neq 0$. This rejection sampling of \mathbf{z} is very efficient since the rejection region is a singleton and has very small probability, particularly in high dimensions. The normalizing constant that arises because of this truncation cancels in the acceptance ratio of TMCMC, as shown in Dutta & Bhattacharya (2014).

3. TTMCMC FOR UPDATING THE DIMENSION AND THE PARAMETERS IN A SINGLE BLOCK USING DETERMINISTIC TRANSFORMATIONS OF A SINGLE RANDOM VARIABLE

First we illustrate the main idea of TTMCMC informally using the additive transformation.

3.1 Illustration of the key idea of TTMCMC with a simple example

Assume that the current state is $\mathbf{x} = (x_1, x_2) \in \mathbb{R}^2$. We first randomly select $u = (u_1, u_2, u_3) \sim \text{Multinomial}(1; w_b, w_d, w_{nc})$, where $w_b, w_d, w_{nc} (> 0)$ such that $w_b + w_d + w_{nc} = 1$ are the probabilities of birth, death, and no-change moves, respectively. That is, if $u_1 = 1$, then we increase the dimensionality from 2 to 3; if $u_2 = 1$, then we decrease the dimensionality from 2 to 1, and if $u_3 = 1$, then we keep the dimensionality unchanged. In the latter case, when the dimensionality is unchanged, the acceptance probability remains the same as in TMCMC, given by (2.1).

If $u_1 = 1$, we can increase the dimensionality by first selecting one of x_1 and x_2 with probability $1/2$; for the sake of clarity, we assume that x_1 has been selected. Here, as in TMCMC, we draw $\epsilon \sim \varrho(\cdot)$, where $\varrho(\cdot)$ is supported on the positive part of the real line, and draw z_2 where $z_2 = 1$ with probability p_2 and $z_2 = -1$ with probability $1 - p_2$. Also, as before, $\mathbf{z}^c = (z_1^c, z_2^c)$ is the conjugate of \mathbf{z} , where $z_i^c = -z_i$. We then construct the move-type $T_{b,\mathbf{z}}(\mathbf{x}, \epsilon) = (x_1 + a_1\epsilon, x_1 - a_1\epsilon, x_2 + z_2 a_2\epsilon) = (g_{1,z_1=1}(x_1, \epsilon), g_{1,z_1^c=-1}(x_1, \epsilon), g_{2,z_2}(x_2, \epsilon))$, say. We re-label $\mathbf{x}' = T_{b,\mathbf{z}}(\mathbf{x}, \epsilon) = (x_1 + a_1\epsilon, x_1 - a_1\epsilon, x_2 + z_2 a_2\epsilon)$ as (x'_1, x'_2, x'_3) . Thus, $T_{b,\mathbf{z}}(\mathbf{x}, \epsilon)$ increases the dimension from 2 to 3.

We accept this birth move with probability

$$a_b(\mathbf{x}, \epsilon) = \min \left\{ 1, \frac{1}{3} \times \frac{w_d}{w_b} \times \frac{p_2^{I_{\{1\}}(z_2^c)} q_2^{I_{\{-1\}}(z_2^c)}}{p_2^{I_{\{1\}}(z_2)} q_2^{I_{\{-1\}}(z_2)}} \times \frac{\pi(x_1 + a_1\epsilon, x_1 - a_1\epsilon, x_2 + z_2 a_2\epsilon)}{\pi(x_1, x_2)} \times \left| \frac{\partial(T_{b,z}(\mathbf{x}, \epsilon))}{\partial(\mathbf{x}, \epsilon)} \right| \right\}. \quad (3.1)$$

In (3.1),

$$\left| \frac{\partial(T_{b,z}(\mathbf{x}, \epsilon))}{\partial(\mathbf{x}, \epsilon)} \right| = \left| \frac{\partial(x_1 + a_1\epsilon, x_1 - a_1\epsilon, x_2 + z_2 a_2\epsilon)}{\partial(x_1, x_2, \epsilon)} \right| = \left| \begin{pmatrix} 1 & 1 & 0 \\ 0 & 0 & 1 \\ a_1 & -a_1 & z_2 a_2 \end{pmatrix} \right| = 2a_1. \quad (3.2)$$

Now let us illustrate the problem of returning to $(x_1, x_2) \in \mathbb{R}^2$ from $T_{b,z}(\mathbf{x}, \epsilon) = (x_1 + a_1\epsilon, x_1 - a_1\epsilon, x_2 + z_2 a_2\epsilon) \in \mathbb{R}^3$. For our purpose, we can select $x_1 + a_1\epsilon$ with probability $1/3$; then select $x_1 - a_1\epsilon$ from the remaining two elements with probability $1/2$, and form the average $x_1^* = ((x_1 + a_1\epsilon) + (x_1 - a_1\epsilon))/2 = x_1$. For non-additive transformations we can consider the averages of the backward moves of each of the selected elements. Even in this additive transformation example, after simulating ϵ as before we can consider the respective backward moves of $x_1 + a_1\epsilon$ and $x_1 - a_1\epsilon$, both yielding x_1 , and then take the average denoted by x_1^* . For the remaining element $x_2 + z_2 a_2\epsilon$, we need to simulate z_2^c and then consider the move $(x_2 + z_2 a_2\epsilon) + z_2^c a_2\epsilon = x_2$. Thus, we can return to (x_1, x_2) using this strategy.

Letting $\mathbf{x}' = (x'_1, x'_2, x'_3)$, and denoting the average involving the first two elements by x_1^* , the death move is then given by $\mathbf{x}'' = T_{d,z}(\mathbf{x}', \epsilon) = (x_1^*, x'_3 + z_2^c a_2\epsilon) = (\frac{x'_1 + x'_2}{2}, x'_3 + z_2^c a_2\epsilon)$. Now observe that for returning to (x'_1, x'_2) from x_1^* , we must have $x_1^* + a_1\epsilon^* = x'_1$ and $x_1^* - a_1\epsilon^* = x'_2$, which yield $\epsilon^* = (x'_1 - x'_2)/2a_1$. Hence, the Jacobian associated with the death move in this case is given by

$$\left| \frac{\partial(T_{d,z}(\mathbf{x}', \epsilon), \epsilon^*, \epsilon)}{\partial(\mathbf{x}', \epsilon)} \right| = \left| \frac{\partial\left(\frac{x'_1 + x'_2}{2}, x'_3 + z_2^c a_2\epsilon, \frac{x'_1 - x'_2}{2a_1}, \epsilon\right)}{\partial(x'_1, x'_2, x'_3, \epsilon)} \right| = \left| \begin{pmatrix} \frac{1}{2} & 0 & \frac{1}{2a_1} & 0 \\ \frac{1}{2} & 0 & -\frac{1}{2a_1} & 0 \\ 0 & 1 & 0 & 0 \\ 0 & z_2^c a_2 & 0 & 1 \end{pmatrix} \right| = \frac{1}{2a_1}. \quad (3.3)$$

We accept this death move with probability

$$\begin{aligned}
a_d(\mathbf{x}'', \epsilon, \epsilon^*) &= \min \left\{ 1, 3 \times \frac{w_b}{w_d} \times \frac{P(\mathbf{z}^c)}{P(\mathbf{z})} \frac{\pi(\mathbf{x}'')}{\pi(\mathbf{x}')} \left| \frac{\partial(T_{d,z}(\mathbf{x}', \epsilon), \epsilon^*, \epsilon)}{\partial(\mathbf{x}', \epsilon)} \right| \right\} \\
&= \min \left\{ 1, 3 \times \frac{w_b}{w_d} \times \frac{p_2^{I_{\{1\}}(z_2^c)} q_2^{I_{\{-1\}}(z_2^c)}}{p_2^{I_{\{1\}}(z_2)} q_2^{I_{\{-1\}}(z_2)}} \times \frac{\pi(\mathbf{x}'')}{\pi(\mathbf{x}')} \times \frac{1}{2a_1} \right\}. \tag{3.4}
\end{aligned}$$

In the general situation, we shall make the birth, death and no-change probabilities w_b , w_d , w_{nc} depend upon the current dimension k , and denote them by $w_{b,k}$, $w_{d,k}$ and $w_{nc,k}$, respectively, satisfying $w_{b,k} + w_{d,k} + w_{nc,k} = 1$ for every $k \geq 1$. Note that when the current dimension $k = 1$, then $w_{d,k} = 0$, as $k \geq 1$. Similarly, if in some cases there is reason to assume that the number of parameters can not exceed some finite quantity denoted by k_{max} , then $w_{b,k_{max}} = 0$.

Figure 3.1 illustrates the idea of TTMCMC schematically, and compares it with the RJMCMC principle, shown diagrammatically in Figure 3.2. As illustrated, for RJMCMC, the necessary “dimension matching” criterion is satisfied, but the criterion is not satisfied, indeed, not necessary, for TTMCMC.

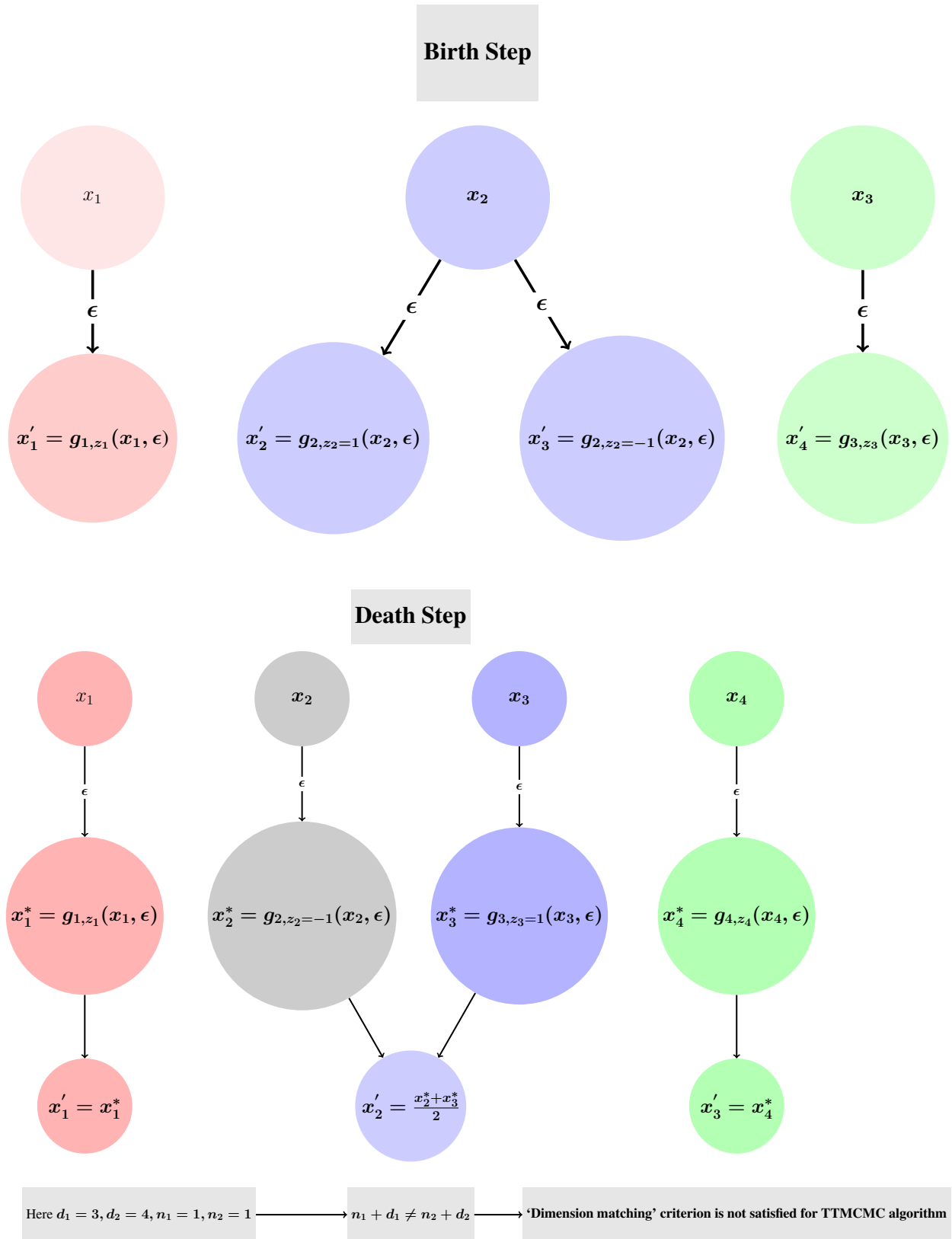


Figure 3.1: Illustration of TTMC algorithm for jumping between dimension 3 and 4.

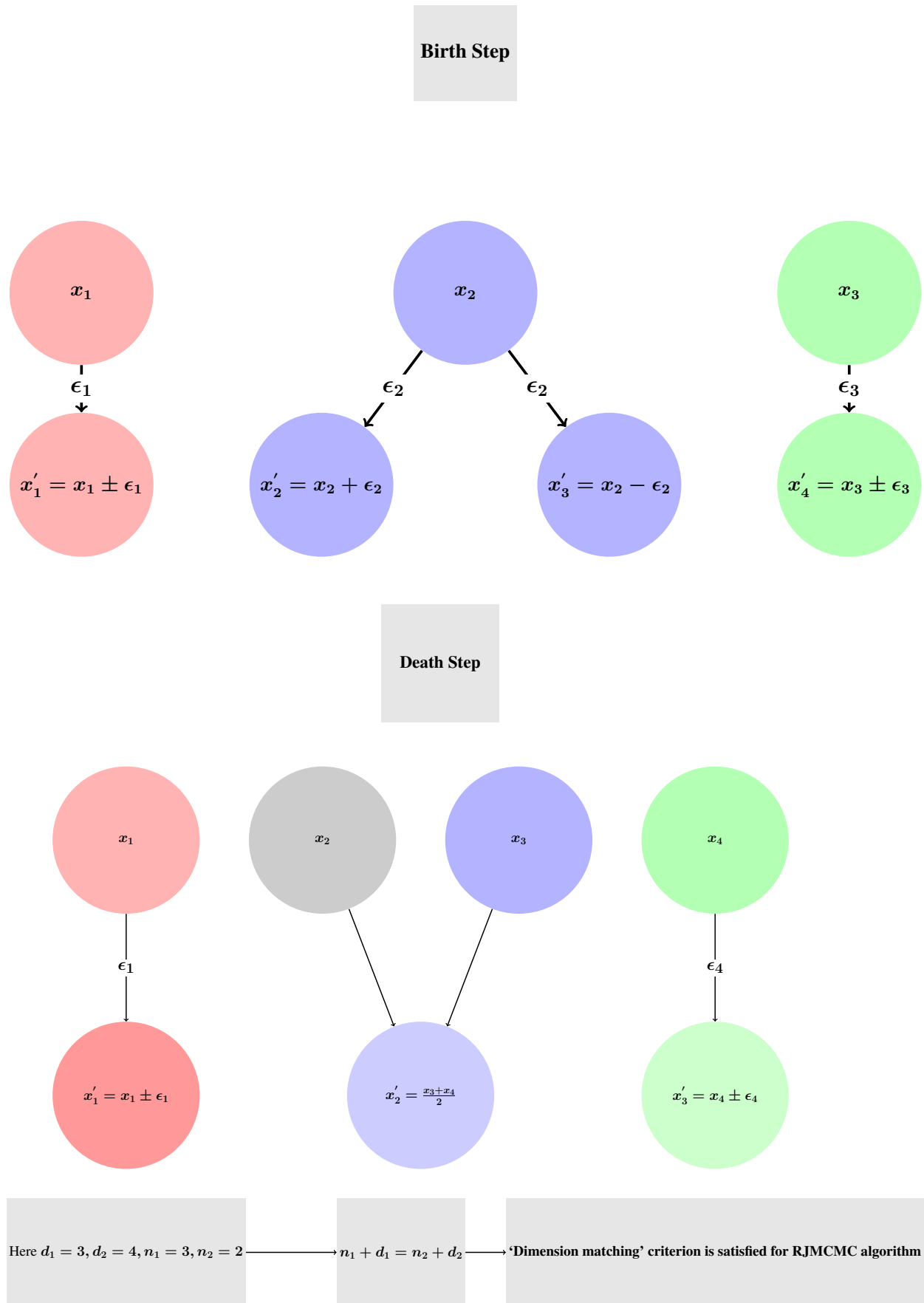


Figure 3.2: Illustration of RJMCMC algorithm for jumping between dimension 3 and 4.

3.2 General TTCCMC algorithm for jumping one dimension at a time

We now provide the TTCCMC algorithm in the general case, as follows.

Algorithm 3.1 *General TTCCMC algorithm based on a single ϵ .*

- Let the initial value be $\mathbf{x}^{(0)} \in \mathbb{R}^k$.
- For $t = 0, 1, 2, \dots$
 1. Generate $u = (u_1, u_2, u_3) \sim \text{Multinomial}(1; w_{b,k}, w_{d,k}, w_{nc,k})$.
 2. If $u_1 = 1$ (increase dimension), then
 - (a) Randomly select a co-ordinate from $\mathbf{x}^{(t)} = (x_1^{(t)}, \dots, x_k^{(t)})$ assuming uniform probability $1/k$ for each co-ordinate. Let j denote the chosen co-ordinate.
 - (b) Generate $\epsilon \sim \rho(\cdot)$ and for $i = 1, \dots, k; i \neq j$ simulate

$$z_i \sim \text{Multinomial}(1; p_i, q_i, 1 - p_i - q_i)$$

independently.

- (c) Propose the following birth move:

$$\begin{aligned} \mathbf{x}' = T_{b,z}(\mathbf{x}^{(t)}, \epsilon) &= (g_{1,z_1}(x_1^{(t)}, \epsilon), \dots, g_{j-1,z_{j-1}}(x_{j-1}^{(t)}, \epsilon), \\ &g_{j,z_j=1}(x_j^{(t)}, \epsilon), g_{j,z_j^c=-1}(x_j^{(t)}, \epsilon), g_{j+1,z_{j+1}}(x_{j+1}^{(t)}, \epsilon), \dots, g_{k,z_k}(x_k^{(t)}, \epsilon)). \end{aligned}$$

Re-label the elements of \mathbf{x}' as $(x'_1, x'_2, \dots, x'_{k+1})$.

- (d) Calculate the acceptance probability of the birth move \mathbf{x}' :

$$a_b(\mathbf{x}^{(t)}, \epsilon) = \min \left\{ 1, \frac{1}{k+1} \times \frac{w_{d,k+1}}{w_{b,k}} \times \frac{P_{(j)}(\mathbf{z}^c)}{P_{(j)}(\mathbf{z})} \frac{\pi(\mathbf{x}')}{\pi(\mathbf{x}^{(t)})} \left| \frac{\partial(T_{b,z}(\mathbf{x}^{(t)}, \epsilon))}{\partial(\mathbf{x}^{(t)}, \epsilon)} \right| \right\},$$

where

$$P_{(j)}(\mathbf{z}) = \prod_{i \neq j=1}^k p_i^{I_{\{1\}}(z_i)} q_i^{I_{\{-1\}}(z_i)},$$

and

$$P_{(j)}(\mathbf{z}^c) = \prod_{i \neq j=1}^k p_i^{I_{\{1\}}(z_i^c)} q_i^{I_{\{-1\}}(z_i^c)}.$$

(e) Set

$$\mathbf{x}^{(t+1)} = \begin{cases} \mathbf{x}' & \text{with probability } a_b(\mathbf{x}^{(t)}, \epsilon) \\ \mathbf{x}^{(t)} & \text{with probability } 1 - a_b(\mathbf{x}^{(t)}, \epsilon). \end{cases}$$

3. If $u_2 = 1$ (decrease dimension), then

(a) Generate $\epsilon \sim \varrho(\cdot)$.

(b) Randomly select co-ordinate j with probability $1/k$, and randomly select co-ordinate j' from the remaining co-ordinates with probability $1/(k-1)$. Let $x_j^* = (g_{j,z_j^c=-1}(x_j, \epsilon) + g_{j',z_{j'}=1}(x_{j'}, \epsilon)) / 2$; replace the co-ordinate x_j drawn first by the average x_j^* , and delete $x_{j'}$.

(c) Simulate \mathbf{z} by generating independently, for $i=1, \dots, k$, but $i \neq j, j'$, $z_i \sim \text{Multinomial}(1; p_i, q_i, 1 - p_i - q_i)$. For $i \neq j, j'$, apply the transformation $x'_i = g_{i,z_i}(x_i^{(t)}, \epsilon)$.

(d) Propose the following death move:

$$\mathbf{x}' = T_{d,\mathbf{z}}(\mathbf{x}^{(t)}, \epsilon) = (g_{1,z_1}(x_1^{(t)}, \epsilon), \dots, g_{j-1,z_{j-1}}(x_{j-1}^{(t)}, \epsilon), x_j^*, g_{j+1,z_{j+1}}(x_{j+1}^{(t)}, \epsilon), \dots, g_{j'-1,z_{j'-1}}(x_{j'-1}^{(t)}, \epsilon), g_{j'+1,z_{j'+1}}(x_{j'+1}^{(t)}, \epsilon), \dots, g_{k,z_k}(x_k^{(t)}, \epsilon)).$$

Re-label the elements of \mathbf{x}' as $(x'_1, x'_2, \dots, x'_{k-1})$.

(e) Solve for ϵ^* from the equations $g_{j,z_j=1}(x_j^*, \epsilon^*) = x_j$ and $g_{j,z_j^c=-1}(x_j^*, \epsilon^*) = x_{j'}$ and express ϵ^* in terms of x_j and $x_{j'}$.

(f) Calculate the acceptance probability of the death move:

$$a_d(\mathbf{x}^{(t)}, \epsilon, \epsilon^*) = \min \left\{ 1, k \times \frac{w_{b,k-1}}{w_{d,k}} \times \frac{P_{(j,j')}(\mathbf{z}^c)}{P_{(j,j')}(\mathbf{z})} \frac{\pi(\mathbf{x}')}{\pi(\mathbf{x}^{(t)})} \left| \frac{\partial(T_{d,\mathbf{z}}(\mathbf{x}^{(t)}, \epsilon), \epsilon^*, \epsilon)}{\partial(\mathbf{x}^{(t)}, \epsilon)} \right| \right\},$$

where

$$P_{(j,j')}(\mathbf{z}) = \prod_{i \neq j, j'=1}^k p_i^{I_{\{1\}}(z_i)} q_i^{I_{\{-1\}}(z_i)},$$

and

$$P_{(j,j)}(\mathbf{z}^c) = \prod_{i \neq j, j'=1}^k p_i^{I_{\{1\}}(z_i^c)} q_i^{I_{\{-1\}}(z_i^c)}.$$

(g) Set

$$\mathbf{x}^{(t+1)} = \begin{cases} \mathbf{x}' & \text{with probability } a_d(\mathbf{x}^{(t)}, \epsilon, \epsilon^*) \\ \mathbf{x}^{(t)} & \text{with probability } 1 - a_d(\mathbf{x}^{(t)}, \epsilon, \epsilon^*). \end{cases}$$

4. If $u_3 = 1$ (dimension remains unchanged), then implement steps (1), (2), (3) of Algorithm 3.1 of Dutta & Bhattacharya (2014).

• End for

In Sections S-1 and S-2 of the supplement we provide the proofs of detailed balance and ergodicity (irreducibility and aperiodicity) of the above TTMC MC method.

3.2.1. Observations regarding Algorithm 3.1

- Note that the acceptance probabilities are independent of the proposal density $\varrho(\cdot)$ irrespective of its form, just as in TMC MC. The reason is that in TTMC MC we simulate $\epsilon \sim \varrho$, for some appropriate density ϱ , for increasing, as well as for decreasing dimension (see the proof of detailed balance in Section S-1 for the precise details). In other words, the “dimension-matching” criterion of RJMC MC is not required for TTMC MC. Indeed, recall that, to accomplish the birth step in RJMC MC one needs to simulate an ϵ , but in the death step two randomly chosen components are averaged to reduce the dimension, and no simulation of ϵ is done. As such, in RJMC MC the dimension-matching criterion is responsible for the presence of the proposal density in the acceptance ratio.
- Consequently, it is not possible to interpret TTMC MC as a special case of RJMC MC. Also, neither is RJMC MC a special case of TTMC MC, even though in fixed-dimensional problems, TMC MC with additive transformations contains the random walk Metropolis algorithm as a special case when as many ϵ ’s as the number of variables to be updated are used for TMC MC.
- Independence of the acceptance ratio of the proposal density ϱ has pleasing consequences for TTMC MC in the sense that for any finite TTMC MC sample (which is always the case

in practice), the possible bias in the acceptance probabilities of birth and death moves due to involvement of ϱ is absent. Since for RJMCMC this is not the case, the performance may be seriously affected. For instance, if ϱ is strictly bounded above by 1, then the birth move will have significantly greater acceptance probability than the death move. The advantage of TTMCMC and disadvantage of RJMCMC in this regard are clearly reflected in all our experiments that we report in this article.

- In the acceptance probabilities, $\frac{P_{(j)}(\mathbf{z}^c)}{P_{(j)}(\mathbf{z})} = 1$ and $\frac{P_{(j,j')}(\mathbf{z}^c)}{P_{(j,j')}(\mathbf{z})} = 1$ if $p_i = q_i$ for each i . This results in simplification of the acceptance ratio computation. The birth, death and the no-change probabilities given by $w_{b,k}$, $w_{d,k}$ and $w_{nc,k}$ can also be chosen to be equal for every $k > 1$, which will result in further simplification of the computation of the acceptance ratio.
- In our algorithm, the new variables created from one variable are never “necessarily adjacent”. Even in the case of adjacency, our method does absolutely fine; indeed, for the death step, we only need to have appropriate positive probability of selecting the two variables for combining them into one (or deleting one) such that the detailed balance holds. Specifically, suppose that we create adjacent variables in the birth move. Then, in the corresponding death move we will choose adjacent pairs with appropriate probability and combine them into one. Alternatively, one may select two variables, but should reject the entire death move if the selected variables are not adjacent. In fact, the issue of adjacency is nothing specific to TTMCMC, and can be handled by RJMCMC as well as by TTMCMC.

3.3 Structured dependence within the moves

In Algorithm 3.1 we have assumed that for $i \in \{1, \dots, k\} \setminus \{j\}$ and for $i \in \{1, \dots, k\} \setminus \{j, j'\}$ (accordingly as the move-type is birth move or death move), z_i are independently simulated in every iteration. Although the co-ordinate-wise moves are dependent since the same ϵ is used for updating them, more flexible and structured dependence can be induced within the moves in the TTMCMC context. Such structured dependence allows for selecting the co-ordinate-wise forward or backward transformations in ways that take account of the posterior correlation between the

parameters, thus facilitating more efficient moves.

Briefly, at each iteration, for $i = 1, \dots, k$, we can reparameterize p_i and q_i as

$$p_i = \frac{\exp(\psi_{1i})}{\sum_{j=1}^3 \exp(\psi_{ji})}; \quad q_i = \frac{\exp(\psi_{2i})}{\sum_{j=1}^3 \exp(\psi_{ji})}; \quad 1 - p_i - q_i = \frac{\exp(\psi_{3i})}{\sum_{j=1}^3 \exp(\psi_{ji})}, \quad (3.5)$$

where, for $j = 1, 2, 3$,

$$(\psi_{j1}, \psi_{j2}, \dots, \psi_{jk}) \sim N_k(\boldsymbol{\mu}_j, \boldsymbol{\Sigma}_j) \quad (3.6)$$

independently, where $(\boldsymbol{\mu}_j, \boldsymbol{\Sigma}_j)$; $j = 1, 2, 3$ may be estimated from a pilot run of TMCMC with the dimensionality fixed at $k = k_{max}$. Specifically, from a pilot run of TMCMC with $p_i = q_i$, for each variable x_i , $i = 1, \dots, k_{max}$, we may consider the three empirical means of x_i associated with $z_i = 1, -1$ and 0 , as good candidates for the i -th components of $\boldsymbol{\mu}_1, \boldsymbol{\mu}_2$ and $\boldsymbol{\mu}_3$, respectively. For the covariance matrices $\boldsymbol{\Sigma}_j$, the empirical estimates of the covariances between x_i and x_j associated with $(z_i = 1, z_j = 1)$, $(z_i = -1, z_j = -1)$, and $(z_i = 0, z_j = 0)$ may be considered as the (i, j) -th elements of $\boldsymbol{\Sigma}_1, \boldsymbol{\Sigma}_2$ and $\boldsymbol{\Sigma}_3$, respectively. The above strategy yields three k_{max} -dimensional vectors $\tilde{\boldsymbol{\mu}}_j$; $j = 1, 2, 3$, and three $k_{max} \times k_{max}$ -dimensional covariance matrices $\tilde{\boldsymbol{\Sigma}}_j$; $j = 1, 2, 3$. The required k -dimensional $\boldsymbol{\mu}_j$ and $k \times k$ -dimensional $\boldsymbol{\Sigma}_j$ are then simply relevant sub-vectors and sub-matrices of $\tilde{\boldsymbol{\mu}}_j$ and $\tilde{\boldsymbol{\Sigma}}_j$ respectively.

At each iteration of TTMCMC we then first simulate $(\psi_{j1}, \psi_{j2}, \dots, \psi_{jk})$; $j = 1, 2, 3$ using (3.6), obtain $\{p_i, q_i, 1 - p_i - q_i; i = 1, \dots, k\}$ using (3.5); then given $\{p_i, q_i, 1 - p_i - q_i; i = 1, \dots, k\}$ we simulate $z_i \sim Multinomial(1; p_i, q_i, 1 - p_i - q_i)$ independently as before, where $i \in \{1, \dots, k\} \setminus \{j\}$ or $i \in \{1, \dots, k\} \setminus \{j, j'\}$.

As in the case of TMCMC, it can be easily verified that our modified TTMCMC algorithm with this hierarchical dependence structure for the distribution of \mathbf{z} satisfies detailed balance.

4. JUMPING MORE THAN ONE DIMENSIONS AT A TIME

We now consider the situations where instead of jumping one dimension, one wishes to jump several dimensions at a time. That is, we now consider the more general framework where $\mathbf{x} = (x_1, \dots, x_k) \in \mathbb{R}^k$ and that we wish to increase the dimension to $k + m$, or to decrease the dimension from $k + m$ to k , where $1 \leq m \leq k$. It follows that TTMCMC can jump from k

to $2k$ dimensions and from $2k$ to k dimensions at the maximum. RJMCMC does not have such restriction, but jumping many dimensions at a time will only add to the general inefficiency of RJMCMC.

For an illustrative TTMC example where jumping more than one dimension is desired, assume that $k = 3$ and $m = 2$, so that it is required to jump from \mathbb{R}^3 to \mathbb{R}^5 . For simplicity, we illustrate with the additive transformation. One may anticipate that this can be accomplished by simulating a single positive $\epsilon \sim \rho(\cdot)$, selecting, say, x_1 and x_2 at random without replacement from $\mathbf{x} = (x_1, x_2, x_3)$, simulating z_3 , and then constructing the birth move $\mathbf{x}' = T_{b,z_2}(\mathbf{x}, \epsilon) = (x_1 + a_1\epsilon, x_1 - a_1\epsilon, x_2 + a_2\epsilon, x_2 - a_2\epsilon, x_3 + z_3a_3\epsilon) = (x'_1, x'_2, x'_3, x'_4, x'_5)$. However, for this move, the dimension of $(\mathbf{x}, \epsilon) = (x_1, x_2, x_3, \epsilon)$ is 4, while that of $\mathbf{x}' = (x'_1, x'_2, x'_3, x'_4, x'_5)$ is 5. In other words, the Jacobian $\left| \frac{\partial(T_{b,z}(\mathbf{x}, \epsilon))}{\partial(\mathbf{x}, \epsilon)} \right|$ is not well-defined.

To get past the above difficulty with dimensions, we need to simulate two ϵ 's from $\rho(\cdot)$: ϵ_1 for splitting x_1 into $x_1 + a_1\epsilon_1$ and $x_1 - a_1\epsilon_1$, and ϵ_2 for splitting x_2 into $x_2 + a_2\epsilon_2$ and $x_2 - a_2\epsilon_2$, and also to update x_3 to $x_3 + z_3a_3\epsilon_2$ (ϵ_1 can also be used to update x_3). Hence the birth move takes the form $\mathbf{x}' = T_{b,z_3}(\mathbf{x}, \epsilon_1, \epsilon_2) = (x_1 + a_1\epsilon_1, x_1 - a_1\epsilon_1, x_2 + a_2\epsilon_2, x_2 - a_2\epsilon_2, x_3 + z_3a_3\epsilon_2) = (x'_1, x'_2, x'_3, x'_4, x'_5)$. Now the dimensions of both $\mathbf{x}' = (x'_1, x'_2, x'_3, x'_4, x'_5)$ and $(\mathbf{x}, \epsilon_1, \epsilon_2) = (x_1, x_2, x_3, \epsilon_1, \epsilon_2)$ are the same and equals 5; hence the Jacobian

$$\left| \frac{\partial(T_{b,z_3}(\mathbf{x}, \epsilon_1, \epsilon_2))}{\partial(\mathbf{x}, \epsilon_1, \epsilon_2)} \right| = \left| \frac{\partial(x_1 + a_1\epsilon_1, x_1 - a_1\epsilon_1, x_2 + a_2\epsilon_2, x_2 - a_2\epsilon_2, x_3 + z_3a_3\epsilon_2)}{\partial(x_1, x_2, x_3, \epsilon_1, \epsilon_2)} \right| = 4a_1a_2,$$

is well-defined. The acceptance probability of the birth move in this example is given by

$$\begin{aligned} a_b(\mathbf{x}, \epsilon_1, \epsilon_2) &= \min \left\{ 1, \frac{1}{(3+2)(3+1)} \times \frac{w_{d,5}}{w_{b,3}} \times \frac{p_3^{I_{\{1\}}(z_3^c)} q_3^{I_{\{-1\}}(z_3^c)}}{p_3^{I_{\{1\}}(z_3)} q_3^{I_{\{-1\}}(z_3)}} \times \frac{\pi(\mathbf{x}')}{\pi(\mathbf{x})} \times \left| \frac{\partial(T_{b,z_3}(\mathbf{x}, \epsilon_1, \epsilon_2))}{\partial(\mathbf{x}, \epsilon_1, \epsilon_2)} \right| \right\} \\ &= \min \left\{ 1, \frac{1}{20} \times \frac{w_{d,5}}{w_{b,3}} \times \frac{p_3^{I_{\{1\}}(z_3^c)} q_3^{I_{\{-1\}}(z_3^c)}}{p_3^{I_{\{1\}}(z_3)} q_3^{I_{\{-1\}}(z_3)}} \frac{\pi(\mathbf{x}')}{\pi(\mathbf{x})} \times 4a_1a_2 \right\}. \end{aligned} \tag{4.1}$$

For the corresponding death move, that is, for moving from $\mathbf{x}' = (x'_1, x'_2, x'_3, x'_4, x'_5)$ to $\mathbf{x}'' = T_{d,z}(\mathbf{x}', \epsilon_1) = (\frac{x'_1+x'_2}{2}, \frac{x'_3+x'_4}{2}, x'_5 + z_3^c a_3 \epsilon_1) = (x''_1, x''_2, x''_3)$, we must have, for the reverse of this death move, $x''_1 + a_1\epsilon_1^* = x'_1$, $x''_1 - a_1\epsilon_1^* = x'_2$, $x''_2 + a_2\epsilon_2^* = x'_3$, $x''_2 - a_2\epsilon_2^* = x'_4$. The first two

equations yield $\epsilon_1^* = \frac{x'_1 - x'_2}{2a_1}$ and the last two equations yield $\epsilon_2^* = \frac{x'_3 - x'_4}{2a_2}$. The Jacobian is given by

$$\left| \frac{\partial(T_{d,z_3}(\mathbf{x}', \epsilon_1); \epsilon_1^*, \epsilon_2^*, \epsilon_1)}{\partial(\mathbf{x}', \epsilon_1)} \right| = \left| \frac{\partial \left(\frac{x'_1 + x'_2}{2}, \frac{x'_3 + x'_4}{2}, x'_5 + z_3^c a_3 \epsilon_1, \frac{x'_1 - x'_2}{2a_1}, \frac{x'_3 - x'_4}{2a_2}, \epsilon_1 \right)}{\partial(x'_1, x'_2, x'_3, x'_4, x'_5, \epsilon_1)} \right| = \frac{1}{4a_1 a_2}. \quad (4.2)$$

We accept this death move with probability

$$\begin{aligned} a_d(\mathbf{x}'', \epsilon_1, \epsilon_1^*, \epsilon_2^*) &= \min \left\{ 1, 5 \times 4 \times \frac{w_{b,3}}{w_{d,5}} \times \frac{P(\mathbf{z}^c)}{P(\mathbf{z})} \frac{\pi(\mathbf{x}'')}{\pi(\mathbf{x}')} \left| \frac{\partial(T_{d,z_3}(\mathbf{x}', \epsilon_1); \epsilon_1^*, \epsilon_2^*, \epsilon_1)}{\partial(\mathbf{x}', \epsilon_1)} \right| \right\} \\ &= \min \left\{ 1, 20 \times \frac{w_{b,3}}{w_{d,5}} \times \frac{p_3^{I_{\{1\}}(z_3)} q_3^{I_{\{-1\}}(z_3)}}{p_3^{I_{\{1\}}(z_3^c)} q_3^{I_{\{-1\}}(z_3^c)}} \times \frac{\pi(\mathbf{x}'')}{\pi(\mathbf{x}')} \times \frac{1}{4a_1 a_2} \right\}. \end{aligned} \quad (4.3)$$

We illustrate the idea of this algorithm in Figure 4.1 diagrammatically for the ease of understanding.

Thus, in general, for moving from dimension k to dimension $k + m$, we need to simulate $\epsilon_1, \dots, \epsilon_m$ for updating $\mathbf{x} = (x_1, \dots, x_k)$ to $\mathbf{x}' = (x'_1, x'_2, \dots, x'_k, x'_{k+1}, \dots, x'_{k+m})$. The associated general TTMC MC algorithm for jumping m dimensions is provided as Algorithm S-3.1 of Section S-3, and the proof of its detailed balance is provided in Section S-4.

In variable dimensional problems such as mixtures, changing the dimension of one set of parameters necessitates changing the dimensions of the other sets of parameters. Thus, more than one dimension must be changed at a time, while the parameters are inter-related. We provide the details and the relevant algorithm (Algorithm S-5.1) in Section S-5 of the supplement. Indeed, for our mixture applications of TTMC MC, we implement Algorithm S-5.1, choosing the additive transformation.

Note that exactly as discussed in Section 3.3 we can incorporate a hierarchical dependence structure on the distribution of \mathbf{z} in Algorithms S-3.1 and S-5.1, which does not hamper the detailed balance condition.

5. TTMC MC: TOWARDS AUTOMATION

Algorithms 3.1, S-3.1 and S-5.1 provide concrete ways to implement our TTMC MC procedure, in general variable dimensional problems. Below we detail the manifold advantages of TTMC MC, which point towards the fact that TTMC MC is close to qualifying as an automatic sampler in variable dimensional problems.

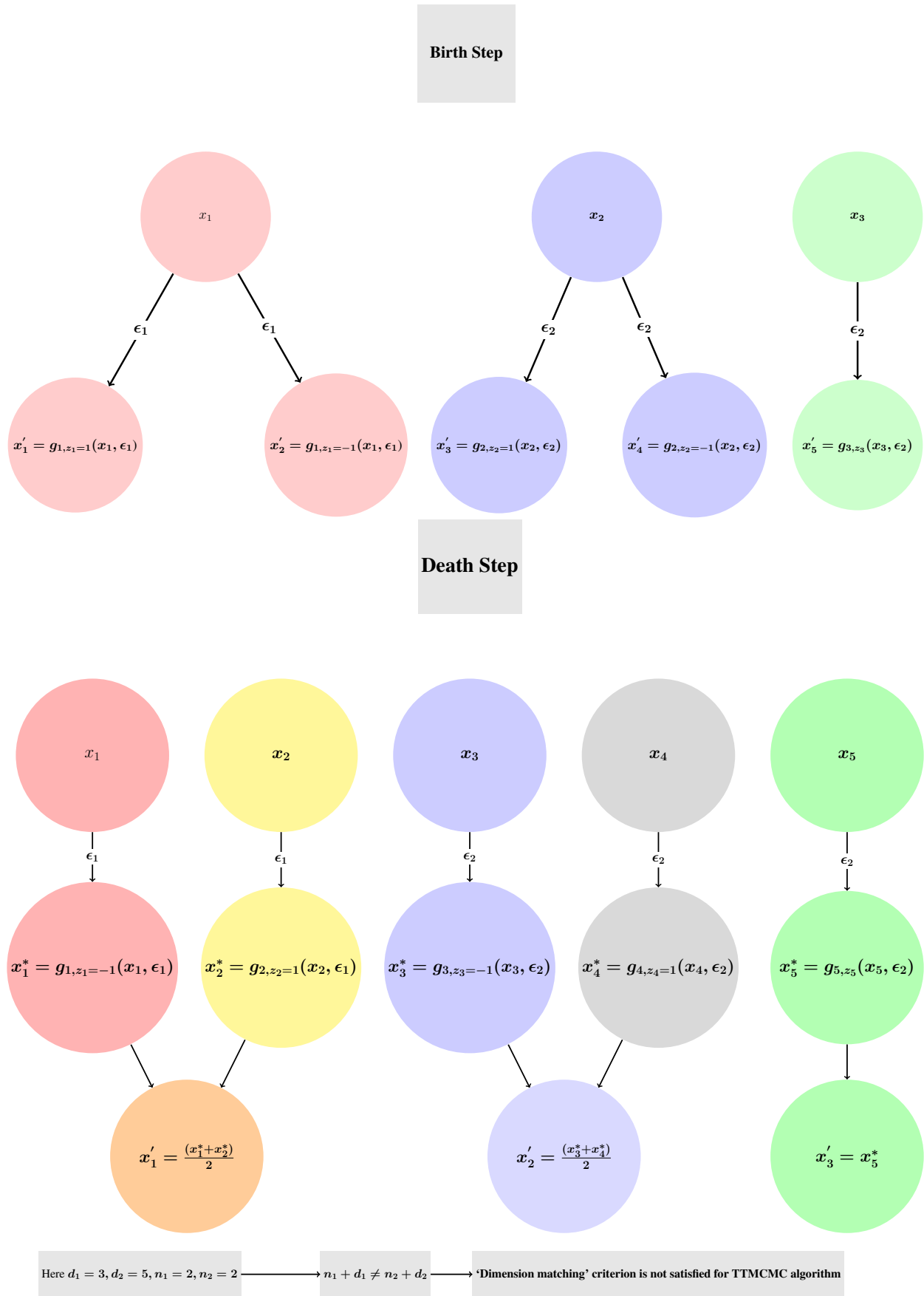


Figure 4.1: Illustration of TTMC algorithm for jumping more than one dimension.

5.1 Reasonably high acceptance rate

The additive and the multiplicative transformations, and combinations of them can be effectively utilized, in conjunction with just a few, fixed number of ϵ 's, to accomplish transdimensional movement. The methodology reduces the variable dimensional problem to effectively fixed dimensional, indexed by a fixed and small number of ϵ 's. The fixed and low-dimensional nature of ϵ (or the set $\{\epsilon_1, \dots, \epsilon_m\}$) ensures reasonably high acceptance rate. Indeed, for high-dimensional proposals, with high probability at least one component would be ill-proposed, which would render the acceptance probability extremely small, even in fixed-dimensional cases. In the context of TMCMC, theoretical and empirical results are provided in Dutta & Bhattacharya (2014), Dey & Bhattacharya (2017b), Dey & Bhattacharya (2017a). Our experiments in this paper provide ample support to our claim of adequate acceptance rate of TTMCMC.

5.2 Good mixing properties in high-dimensional and multimodal cases

Dutta & Bhattacharya (2014) discussed that in one-dimensional situations, TMCMC reduces to a Metropolis-Hastings algorithm with a specialized mixture proposal density, and hence, is expected to explore multimodal target densities quite efficiently (see Guan & Krone (2007), for example). In higher dimensions, due to singularity, the proposal does not admit a Lebesgue-measure-dominated mixture density form directly, but since the method employs similar principles, good convergence properties of TMCMC are to be expected for high-dimensional multimodal targets as well. Since TTMCMC samplers are also based on the same principles of deterministic transformations and construction of move types within each of the birth, death and no-change move types, good convergence properties are expected when the target density is multimodal for each dimension. In the context of TMCMC, Dey & Bhattacharya (2017c), Dey & Bhattacharya (2017b) and Dey & Bhattacharya (2017a) demonstrate far superior mixing of TMCMC compared to random walk Metropolis-Hastings. The results of our TTMCMC applications reported in this paper provide ample support to this discussion.

5.3 Applicability to all variable dimensional problems

The construction of TTMC MC sampler does not require any assumptions regarding the model, such as existence of moments or unimodality. Note that in the attempts made so far for constructing generic RJMC MC samplers, these assumptions are quite crucial; see Sisson (2005), Fan & Sisson (2011) for comprehensive discussions regarding these assumptions. So, for the construction of TTMC MC sampler for switching between two models, namely, from \mathcal{M}_k to $\mathcal{M}_{k'}$, we only need to determine if some sets of parameters are related and decide on the number of parameters to be added or deleted, in a single step. Accordingly we will choose one of the above mentioned algorithms and update all the parameters in a single block. Hence, our proposed sampler is very much applicable to any variable dimensional problem.

5.4 Default TTMC MC algorithm and its tuning

In order to design efficient MCMC algorithms it has become standard practice to tune the proposals. For the default, random walk proposals, this is synonymous with choosing the scales optimally. Dutta & Bhattacharya (2014) recommended additive TMC MC as the default TMC MC proposal since this transformation requires much smaller number of move-types and the corresponding acceptance probability has a simple form in that it is free of the Jacobian of transformations. Already Dey & Bhattacharya (2017b), Dey & Bhattacharya (2017a) have developed some theory on optimal scaling in the context of additive TMC MC. In keeping with Dutta & Bhattacharya (2014) we advocate additive TTMC MC as the default TTMC MC sampler, which again requires specification of the scaling constants. In this regard, in Section S-8.2 of the supplement we propose a convergence diagnostic that is generally applicable. Guided by our proposed convergence diagnostic it is possible to find the appropriate value of scaling constants. Instances of the idea are illustrated in Sections 6 and 7. The results of our experiments demonstrate great ease of implementation and excellent performance of the default additive TTMC MC sampler in all the examples. Further experiments with additive TTMC MC, conducted by these authors and their colleagues in challenging, high-dimensional spatio-temporal problems (see, for example, Das & Bhattacharya (2016)), variable-selection problems, (high-dimensional) curve-fitting problems also yielded excellent re-

sults. Thus, it seems that additive TTMC is close towards the kind of automation that we desire.

6. SIMULATION STUDIES WITH MIXTURES OF GAMMA DISTRIBUTIONS WITH UNKNOWN NUMBER OF COMPONENTS

Wiper, Insua & Ruggeri (2001) implement RJMCMC in mixtures of gamma distributions of the form $\mathcal{G}\left(\nu, \frac{\nu}{\mu}\right)$, where by $\mathcal{G}(a, b)$ we mean a gamma distribution with mean a/b and variance a/b^2 .

In other words, Wiper et al. (2001) consider the following mixture density for $y > 0$:

$$f(y|\boldsymbol{\nu}_k, \boldsymbol{\mu}_k, \boldsymbol{\pi}_k, k) = \sum_{j=1}^k \pi_j \frac{(\nu_j/\mu_j)^{\nu_j}}{\Gamma(\nu_j)} y^{\nu_j-1} \exp\left(-\frac{\nu_j}{\mu_j} y\right), \quad (6.1)$$

where $\boldsymbol{\nu}_k = (\nu_1, \dots, \nu_k)$, $\boldsymbol{\mu}_k = (\mu_1, \dots, \mu_k)$, and $\boldsymbol{\pi}_k = (\pi_1, \dots, \pi_k)$. Given $k > 0$, for each j , $\nu_j > 0$, $\mu_j > 0$, $0 < \pi_j < 1$ such that $\sum_{j=1}^k \pi_j = 1$. We assume k to be unknown, so that the dimension of the model (that is, the number of the component parameters) is unknown and considered random.

6.1 Prior structure

Wiper et al. (2001) assumed the following prior structure given k :

$$\boldsymbol{\pi}_k \sim \mathcal{D}(1, \dots, 1); \quad (6.2)$$

$$\nu_j \stackrel{iid}{\sim} \mathcal{E}(100); \quad j = 1, \dots, k; \quad (6.3)$$

$$\mu_j^{-1} \stackrel{iid}{\sim} \mathcal{G}(1, 1); \quad j = 1, \dots, k, \quad (6.4)$$

such that $\mu_1 < \dots < \mu_k$. In (6.2), $\mathcal{D}(1, \dots, 1)$ denotes the Dirichlet distribution with all the parameters equal to 1, and in (6.3), $\mathcal{E}(100)$ stands for the exponential distribution with mean 100. As regards k , Wiper et al. (2001) consider the discrete uniform distribution on $\{1, \dots, 10\}$.

For the implementation purpose, we reparameterize ν_j and μ_j as $\exp(\nu_j^*)$ and $\exp(\mu_j^*)$, where $\nu_j^* \sim \log(\text{Exponential}(100))$ and $(\mu_j^*)^{-1} \sim \log(\mathcal{G}(1, 1))$. Since $-\infty < \nu_j^* < \infty$ and $-\infty < \mu_j^* < \infty$, this reparameterization frees the parameter space from any restrictions, allowing TTMC to move freely, while keeping the original prior distributions intact. We denote $(\nu_1^*, \dots, \nu_k^*)$ by $\boldsymbol{\nu}_k^*$ and $(\mu_1^*, \dots, \mu_k^*)$ by $\boldsymbol{\mu}_k^*$.

For π we propose the following prior based on reparameterization: for $j = 1, \dots, k$,

$$\pi_j = \frac{\exp(\omega_j)}{\sum_{\ell=1}^k \exp(\omega_\ell)}; \quad \omega_1, \dots, \omega_k \stackrel{iid}{\sim} N(\mu_\omega, \sigma_\omega^2), \quad (6.5)$$

where $\omega_j \stackrel{iid}{\sim} \log(\mathcal{G}(1, 1))$, so that the prior (6.2) remains intact. Thus, we need to update $\omega_k = (\omega_1, \dots, \omega_k)$, instead of π , using TTMC MC.

6.2 Label switching

A brief account of the so-called “label-switching problem” associated with identifiability of mixtures is provided in Section S-6 of the supplement. In this article our goal is to demonstrate TTMC MC with inference regarding posterior distributions of densities. Since inference on densities is not affected by label switching, the problem of label switching is not of much importance in our context. Moreover, we argue in Section S-6 that identifiability in the mixture context is not generally desirable. However, since Wiper et al. (2001) enforced the restriction $\mu_1 < \dots < \mu_k$ in an attempt to mitigate identifiability problems, for fair comparison we also impose the same restriction.

6.3 Posterior summary

An important aspect to any Bayesian analysis is summarization of the posterior in the sense of obtaining a measure of central tendency and appropriate credible regions. Here we are interested in the posterior distribution of the entire mixture density, induced by the posterior of the unknown number of parameters. Thus, we need a measure of central tendency for the set of mixture densities supported by the posterior, and appropriately constructed credible regions. Indeed, in Section S-7 of the supplement, we develop a methodology for obtaining the modal mixture density associated with the posterior, along with the desired credible regions and highest posterior density (HPD) credible regions. In the context of our experiments we shall display the modal mixture densities and several other mixture densities falling within the 95% HPD regions.

6.4 Convergence diagnostics

Convergence assessment even in fixed-dimensional set-ups is a difficult proposition; in variable-dimensional problems, the challenges increase manifold. We provide a briefing on these in Section S-8.1 of the supplement. As an attempt to make some progress on convergence assessment in variable-dimensional problems we propose a convergence diagnostic in Section S-8.2 of the supplement, which is based on the methodology for summarizing the posterior. In a nutshell, we obtain 95% (or any other desired) credible regions from the first and second halves of a complete run of TTMC MC, and then obtain the minimum increments of the radii required for the credible regions to contain one another; small values of the increments indicate convergence of TTMC MC. Not only do we assess convergence of TTMC MC with this method, we exploit this idea to select the scales of the additive transformation that we employ for the illustrations.

6.5 General TTMC MC strategy for our experiments

We conduct four simulation studies, with data generated from the same 1-component, 2-component, 3-component and 4-component gamma mixtures as considered by Wiper et al. (2001) and apply TTMC MC and compare our results with those obtained by the RJMC MC algorithm of Wiper et al. (2001). In particular, we apply Algorithm S-3.1, updating $(k, \boldsymbol{\nu}^*, \boldsymbol{\mu}^*, \boldsymbol{\omega})$ simultaneously in a single block using the additive transformation; we choose the proposal density to be $\varrho(\boldsymbol{\epsilon}) \equiv N(\boldsymbol{\epsilon} : 0, 1) \mathbb{I}_{(0, \infty)}(\boldsymbol{\epsilon})$, where $N(\boldsymbol{\epsilon} : 0, 1)$ denotes the normal density with mean 0, variance 1, and evaluated at $\boldsymbol{\epsilon}$; $\mathbb{I}_{(0, \infty)}(\cdot)$ denotes the indicator function for the set $(0, \infty)$. For every iteration of TTMC MC we choose equal move-type probabilities of birth, death and no-change strategies. Also, for the underlying additive transformation, we choose equal probabilities of forward and backward transformations. The forms of the Jacobian for the birth and the death moves are given by $8a_{\nu_j^*} a_{\mu_j^*} a_{\omega_j}$ and $(8a_{\nu_j^*} a_{\mu_j^*} a_{\omega_j})^{-1}$ respectively, where $a_{\nu_j^*}$, $a_{\mu_j^*}$ and a_{ω_j} are the scales for additive TTMC MC updating of ν_j^* , μ_j^* and ω_j respectively. We base the choices of these scales on the convergence diagnostic proposed in Section S-8.2 of the supplement. The experimental details are provided in the context-specific applications. All our codes are written in C and implemented on a 32 bit, dual core (2.53 GHz \times 2) laptop with 2.8 GiB memory. However, for high-dimensional multivariate

experiments we implemented our C codes on a VMWare.

6.6 An RJMCMC algorithm based on random walk proposals

Since, in this paper, we apply additive TTMC MC to our examples, it makes sense to compare our TTMC MC results with those obtained by the RJMCMC algorithm based on random walk, which is the closest to additive TTMC MC among all RJMCMC algorithms. Recall that random walk involves additive transformations of the same form as additive TTMC MC, but with independent jump sizes for every variable, unlike TTMC MC. Also, unlike TTMC MC, the acceptance ratios for the birth and death moves involves products of the densities $\varrho(u_i) \equiv N(u_i : 0, 1)\mathbb{I}_{(0,\infty)}(u_i)$; $i = 1, 2, 3$, corresponding to the birth proposals for $(\nu_1^*, \tau_1^*, \omega_1)$. Since the proposals of additive TTMC MC and random walk have the same additive form, the variabilities of the jump sizes of the competing proposals are not expected to be different. This is confirmed by the optimal scaling theory of TMC MC developed by Dey & Bhattacharya (2017b), where it is shown that the optimal scales of additive TMC MC and random walk are the same. Hence, in this work, we choose the same scales of random walk RJMCMC as additive TTMC MC.

The main difference between our random walk RJMCMC and the proposal of Green (2003) is that the latter is deterministic unless movement to a higher dimension is attempted; the moves also involve dimension-specific mean vectors and covariance matrices, which are to be estimated from the dimension-specific posteriors. Even for moderate number of models this is a difficult and computationally burdensome proposition; see Fan & Sisson (2011) for example. Indeed, as stressed in Green (2003), the approach is unlikely to be useful for more than a small set of models.

However, for all our examples related to the gamma mixture, our random walk RJMCMC had very small overall acceptance rate, and completely failed to change the dimension in any such example. Hence, we do not provide further details regarding the performance of the random walk RJMCMC in gamma mixtures. In the normal mixture context, random walk RJMCMC performed somewhat better, although still not at all satisfactorily. Since this algorithm fails even in univariate contexts, we do not pursue this for the multivariate situations.

6.7 First simulation study with data generated from a one-component gamma mixture

Following Wiper et al. (2001) we generate 400 realizations from $\mathcal{Gamma}(3, 3)$, and model the realized data with the gamma mixture of the form (6.1). Assuming the same prior structure described in Section 6.1, we then simulate from the resulting variable-dimensional posterior using TTMCMC.

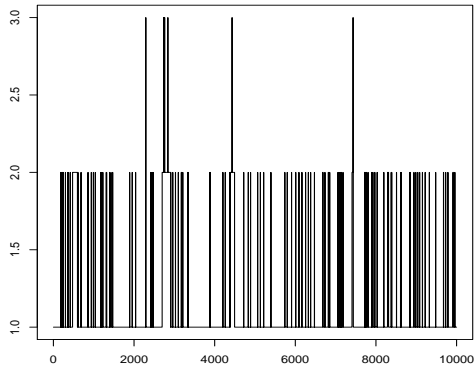
For implementing TTMCMC it is necessary to select the scales $a_{\nu_j^*}, a_{\tau_j^*}, a_{\omega_j}$ appropriately for each $j = 1, \dots, k$. Rather than selecting the scales in order to optimize the acceptance rate (see Dey & Bhattacharya (2017b) for optimal scaling theory in the context of additive TMCMC), here we choose the scales by directly quantifying convergence of the TTMCMC chain using the convergence diagnostic procedure proposed in Section S-8.2 of the supplement. We experimented by setting, for every $j = 1, \dots, k$, the scale values $a_{\nu_j^*} = a_{\nu^*}$; $a_{\mu_j^*} = a_{\mu^*}$, and $a_{\omega_j} = a_{\omega}$, with $a_{\nu^*}, a_{\tau^*}, a_{\omega}$ being one of the trial values 0.05, 0.1, 0.12, 0.15, 0.20, 0.25, 0.50. With every trial value, we ran our TTMCMC algorithm for a burn-in of 750,000 iterations, and a further 1,500,000 iterations, storing one in 150 iterations, thus obtaining a total of 10,000 realizations from the posterior distribution. For each trial run we assessed convergence of our TTMCMC chain using the method proposed in Section S-8.2. We divided our TTMCMC samples into two parts, one part consisting of the first 5,000 realizations and the other part containing the next 5,000 realizations. Constructing the approximate 95% credible regions as prescribed, we then obtained the minimum increment, η_1 , of the radius of the first credible region such that the increased first credible region wholly contains the second credible region. Similarly, we obtained η_2 , the radius increment associated with the second credible region. Small values of η_1 and η_2 indicate convergence of the algorithm. We selected that set of trial values of the scales which yielded the smallest η_1 and η_2 among the trial runs. Indeed, the smallest η_1 and η_2 turned out to be $\eta_1 = 0.041460$ and $\eta_2 = 0.027130$, which corresponded to $a_{\nu} = a_{\mu} = 0.5$ and $a_{\omega} = 1.5$. Hence, we report our results with respect to these trial values. Moreover, since both these quantities are small, we conclude that convergence has taken place appropriately. We remark here that the rather long burn-in that we had considered was unnecessary, as further experiments showed that the chain converged in far less number of iterations. But we feel

it is a good practice to allow large enough burn-in when it is feasible computationally. The overall acceptance rate, evaluated empirically, turned out to be 0.036596. The birth, death, and no-change rates are 0.004206, 0.053131 and 0.067679, respectively. Our TTMC MC implementation with the scales selected as above took 10 minutes and 57 seconds.

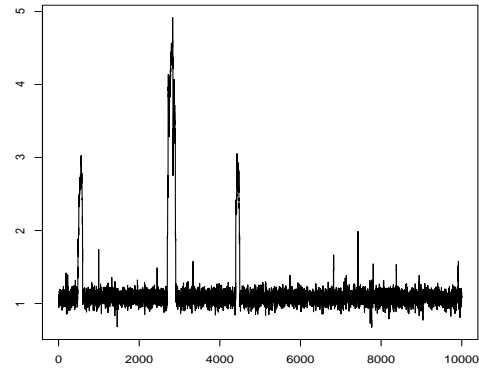
The trace plots of k , ν_1^* , μ_1^* and ω_1 , provided in Figure 6.1, exhibits quite adequate mixing properties consistent with our more formal test of convergence. Also very encouragingly, the posterior distribution of k gives probabilities 0.9344, 0.0649 and 0.0007 to $k = 1, 2, 3$ respectively, heavily supporting the true, single-component gamma mixture. Since the data size is rather large, such high support to the truth is expected. Indeed, with further simulation studies we demonstrate in Section S-9.1 of the supplement, that as the data size increases, the posterior distribution of k concentrates around the truth, namely, $k = 1$.

Figure 6.2 shows the modal density (thick, black curve), along with some other densities within the 95% HPD region overlapped on the histogram of the simulated data. Excellent fit of the posterior distribution of the densities to the data is indicated by the diagram.

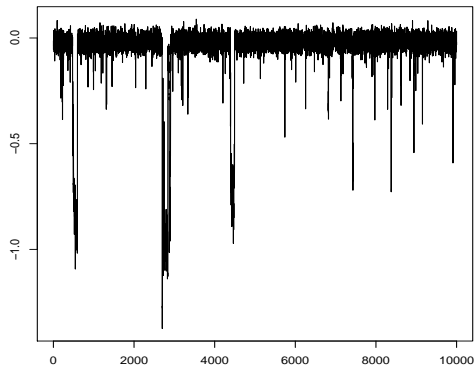
6.7.1. Comparison with the results obtained by Wiper et al. (2001) In sharp contrast with our TTMC MC results, Wiper et al. (2001), using an RJMC MC algorithm that is very similar to that proposed by Richardson & Green (1997) for normal mixtures, obtained a posterior distribution that supports all possible values of $k \in \{1, \dots, 10\}$. In particular, their posterior probabilities of $k = 1, 2, 3, 4, 5$ turned out to be 0.41, 0.24, 0.12, 0.08 and 0.05, respectively, with other values of k having posterior probabilities less than 0.03. In other words, driven by RJMC MC, the true value $k = 1$ received lower posterior support, in comparison with our TTMC MC based posterior. This performance can possibly be attributed to the $\mathcal{G}(5, 5)$ proposal density they used for their dimension-changing move. Since this density is uniformly less than one and features in the acceptance ratio, heavy bias towards large values of k is to be expected as per our discussion in the third point following Algorithm 3.1. Thus, there seems to be good reasons to suspect the convergence of the RJMC MC algorithm in this case. In fact, as we shall show, the same issue hinders convergence of the RJMC MC algorithms for the remaining experiments as well.



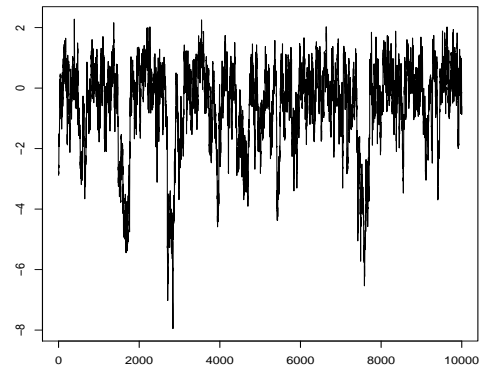
(a) Trace plot of k .



(b) Trace plot of ν_1^* .



(c) Trace plot of μ_1^* .



(d) Trace plot of ω_1 .

Figure 6.1: **TTMCMC for 1-component gamma mixture:** Trace plots of k , ν_1^* , μ_1^* and ω_1 .

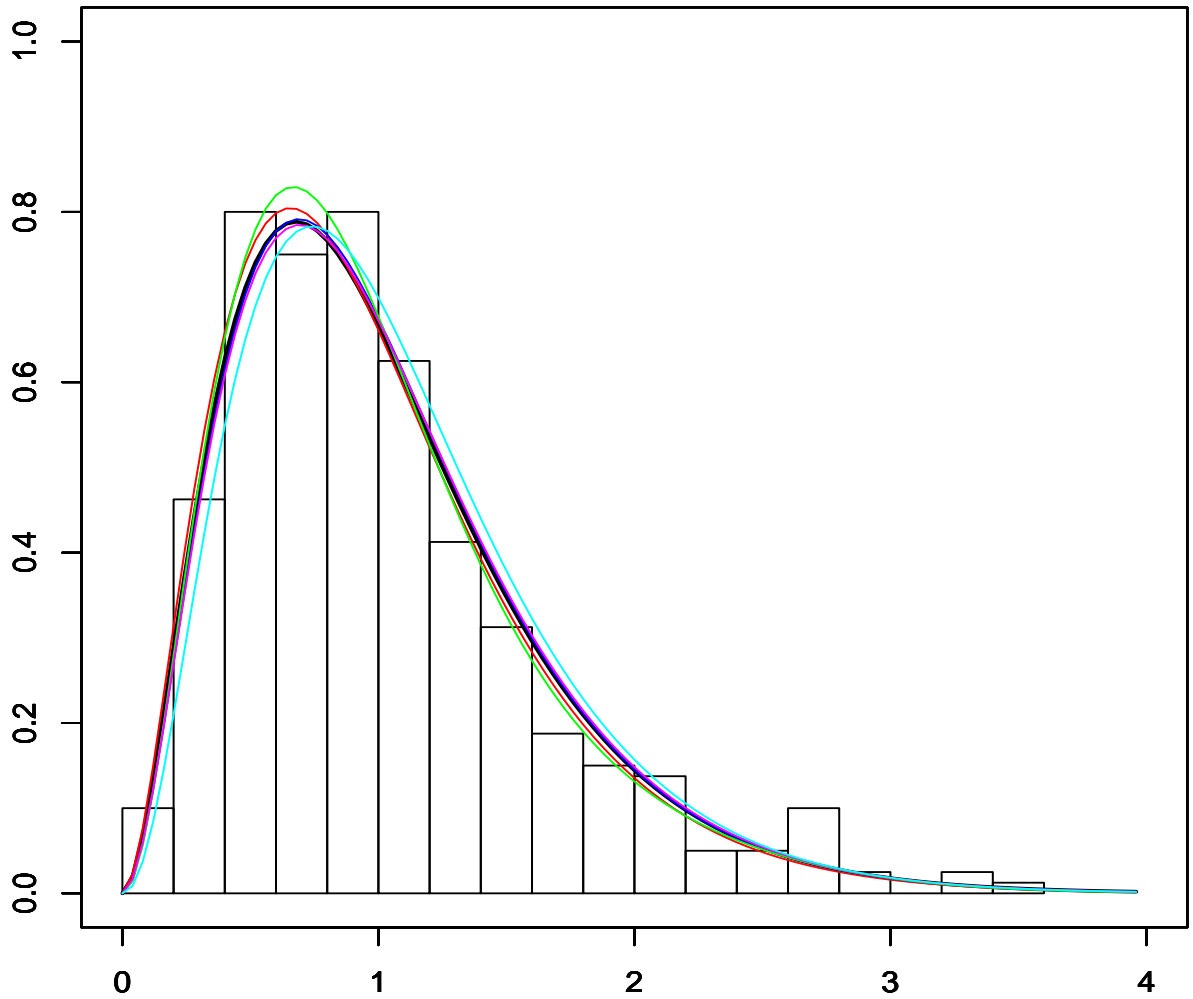


Figure 6.2: **TTMCMC for 1-component gamma mixture:** Goodness of fit of the posterior distribution of densities (coloured curves) to the simulated data (histogram). The thick black curve is the modal density and the other coloured curves are some densities contained in the 95% HPD.

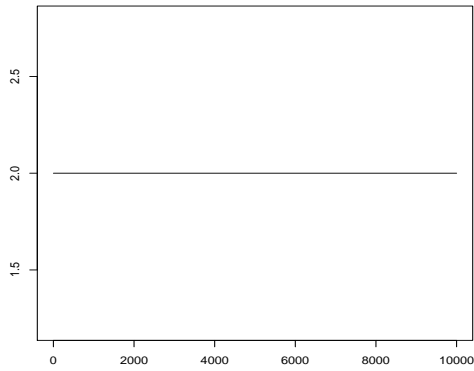
It is important to remark in this context that the actual mixture density can be approximated well in spite of poor mixing, provided that k takes on large values with significant posterior probabilities. Therefore fitting the actual density alone can be very misleading as a criterion of assessment of variable-dimensional algorithms, particularly for RJMCMC algorithms, because of their inherent bias towards large values of k in any practical implementation. In all the four simulation examples considered by Wiper et al. (2001), the actual densities are well-approximated by RJMCMC, but in all the cases, large values of k seemed to play vital important roles in this regard. Such an issue is clearly of more concern in real data cases where the truth is unknown. As we demonstrate with TTMCMC in the supplement with the real galaxy data example of Richardson & Green (1997), their prior structure perhaps actually supports unimodal density, while the histogram is highly multimodal. However, because of large values of k supported by RJMCMC, the approximated density seems to appear as a good fit.

6.8 Second simulation study with data generated from a two-component gamma mixture

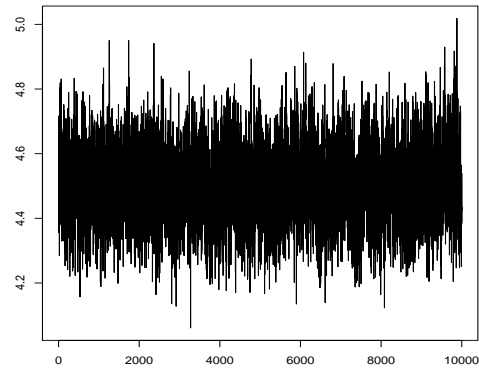
Following Wiper et al. (2001) we now generate 400 realizations from the two-component mixture $0.1 \times \mathcal{G}(9, 27) + 0.9 \times \mathcal{G}(90, 270)$.

In this case, for TTMCMC implementation we obtained $a_{\nu^*} = 0.05$; $a_{\mu^*} = 0.005$, and $a_{\omega} = 0.05$ using our convergence diagnostic procedure. We set a considerably large burn-in time of 30,00,000 iterations as convergence seemed to be somewhat slow compared to the one-component example. We stored one in 150 iterations of a further run of 1, 500, 000 iterations, so that, as before we stored a total of 10,000 realizations from the posterior distribution. This took 31 minutes 6 seconds and yielded an overall acceptance rate 0.229365. Also, the birth, death and no-change rates are 0.000017, 0.000022 and 0.688025, respectively. In this case, we obtained $\eta_1 = 0.28333$ and $\eta_2 = 0.30828$, which are reasonably small, providing reasonably strong evidence in support of convergence of our TTMCMC chain. This is further supported strongly by the visual information carried by the trace plots of k , ν_1^* , μ_1^* and ω_1 , shown in Figure 6.3.

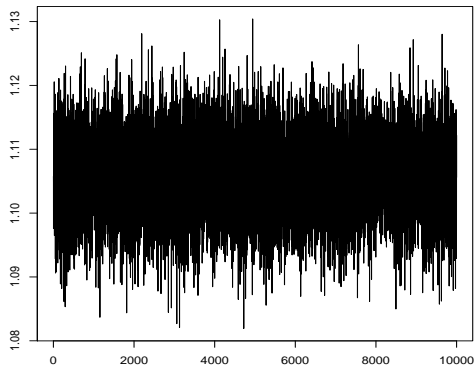
Interestingly, after burn-in, TTMCMC gives full mass to 2 components, thus completely supporting the truth. However, as demonstrated in Section S-9 of the supplement with simulation



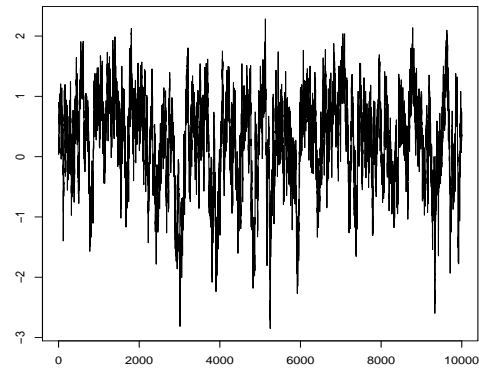
(a) Trace plot of k .



(b) Trace plot of ν_1^* .



(c) Trace plot of μ_1^* .



(d) Trace plot of ω_1 .

Figure 6.3: **TTMCMC for 2-component gamma mixture:** Trace plots of k , ν_1^* , μ_1^* and ω_1 .

studies for different data sizes (see Section S-9.2 for simulations with this 2-component mixture), it is possible that the actual posterior distribution of k gives “almost” point mass to $k = 2$, such that with probability close to zero some other components may also occur, but might have been missed by us in this case due to the finite run length of our algorithm.

As before, Figure 6.4 shows excellent fit of the posterior distribution of the densities to the simulated data.

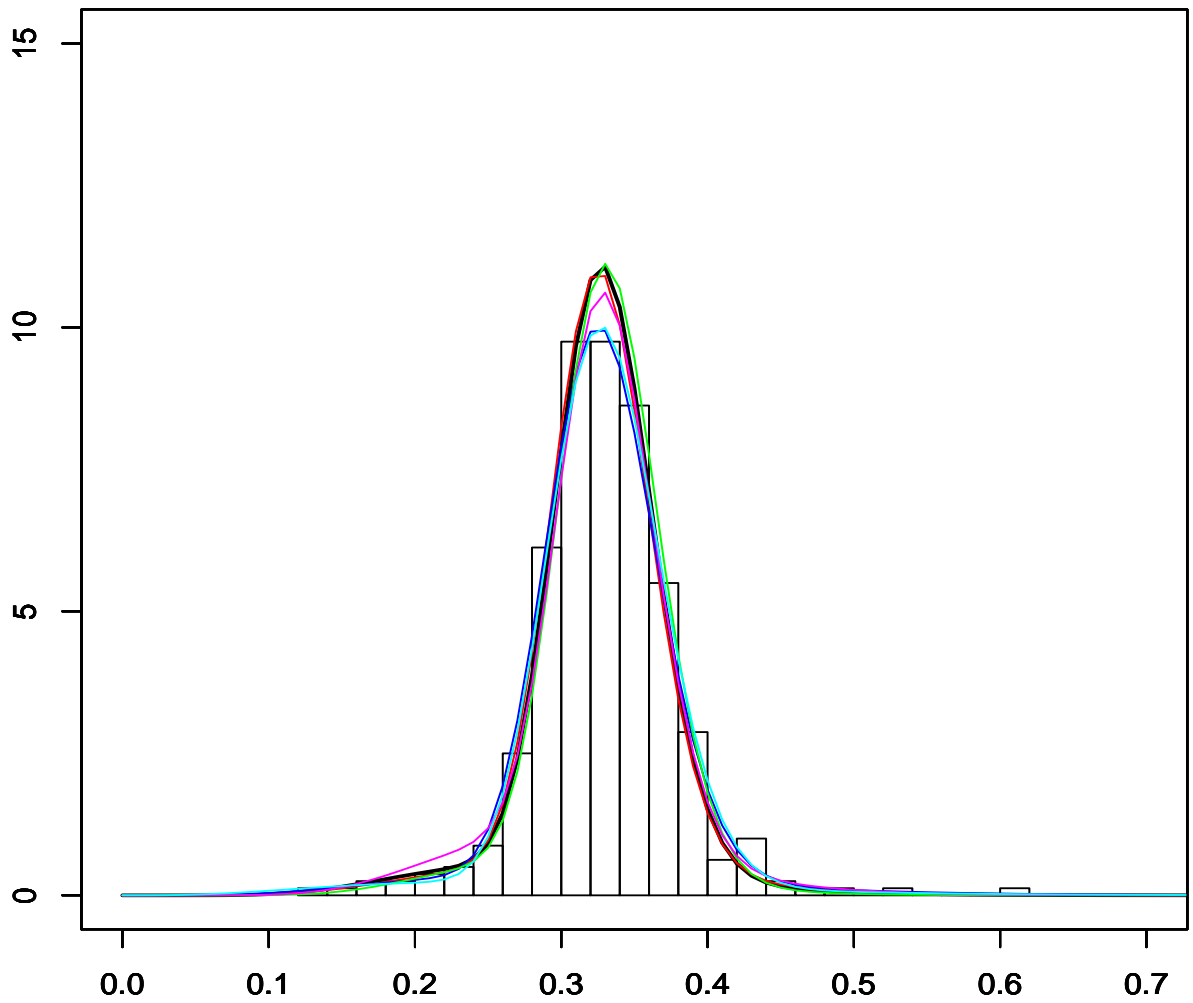


Figure 6.4: **TTMCMC for 2-component gamma mixture:** Goodness of fit of the posterior distribution of densities (coloured curves) to the simulated data (histogram). The thick black curve is the modal density and the other coloured curves are some densities contained in the 95% HPD.

6.8.1. Comparison with the results obtained by Wiper et al. (2001) As to be anticipated, bias towards large values of k continued in this example. Indeed, although Wiper et al. (2001) obtained $k = 2$ as the mode of their RJMCMC based posterior of k , they also found that their RJMCMC algorithm yielded the posterior probability about 0.01 for $k = 1$, and supported other larger values of k . Thus, compared to TTMCMC, which identifies the truth very precisely, RJMCMC manages to facilitate only weak inference because of its lack of convergence.

6.9 Third simulation study with data generated from a three-component gamma mixture

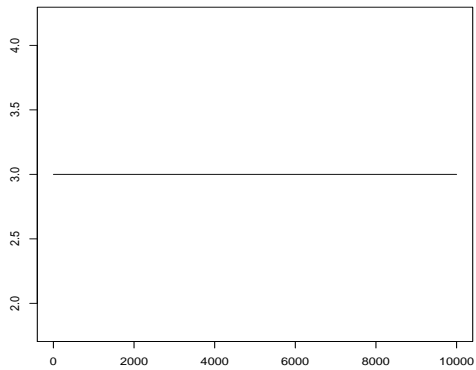
Here we generate 400 realizations from the three-component mixture $0.2 \times \mathcal{G}(40, 20) + 0.6 \times \mathcal{G}(6, 1) + 0.2 \times \mathcal{G}(200, 20)$, following Wiper et al. (2001).

Again we obtained $a_{\nu^*} = 0.05$; $a_{\mu^*} = 0.005$, and $a_{\omega} = 0.05$ using our convergence diagnostic procedure. Here a burn-in of 15,00,000 iterations turned out to be more than sufficient. As before we stored 10,000 realizations from the posterior distribution out of a further 1,500,000 iterations after the burn-in with a thinning of size 150. The overall acceptance rate was 0.240443 and the time taken was 36 minutes and 5 seconds. The birth, death and no-change rates are 0.00001, 0.000017 and 0.720547, respectively. As regards the convergence diagnostic, $\eta_1 = 0.01602$ and $\eta_2 = 0.01757$, which are both small enough to let us conclude that the TTMCMC chain has converged very well. The trace plots displayed in Figure 6.5 completely support our conclusion regarding convergence.

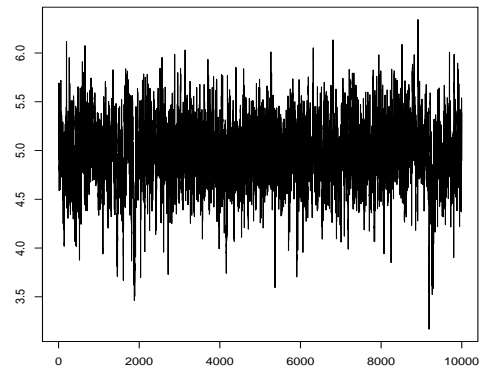
Again, the posterior distribution of k completely supports the truth, giving full mass to 3, which, in this example, is the correct number of components. The simulation study in Section S-9.3 of the supplement demonstrates that it is possible that here TTMCMC has missed $k = 4$, which might have occurred with extremely small probability.

As to be expected, Figure 6.6 confirms excellent fit of the posterior distribution of the densities to the simulated data.

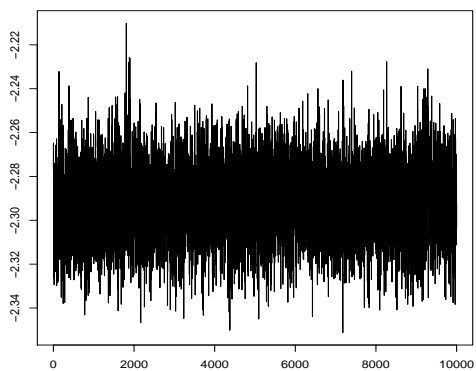
6.9.1. Comparison with the results obtained by Wiper et al. (2001) Specific RJMCMC based results pertaining to the three component mixture are not provided in Wiper et al. (2001),



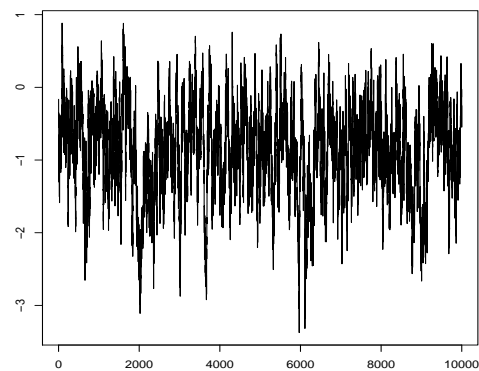
(a) Trace plot of k .



(b) Trace plot of ν_1^* .



(c) Trace plot of μ_1^* .



(d) Trace plot of ω_1 .

Figure 6.5: **TTMCMC for 3-component gamma mixture:** Trace plots of k , ν_1^* , μ_1^* and ω_1 .

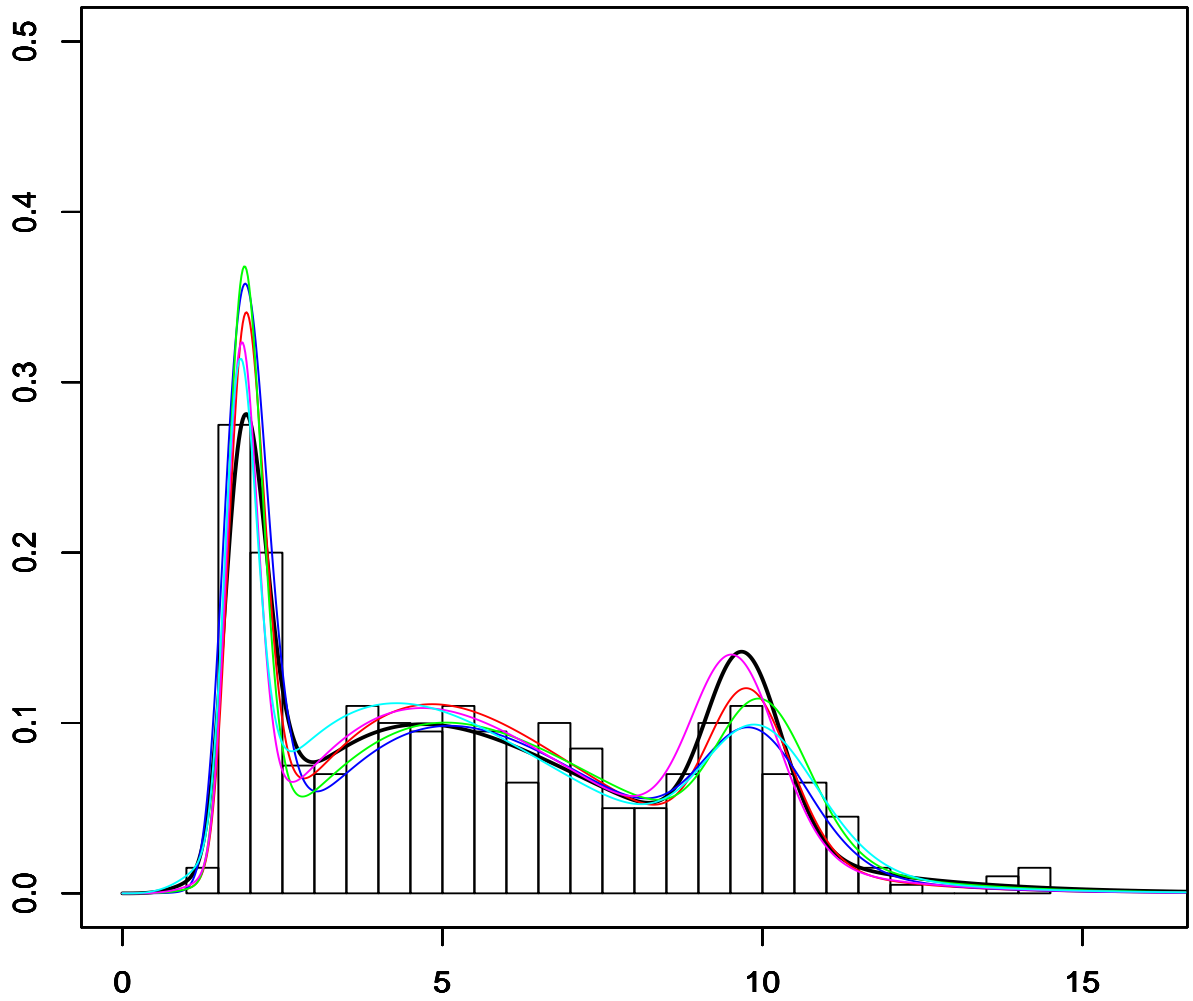


Figure 6.6: **TTMCMC for 3-component gamma mixture:** Goodness of fit of the posterior distribution of densities (coloured curves) to the simulated data (histogram). The thick black curve is the modal density and the other coloured curves are some densities contained in the 95% HPD.

but larger values of k compared to the truth, are certain to occur with significant probabilities.

6.10 Fourth simulation study with data generated from a four-component gamma mixture

For the final simulation study with gamma mixtures, following Wiper et al. (2001) we generate 400 realizations from the four-component mixture $0.25 \times \mathcal{G}(200, 100) + 0.25 \times \mathcal{G}(400, 100) + 0.25 \times \mathcal{G}(600, 100) + 0.25 \times \mathcal{G}(800, 100)$.

Here we obtained $a_{\nu^*} = 0.05$; $a_{\mu^*} = 0.005$, and $a_{\omega} = 0.12$, with a burn-in of 15,00,000 iterations and with respect to 10,000 realizations from the posterior distribution stored as before after burn-in with a thinning of size 150. The time to implement TTMC MC was 40 minutes and 35 seconds and we obtained an overall acceptance rate 0.117432. The birth, death and no-change rates are 0.000417, 0.000401 and 0.345363, respectively. That the chain converged reasonably well can be inferred since $\eta_1 = 0.08154$ and $\eta_2 = 0.11839$ are both reasonably small. As before, the trace plots displayed in Figure 6.7 confirm our conclusion regarding convergence.

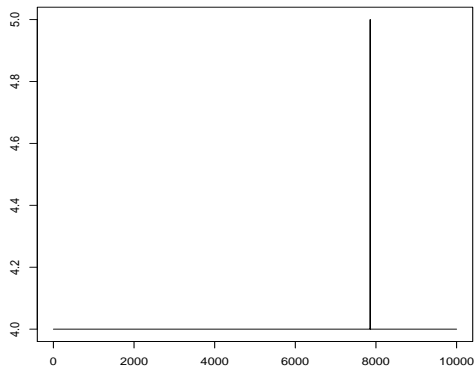
Here the posterior distribution of k gives almost full mass to the truth $k = 4$, and seems to be consistent with the further simulation study conducted in Section S-9.4 of the supplement, considering a data of size 1000.

As before, Figure 6.8 shows that excellent fit of the posterior distribution of the densities to the simulated data has been achieved.

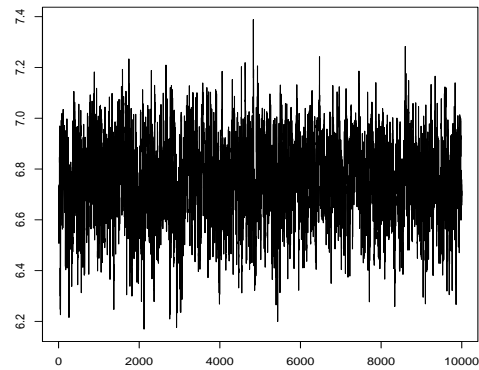
6.10.1. Comparison with the results obtained by Wiper et al. (2001) Even for this 4-component example specific RJMCMC based results are not provided in Wiper et al. (2001), but as in the other RJMCMC based examples, larger values of k compared to the truth, are certain to occur with significant probabilities.

7. COMPARISON OF TTMC MC AND RJMCMC IN THE NORMAL MIXTURE SET UP WITH UNKNOWN NUMBER OF COMPONENTS

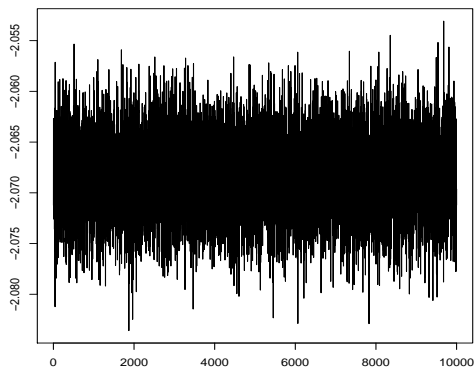
We now illustrate TTMC MC on normal mixture models with unknown number of components with application to the well-studied enzyme, acidity and the galaxy data sets. Richardson &



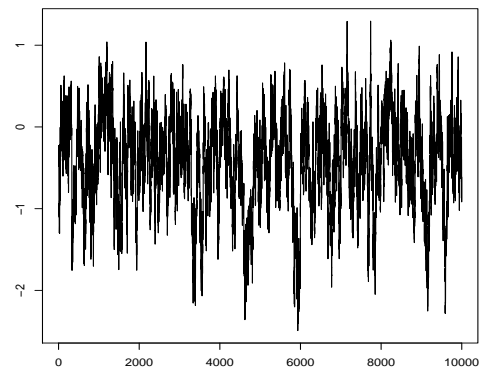
(a) Trace plot of k .



(b) Trace plot of ν_1^* .



(c) Trace plot of μ_1^* .



(d) Trace plot of ω_1 .

Figure 6.7: **TTMCMC for 4-component gamma mixture:** Trace plots of k , ν_1^* , μ_1^* and ω_1 .

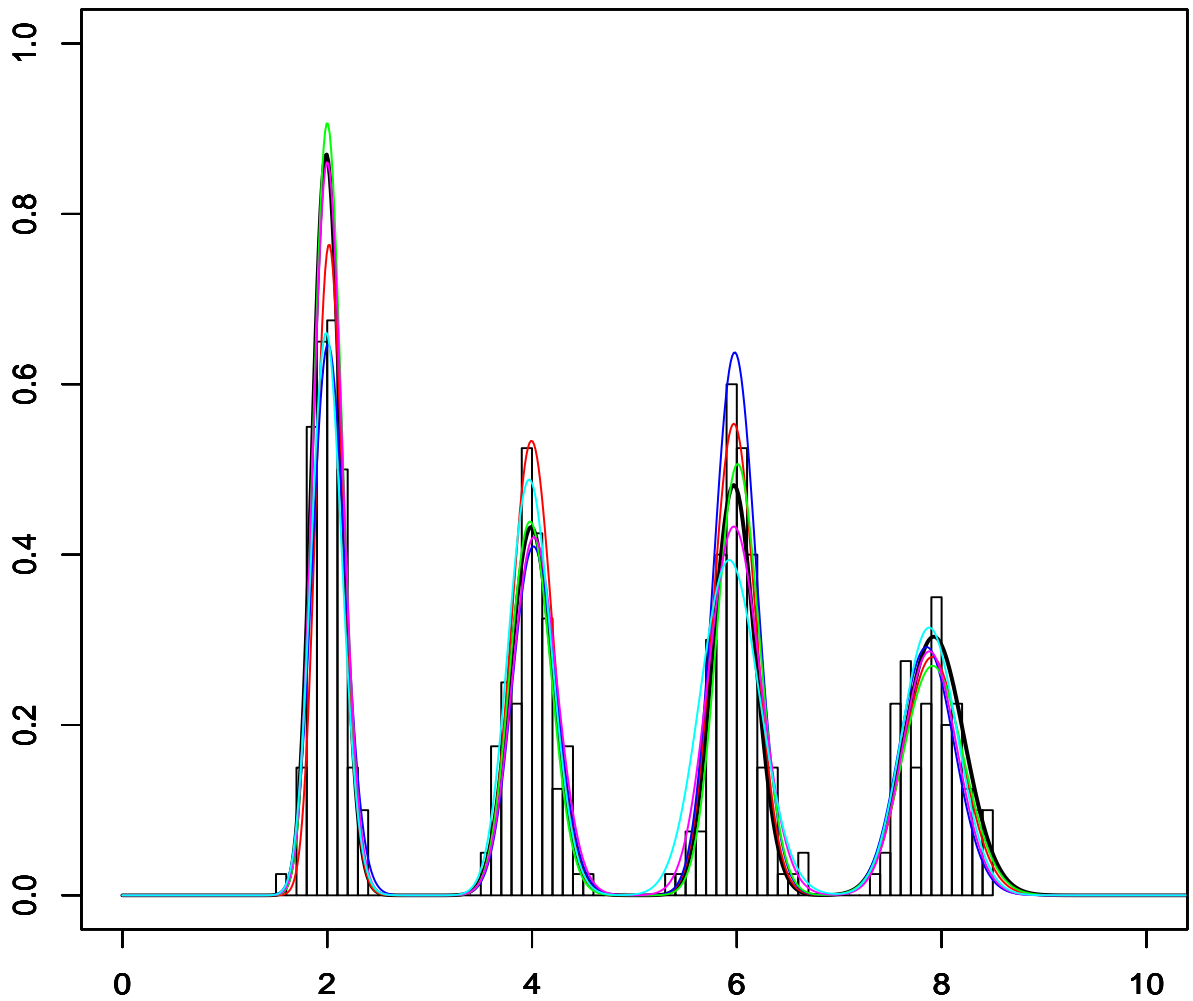


Figure 6.8: **TTMCMC for 4-component gamma mixture:** Goodness of fit of the posterior distribution of densities (coloured curves) to the simulated data (histogram). The thick black curve is the modal density and the other coloured curves are some densities contained in the 95% HPD.

Green (1997) modeled these data sets using parametric normal mixtures and applied RJMCMC for Bayesian inference. On the other hand, Bhattacharya (2008) (see also Escobar & West (1995)) proposed a semi parametric normal mixture model based on Dirichlet process and used Gibbs sampler for Bayesian inference.

7.1 Normal mixture

Let the data points y_1, \dots, y_n be independently and identically distributed (*iid*) as the normal mixture of the following form: for $i = 1, \dots, n$

$$f(y_i | \boldsymbol{\nu}_k, \boldsymbol{\tau}_k, \boldsymbol{\pi}_k, k) = \sum_{j=1}^k \pi_j \sqrt{\frac{\tau_j}{2\pi}} \exp \left\{ -\frac{\tau_j}{2} (y_i - \nu_j)^2 \right\}, \quad (7.1)$$

where $\boldsymbol{\nu}_k = (\nu_1, \dots, \nu_k)$, $\boldsymbol{\tau}_k = (\tau_1, \dots, \tau_k)$, and $\boldsymbol{\pi}_k = (\pi_1, \dots, \pi_k)$. Given $k > 0$, for each j , $-\infty < \nu_j < \infty$, $\tau_j > 0$, $0 < \pi_j < 1$ such that $\sum_{j=1}^k \pi_j = 1$. As before, we assume that k is unknown.

7.2 Prior structure

Note that the semi parametric mixture model of Bhattacharya (2008) can be viewed as a parametric model when the scale parameter associated with the base distribution of the Dirichlet process prior tends to infinity. Hence, from that perspective, the base distributions of ν_j and τ_j may be regarded as the respective priors for our current parametric mixture context. Thus, motivated by Bhattacharya (2008), we consider the following prior for $\boldsymbol{\nu}$ and $\boldsymbol{\tau}$:

$$[\tau_j] \sim \mathcal{G} \left(\frac{s}{2}, \frac{S}{2} \right); \quad (7.2)$$

$$[\nu_j | \tau_j] \sim N \left(\nu_0, \frac{\psi}{\tau_j} \right). \quad (7.3)$$

In the above, $N(\mu, \sigma^2)$ denotes the normal distribution with mean μ and variance σ^2 . Specifications of the values of the hyperparameters s, S, ν_0, ψ are discussed in the context of the applications.

Analogous to the gamma mixture context here we reparameterize τ_j as $\exp(\tau_j^*)$, where $\tau_j^* \sim \log(\mathcal{G}(s/2, S/2))$. We denote $(\tau_1^*, \dots, \tau_k^*)$ by $\boldsymbol{\tau}_k^*$.

For π we propose the same reparameterization (6.5). In this case, we consider two kinds of priors on ω . One is $\omega_j \sim N(\mu_\omega, \sigma_\omega^2)$, and the other is $\omega_j \sim \log(\mathcal{G}(\alpha_j, 1))$ independently, for $j = 1, \dots, k$, where $\alpha_j > 0$; $j = 1, \dots, k$. Note that, for the normal prior on ω_j , the induced prior on π is not the traditional Dirichlet distribution, while the second prior implies that $\pi \sim \mathcal{D}(\alpha_1, \dots, \alpha_k)$.

As regards the prior on k , we consider the uniform distribution on $\{1, 2, \dots, 30\}$, the truncated Poisson distribution on $\{1, 2, \dots, 30\}$ and the discretized normal with mean μ_k and variance σ_k^2 on $\{1, 2, \dots, 30\}$ (that is, the normal density with mean μ_k and variance σ_k^2 evaluated and re-normalized on $\{1, 2, \dots, 30\}$ to render it a discrete probability mass function).

We fit normal mixture models to each of the three data sets – enzyme, acidity, and galaxy, using the general TTMCMC strategy provided in Section 6.5. The details are provided in the context-specific applications.

We compare the performance of additive TTMCMC with random walk RJMCMC, which is analogous to additive TTMCMC but with independent jump-sizes for every co-ordinate and with the proposal density associated with the birth move incorporated within the acceptance ratio, unlike TTMCMC; see Section 6.6.

Our main aim is to demonstrate that the simplest version of TTMCMC, namely, TTMCMC with the additive transformation, is efficient enough for adequately exploring the complicated mixture-based posteriors in all the three applications, while the corresponding RJMCMC version, composed of random walk based moves, fails miserably.

Specific details of inference and implementation of our methodologies follow.

7.3 Enzyme data

Following Bhattacharya (2008) we set $s = 4.0$; $S = 2 \times (0.2/1.22) = 0.3278689$; $\nu_0 = 1.45$; $\psi = 33.3$. Rather than assuming $\omega_j \sim \log(\mathcal{G}(\alpha_j, 1))$ which induce the traditional Dirichlet distribution for π , here we assume that $\omega_j \sim N(\mu_{\omega_j}, \sigma_{\omega_j}^2)$, with $\mu_\omega = 0$ and $\sigma_\omega^2 = 0.25$. We chose somewhat small variance to reflect our belief that ω_j 's are relatively close to constant, so that *a priori* the mixing probabilities π are approximately the same. We specify the uniform distribution on $\{1, \dots, 30\}$ as the prior on k .

As in the gamma mixture set-up we experimented by setting, for every $j = 1, \dots, k$, the scale values $a_{\nu_j^*} = a_{\nu^*}$; $a_{\tau_j^*} = a_{\tau^*}$, and $a_{\omega_j} = a_{\omega}$, with $a_{\nu^*}, a_{\tau^*}, a_{\omega}$ being one of the trial values 0.05, 0.1, 0.12, 0.15, 0.20, 0.25, 0.50. We considered a burn-in of 375,000 iterations and a further 15,00,000 iterations, storing as before one in 150 iterations to obtain 10,000 realizations from the posterior. Here η_1 and η_2 turned out to be $\eta_1 = 0.07291$ and $\eta_2 = 0.039230$, which corresponded to $a_{\nu} = a_{\tau} = a_{\omega} = 0.05$. The results we report are with respect to these trial values. Since both η_1 and η_2 are small, we conclude that convergence has taken place appropriately. The overall acceptance rate, evaluated empirically, turned out to be 0.05284032, and the birth, death, no-change rates are 0.000306, 0.000304 and 0.157810, respectively. Our TTMC implementation with the scales selected as above took 2 minutes and 56 seconds.

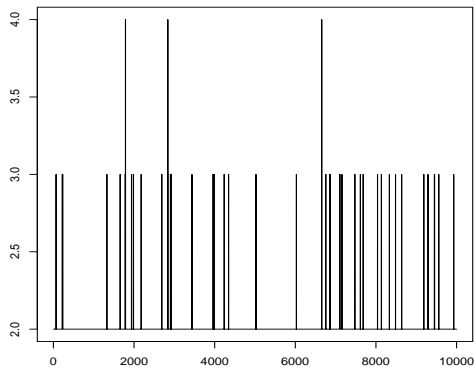
We also verified convergence of our TTMC chain with informal trace plots. Figure 7.1 displays the trace plots of k , ν_1^* , τ_1^* and ω_1 . As seen in panel (a) of Figure 7.1 the posterior distribution of k placed highest mass on 2 components (posterior probability 0.986), followed by 3 components (posterior probability 0.0137), and then by 4 components (probability 0.0003). In other words, our Bayesian analysis strongly supports bimodality. Indeed, the information regarding bimodality is particularly strong thanks to the small range on which the data are supported and the large size of the data (the data set contains 245 observations on an effective support $(0, 3)$). Panels (b), (c) and (d) of Figure 7.1 show adequate mixing properties of the chain. Thus, the mixing information provided by these trace plots supports the conclusion obtained by our proposed credible region based convergence assessment method.

Figure 7.2 shows excellent fit of the posterior distribution of the densities to the data.

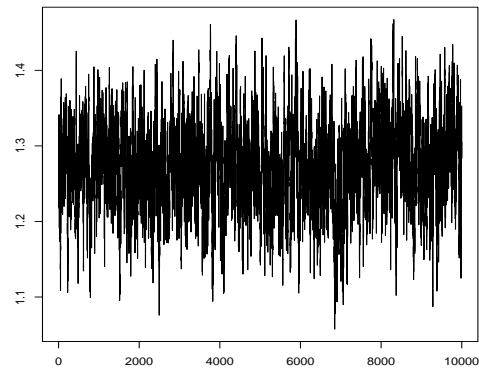
7.4 Acidity data

Again following Bhattacharya (2008) we set $s = 4.0$; $S = 2 \times (0.2/0.573) = 0.6980803$; $\nu_0 = 5.02$; $\psi = 33.3$. Here also we assume that $\omega_j \sim N(\mu_{\omega_j}, \sigma_{\omega_j}^2)$, with $\mu_{\omega} = 0$ and $\sigma_{\omega}^2 = 0.25$. As before we put the uniform prior distribution on $\{1, \dots, 30\}$ on k .

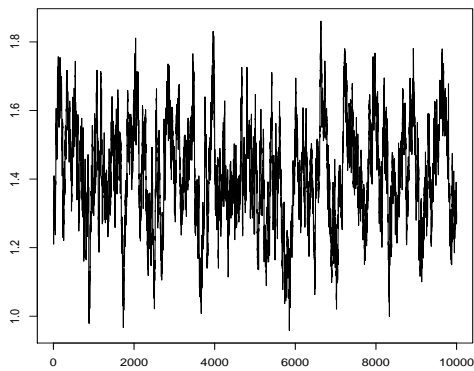
Following the convergence diagnostic method detailed above for choosing appropriate scales here we obtain $a_{\nu_j^*} = a_{\tau_j^*} = a_{\omega_j^*} = 0.05$ for $j = 1, \dots, k$. For these scales we obtained $\eta_1 = 0.0049$



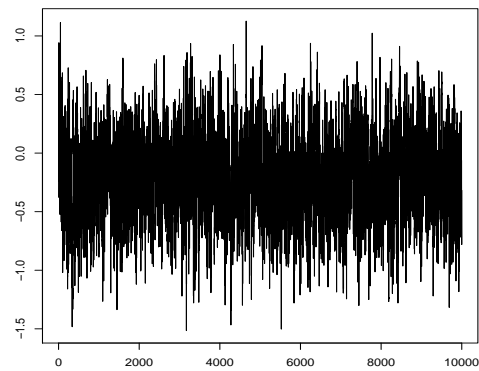
(a) Trace plot of k .



(b) Trace plot of ν_1^* .



(c) Trace plot of τ_1^* .



(d) Trace plot of ω_1 .

Figure 7.1: **TTMCMC for the enzyme data:** Trace plots of k , ν_1^* , τ_1^* and ω_1 .

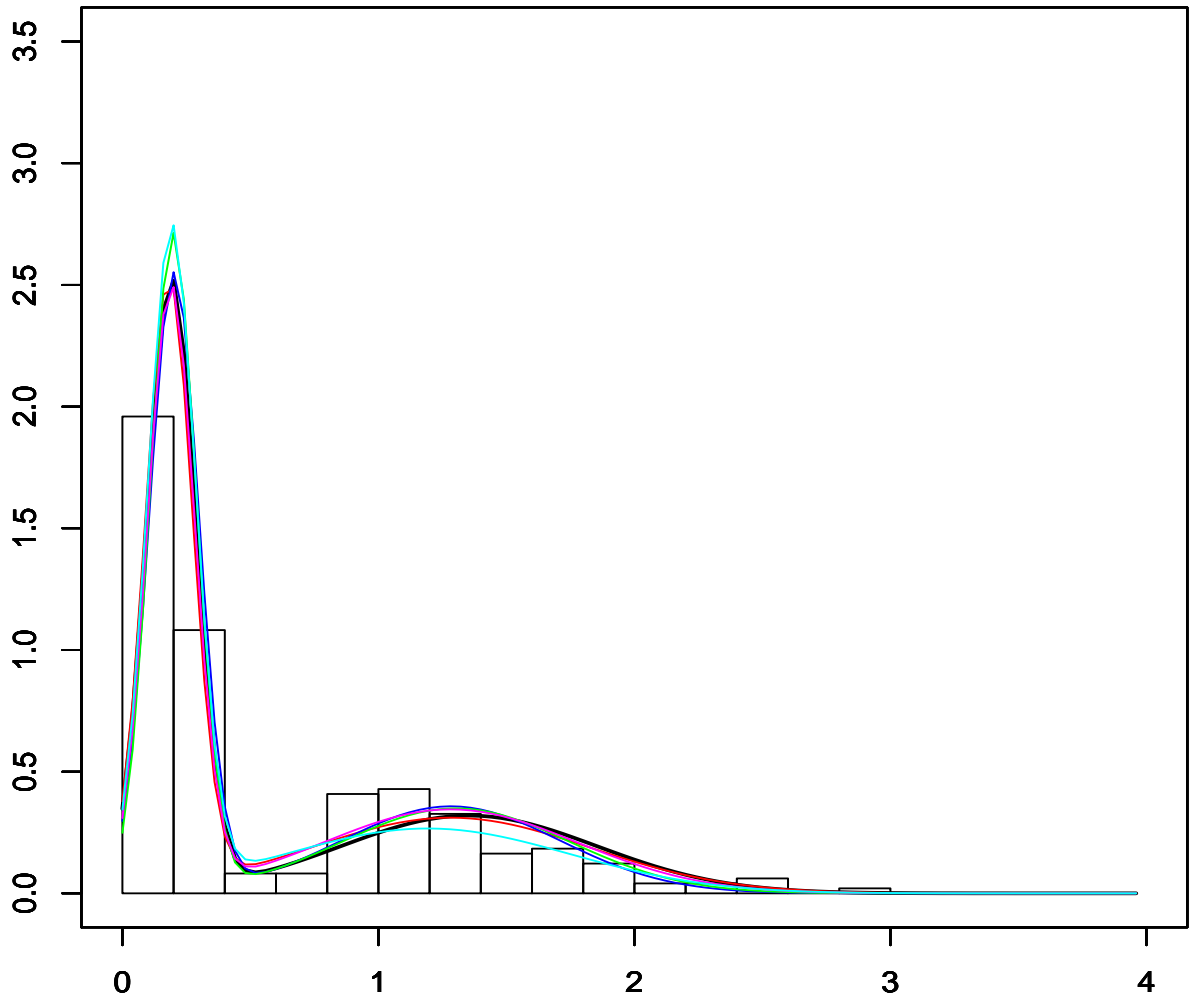


Figure 7.2: **TTMCMC for the enzyme data:** Goodness of fit of the posterior distribution of densities (coloured curves) to the observed data (histogram). The thick black curve is the modal density and the other coloured curves are some densities contained in the 95% HPD.

and $\eta_2 = 0.0080$, which are very small, indicating very good convergence.

With the chosen scales our implementation took 1 minute and 43 seconds to yield 10,000 realizations following a burn-in of 300,000 iterations, after storing one in 150 iterations out of further 15,000,000 iterations after the burn-in period. The overall acceptance rate turned out to be 0.198572, and the birth, death, no-change rates turned out to be 0.000795, 0.000842 and 0.593601, respectively.

The trace plots of k, ν_1^*, τ_1^* and ω_1 , shown in Figure 7.3, again indicate quite good mixing properties and are consistent with the conclusions of our proposed credible region based convergence assessment criterion.

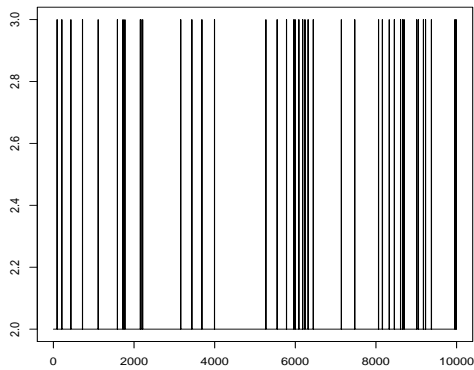
With our prior structure here the posterior distribution of k again strongly favoured 2 and 3 components, with $k = 2$ receiving significantly larger posterior mass 0.9941 compared to the posterior probability of $k = 3$. The reason for the strong support for bimodality can be attributed to the large size of the data contained in the relatively small interval (2, 8).

The modal density and sample densities falling in the 95% HPD region, overlapped on the histogram of the observed data are shown in Figure 7.4. Once again, good fit to the data is indicated.

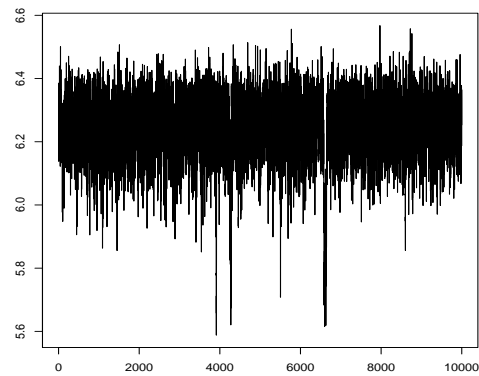
7.5 Galaxy data

In contrast with the previous two cases of the enzyme and the acidity data, the galaxy data, which is much more sparse and seems to exhibit far greater number of modes, seems to be much more challenging to analyze. Thus, we consider a somewhat different prior structure to reflect our beliefs regarding the Bayesian mixture analysis.

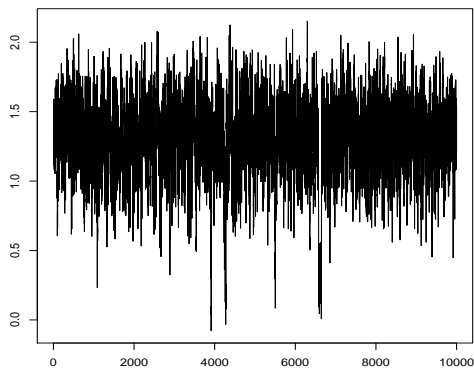
Here, following Bhattacharya (2008) we set $s = 4.0$; $S = 2$; $\nu_0 = 20$; $\psi = 33.3$. However, unlike the previous two cases here we assume that $\omega_j \sim \log(\mathcal{G}(5, 1))$, so that π follows the Dirichlet distribution with all the parameters equal to 5. The prior mean and mode of π_j associated with this Dirichlet distribution are $1/k$ and the variance is $(k - 1)/6k^2$. Note that the mean and the variance of the uniform Dirichlet distribution, which corresponds to taking all the parameters equal to 1, are $1/k$ and $(k - 1)/\{k(k + 1)\}$, respectively. Hence, for large k , the variance of our



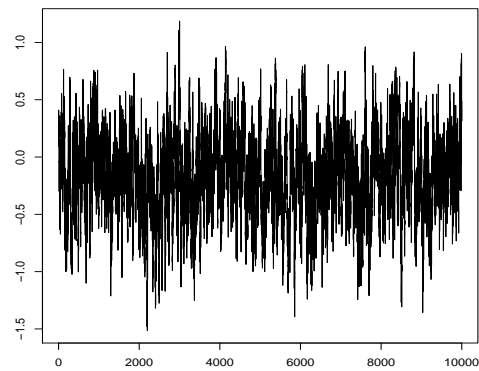
(a) Trace plot of k .



(b) Trace plot of ν_1^* .



(c) Trace plot of τ_1^* .



(d) Trace plot of ω_1 .

Figure 7.3: **TTMCMC for the acidity data:** Trace plots of k , ν_1^* , τ_1^* and ω_1 .

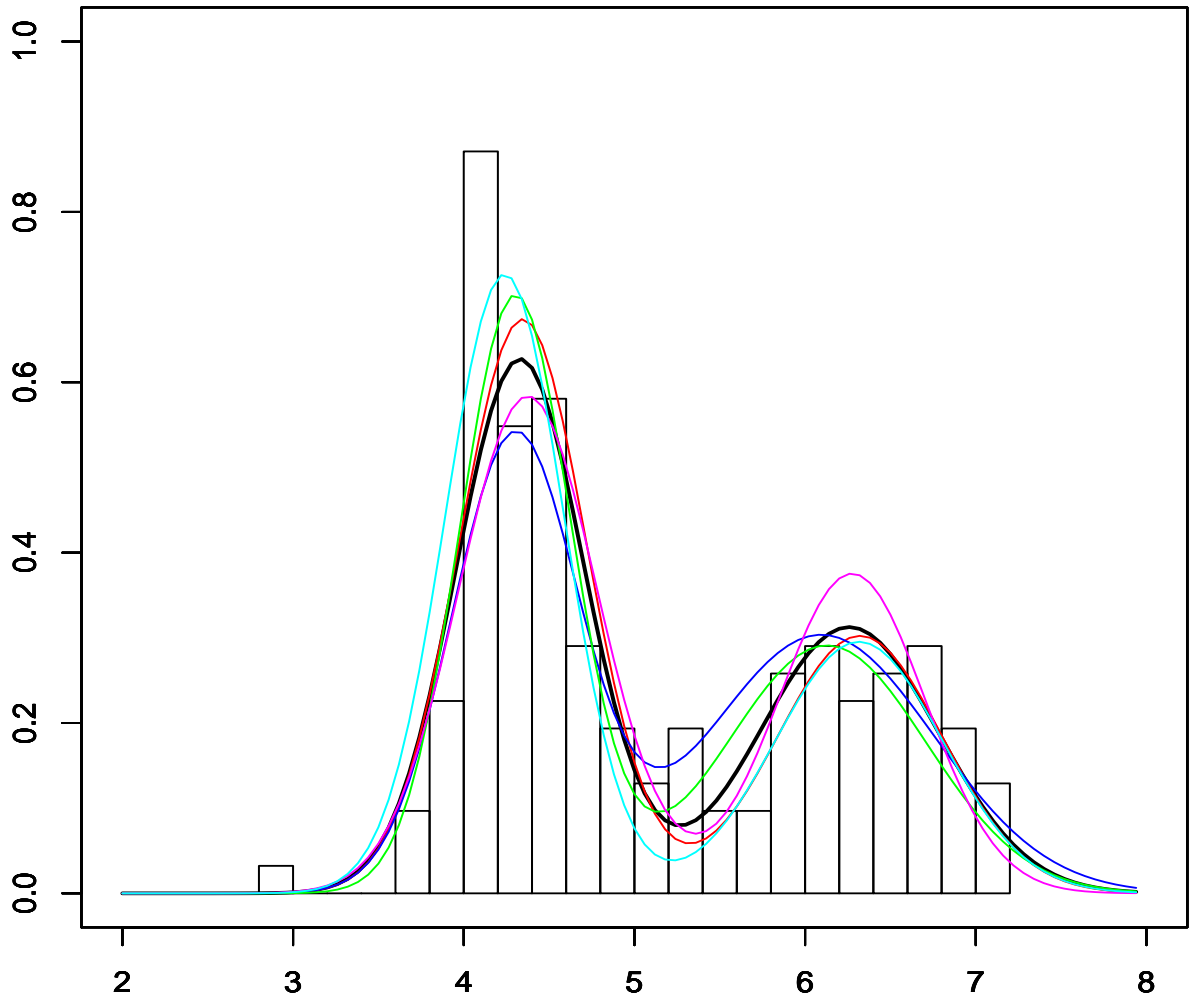


Figure 7.4: **TTMCMC for the acidity data:** Goodness of fit of the posterior distribution of densities (coloured curves) to the observed data (histogram). The thick black curve is the modal density and the other coloured curves are some densities contained in the 95% HPD.

prior distribution is about $1/6$ times that of the uniform Dirichlet. This lesser variability ensures that the minor local modes receive non-negligible prior weights, and hence makes sense in this galaxy data scenario. As regards the prior on k , here we choose a discretized normal distribution on $\{1, \dots, 30\}$ with mean 15 and variance 50. This reflects our belief that although all the values in $\{1, \dots, 30\}$ receive significant prior masses, relatively large number of components is preferable in this application where many local modes are exhibited by the data.

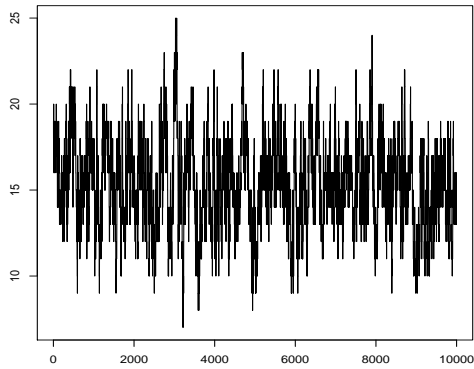
In this application, following the previous convergence diagnostic method, we found the appropriate scales to be $a_{\nu_j^*} = a_{\tau_j^*} = a_{\omega_j} = 1$ for $j = 1, \dots, k$. These scales correspond to $\eta_1 = 0.01657$ and $\eta_2 = 0.01039$, which indicate good convergence. Here the overall acceptance rate, computed over 18,000,000 iterations, turned out to be 0.036388, while the birth, death and no-change rates are 0.007517, 0.007559 and 0.094195, respectively.

The implementation of TTMC in this application took 6 minutes and 33 seconds to yield 10,000 realizations after discarding a burn-in of 300,000 iterations, and then storing one iteration in every 150 iterations out of further 15,000,000 iterations following the burn-in period.

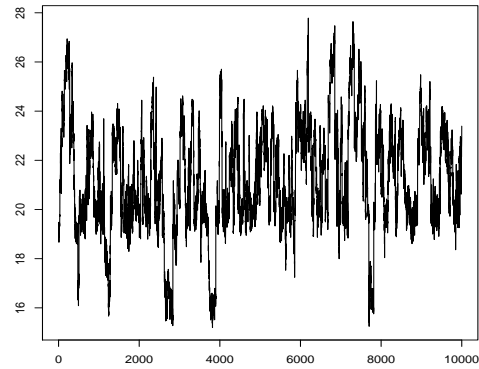
Note that, even in this challenging galaxy data application, the trace plots turned out to be quite reasonable, as shown in Figure 7.5. Thus, reasonable overall mixing behavior of the TTMC chain is indicated by the trace plots, consistent with the results of our credible region based convergence assessment criterion.

In this problem the posterior distribution of k turned out to be much more variable than in the previous two cases. Here $k \in \{7, 8, 9, 10, 11, 12, 13, 14, 15, 16, 17, 18, 19, 20, 21, 22, 23, 24, 25\}$ with respective probabilities $\{0.0002, 0.0005, 0.0059, 0.0191, 0.0455, 0.0784, 0.1044, 0.1371, 0.1596, 0.1457, 0.1115, 0.0869, 0.0513, 0.0277, 0.0128, 0.0097, 0.0018, 0.0016, 0.0003\}$. Thus most of the possible values of k received positive posterior masses. It is also difficult to single out any particular value of k that is very strongly favoured by the posterior, unlike the previous two applications.

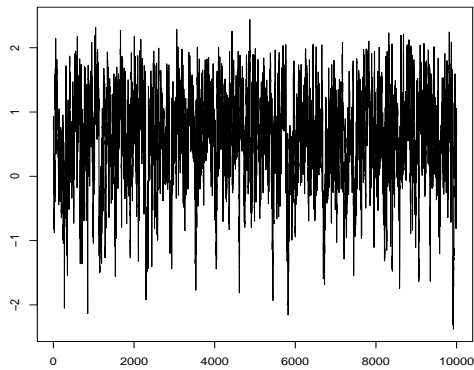
Figure 7.6 depicts the modal density and sample densities falling in the 95% HPD region, overlapped on the histogram of the observed data. The fit to the data seems to be quite encouraging with the sample densities capturing even the minor modes located at the extreme ends of the support of the data.



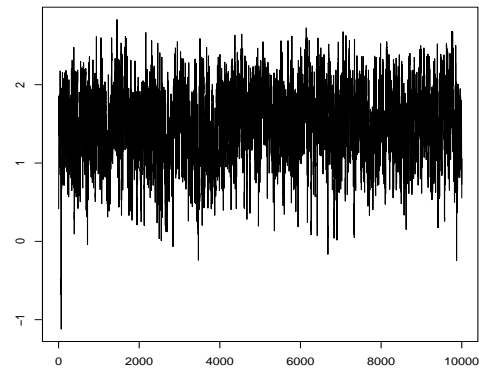
(a) Trace plot of k .



(b) Trace plot of ν_1^* .



(c) Trace plot of τ_1^* .



(d) Trace plot of ω_1 .

Figure 7.5: **TTMCMC for the galaxy data:** Trace plots of k , ν_1^* , τ_1^* and ω_1 . Good mixing behavior of the TTMCMC chain is exhibited by the above panels.

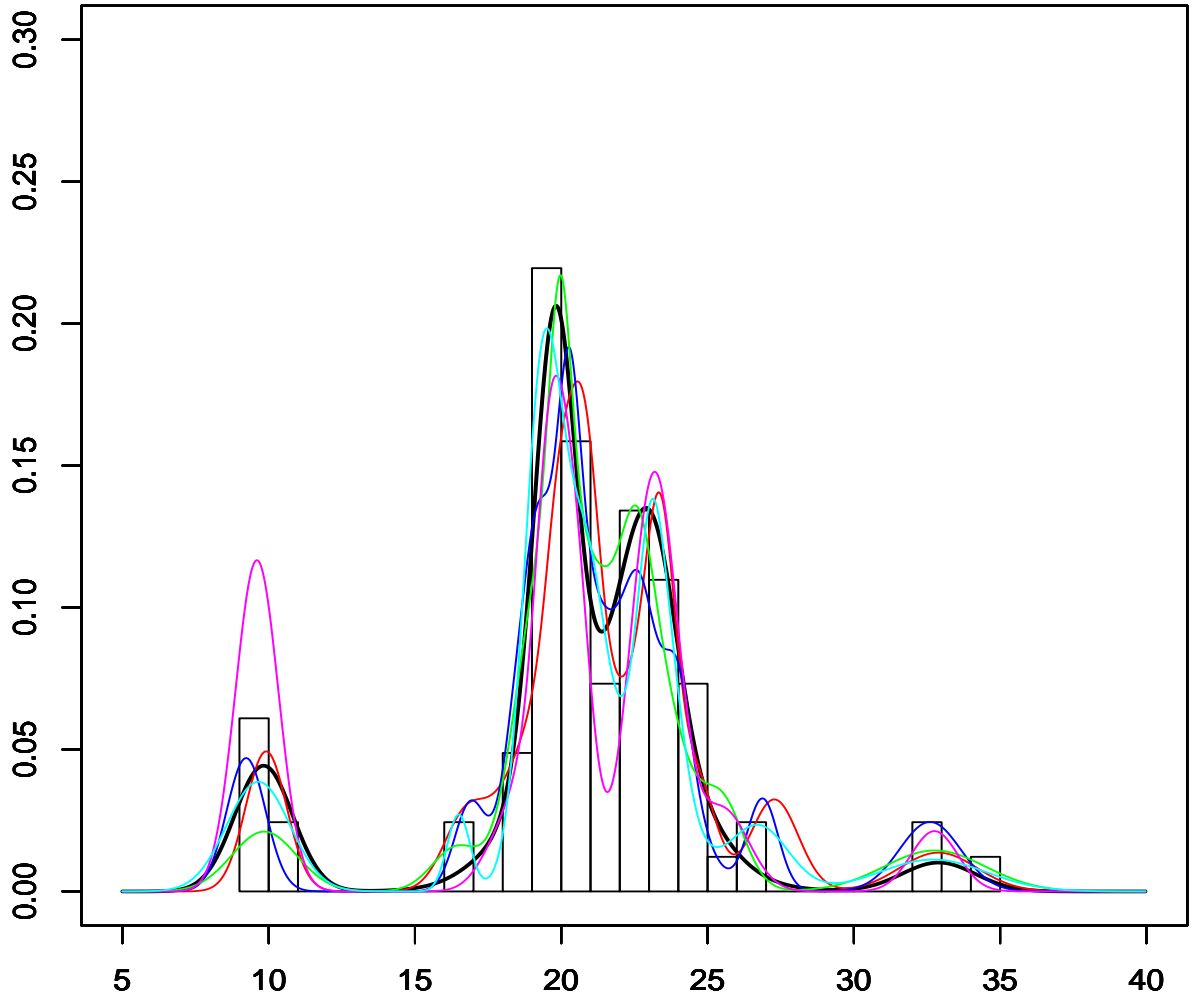


Figure 7.6: **TTMCMC for the galaxy data:** Goodness of fit of the posterior distribution of densities (coloured curves) to the observed data (histogram). The thick black curve is the modal density and the other coloured curves are some densities contained in the 95% HPD.

7.6 **Comparison of TTMCMC with random walk RJMCMC with respect to the three real data sets**

To save space, we have provided the details of the comparisons in Section S-10 of the supplement. Briefly, in all the three examples, random walk RJMCMC places much higher posterior mass to large number of components that are very implausible. The reason for this can be attributed to the product of the left truncated standard normal densities that features in the denominator of the acceptance ratio of the birth move of RJMCMC; since the aforementioned densities are bounded above by 1, this makes the acceptance rate for the birth move exceeding large, which, in effect, seriously slows down convergence. In addition, for the somewhat challenging galaxy data set, the random walk RJMCMC chain has extremely poor acceptance rate, and the chain hardly moved. Recall that this was the case for all the four gamma mixture examples as well. Thus, random walk RJMCMC completely fails to act as the default RJMCMC algorithm.

7.7 **Relevance of autocorrelation plots for convergence diagnosis in variable dimensions**

Convergence assessment with the help of autocorrelations is not always appropriate in variable dimensional MCMC algorithms. Since there is no fixed Euclidean structure, parameters may not retain the same meaning throughout the iterations. To proceed with autocorrelation plots, it is necessary to focus attention on those parameters which retain constant interpretation across all models. In the mixture case the number of components may be considered. In this regard, the autocorrelation plots presented in Figure S-4 of the supplement reveal far superior mixing of the k -chain obtained by our TTMCMC sampler compared to random walk RJMCMC for all the three real data sets. In particular, for the galaxy data set, the RJMCMC based autocorrelations are simply hopeless!

7.8 **Comparison between TTMCMC and RJMCMC when the prior of Richardson and Green (1997) is considered**

Further comparisons between TTMCMC and RJMCMC with respect to the prior structure and the algorithm of Richardson & Green (1997), are provided in Section S-10 of the supplement,

in the context of the challenging galaxy data. We argue that actually their prior structure, where τ are made dependent in a way that they are approximately of the same size, is not expected to provide good fit to the observed histogram, but the large number of components supported by their algorithm as a result of its inherent bias as discussed, create the appearance of good fit. We further argue that the prior structure of Cappé, Robert & Rydén (2003), which is essentially the prior of Richardson & Green (1997) but τ are independent *a priori*, is a more appropriate prior for capturing the varieties of modes in the galaxy data.

8. TTMC MC FOR MULTIVARIATE NORMAL MIXTURES

We now consider *iid* p -variate data $\{\mathbf{y}_i = (y_{i1}, \dots, y_{ip})^T; i = 1, \dots, n\}$ arising from the p -variate normal mixture having the following density when the number of components is k : for $i = 1, \dots, n$,

$$f(\mathbf{y}_i | \Theta_k) = \sum_{j=1}^k \pi_j \frac{1}{(2\pi)^{p/2} |\Sigma_j|^{1/2}} \exp \left\{ -\frac{1}{2} (\mathbf{y}_i - \boldsymbol{\mu}_j)^T \boldsymbol{\Sigma}^{-1} (\mathbf{y}_i - \boldsymbol{\mu}_j) \right\}, \quad (8.1)$$

where $\Theta_k = \{\boldsymbol{\mu}_1, \dots, \boldsymbol{\mu}_k, \boldsymbol{\Sigma}_1, \dots, \boldsymbol{\Sigma}_k, \pi_1, \dots, \pi_k\}$.

Letting $\bar{\mathbf{y}}$ denote the p -dimensional sample mean vector and $\mathbf{S} = \text{diag} \{s_1^2, \dots, s_p^2\}$ denote the diagonal matrix with the sample variances in the diagonal, we transform the data y_i , following Dellaportas & Papageorgiou (2006), to $\mathbf{S}^{-1/2} (\mathbf{y}_i - \bar{\mathbf{y}})$, once the data are generated.

8.1 Prior structure

Following Dellaportas & Papageorgiou (2006), we assume that *a priori*

$$[\boldsymbol{\mu}_j | \boldsymbol{\Sigma}_j] \sim N_p(\mathbf{0}, \boldsymbol{\Sigma}_j), \quad (8.2)$$

a p -variate normal with mean $\mathbf{0}$ and covariance matrix $\boldsymbol{\Sigma}_j$. We also assume following Dellaportas & Papageorgiou (2006) that

$$[\boldsymbol{\Sigma}_j] \sim W^{-1}(p+1, \boldsymbol{\Omega}), \quad (8.3)$$

an inverse-Wishart distribution with $(p+1)$ degrees of freedom and diagonal matrix $\boldsymbol{\Omega}$. However, instead of considering the gamma prior on the diagonal elements of $\boldsymbol{\Omega}$ as in Dellaportas & Papageorgiou (2006), we set all the diagonal elements equal to 1. This we do to avoid oversmoothness

induced by the dependence structure between the $\Sigma_j; j = 1, \dots, k$, and to facilitate adaptive learning from the data. Recall that (see Section 7.8) a similar issue of oversmoothness seems to render the prior of Richardson & Green (1997) less appropriate for capturing the varieties of modes as compared to the prior of Cappé et al. (2003), in the univariate normal mixture case.

As before, we consider a discrete uniform prior for k on $\{1, 2, \dots, 30\}$. Here we remark that although Dellaportas & Papageorgiou (2006) also report a discrete uniform prior on k , they did not specify the range.

8.2 TTMCMC strategy for multivariate situations

As before we reparameterize π_j as $\exp(w_j) / \sum_{i=1}^k \exp(w_i)$. As for Σ_j , we consider the Cholesky decomposition $\Sigma_j = \mathbf{L}\mathbf{L}^T$, where $\mathbf{L} = (L_{rs})_{r,s=1,\dots,p}$ is the appropriate lower triangular matrix. Thus, there are $1+p+p(p+1)/2$ number of parameters to be split in any given birth move given that the j -th mixture component is chosen; w_j , the p components of $\boldsymbol{\mu}_j = (\mu_{j1}, \dots, \mu_{jp})^T$ and $p(p+1)/2$ non-zero elements of \mathbf{L}_j . Thus, we need $1+p+p(p+1)/2$ ϵ 's to define our additive TTMCMC move types. The Jacobian of the birth move is given $2^{1+p+p(p+1)/2} \times a_{w_j} \times \prod_{r=1}^p a_{\mu_{jr}} \prod_{r \geq s=1}^p a_{L_{jrs}}$, where $a_{\mu_{jr}}$ is the scale for the additive transformation of the r -th component of $\boldsymbol{\mu}_j$ and $a_{L_{jrs}}$ is the same for the (r, s) -th element of \mathbf{L}_{jrs} , where $r \geq s$. The Jacobian for the death move is the inverse of that of the birth move with the relevant scale values. We reject the entire move if any of the diagonal elements of \mathbf{L} becomes negative.

8.3 Simulation experiment with $p = 3$

Following Dellaportas & Papageorgiou (2006) we set generate 80, 100 and 100 data points from 3-

variate normal distributions with means $\boldsymbol{\mu}_1 = (6, 4, 2)^T$, $\boldsymbol{\mu}_2 = (-11, -4, -1)^T$, $\boldsymbol{\mu}_3 = (-7, -11, -5)^T$ and covariance matrices $\Sigma_1 = \begin{pmatrix} 3 & 2 & 1 \\ 2 & 5 & 0 \\ 1 & 0 & 4 \end{pmatrix}$, $\Sigma_2 = \begin{pmatrix} 2 & -1.5 & 1 \\ -1.5 & 5 & 2 \\ 1 & 2 & 3 \end{pmatrix}$, $\Sigma_3 = \begin{pmatrix} 5 & -1 & 1 \\ -1 & 4 & -2 \\ 1 & -2 & 3 \end{pmatrix}$,

respectively, and fit our 3-variate mixture model to the data assuming unknown number of components.

Considering a burn-in of 3,000,000 iterations, we ran the TTMCMC algorithm for a further

3,000,000 iterations, storing one in 300 iterations, to obtain 10,000 realizations from the posterior. The implementation took 49 minutes and 14 seconds on our laptop. The overall acceptance rate turned out to be 0.038231 when the scales of the additive transformations are set to be 0.05 and 0.05 for the means and the elements of the Cholesky factors, and 0.5 for the weights. The birth, death and the no-change rates are 0.000002, 0.000015 and 0.114539, respectively. The trace plots shown in Figure 8.1 confirm excellent convergence properties of our algorithm, even in the multivariate case. Importantly, we obtained point mass at the true number of mixture components (as before, we do not rule out the possibility of missing some component other than 3 in our finite TTMC run). In contrast, Dellaportas & Papageorgiou (2006) report 6 models associated with $k = 1, \dots, 6$, with 3 components receiving 0.9493 posterior probability.

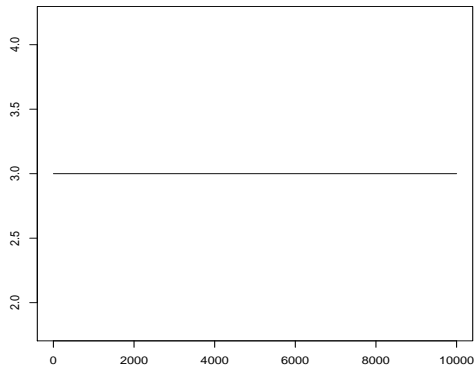
Figure 8.2 depicts the modal density and sample densities falling in the 95% HPD region, overlapped on the histogram of the first component $\{y_{i1}; i = 1, \dots, n\}$ (here $n = 280$) of the observed data. Excellent fit to the data is clearly indicated.

8.4 Simulation experiment with $p = 10$

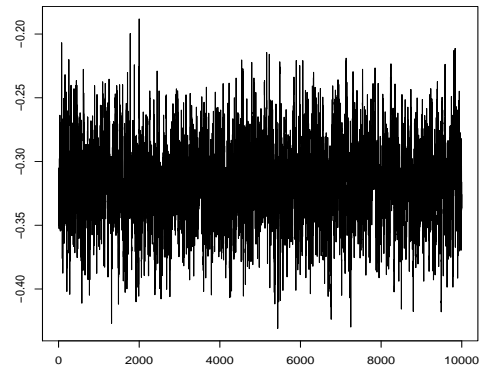
We now consider application of TTMC to mixtures of $p = 10$ dimensional multivariate normals. Specifically, we first generate two mean vectors $\boldsymbol{\mu}_1$ and $\boldsymbol{\mu}_2$ from two 10-dimensional, normal distributions $N_{10}(4\mathbf{1}_{10}, \mathbf{I}_{10})$ and $N_{10}(-5\mathbf{1}_{10}, \mathbf{I}_{10})$, where, for any integer $p \geq 1$, $\mathbf{1}_p$ is a d -component vector with each component 1, and \mathbf{I}_p is the identity matrix of order p . Corresponding to the mean vectors $\boldsymbol{\mu}_1$ and $\boldsymbol{\mu}_2$, we specify covariance matrices $\boldsymbol{\Sigma}_1$ and $\boldsymbol{\Sigma}_2$ of the following form: the off-diagonal elements are given by $\sigma_j^2 \rho$ and the diagonal elements are all equal to σ_j^2 , for $j = 1, 2$. For our illustration we consider $\sigma_1^2 = 4$, $\sigma_2^2 = 3$ and $\rho = 0.5$.

We then generate 300 realizations from $N_{10}(\boldsymbol{\mu}_1, \boldsymbol{\Sigma}_1)$ and 300 realizations from $N_{10}(\boldsymbol{\mu}_2, \boldsymbol{\Sigma}_2)$, which constitute our data set $\{\mathbf{y}_1, \dots, \mathbf{y}_{600}\}$ of size 600.

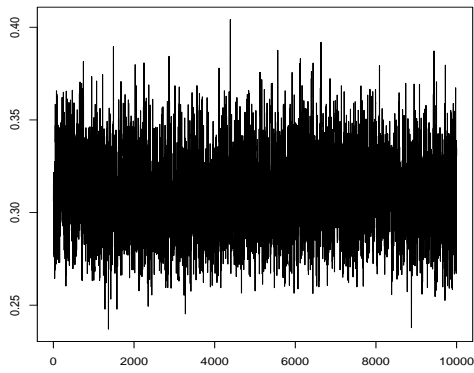
We use the same TTMC algorithm as in the 3-dimensional experiment, but as to be anticipated for higher dimensions, the convergence was slower compared to the 3-dimensional example. To improve mixing, we employed the following strategy. At the end of each iteration $t \geq 1$, we simulated $r^{(t)} \sim N(0, 1)$ and proposed the further additive transformation $\boldsymbol{\Theta}^{(t)} \mapsto \boldsymbol{\Theta}^{(t)} + \mathbf{a}r^{(t)}$,



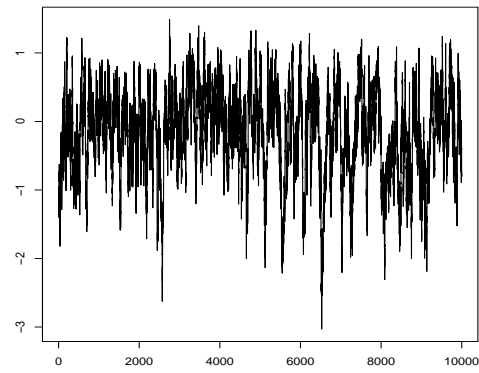
(a) Trace plot of k .



(b) Trace plot of μ_{11} .



(c) Trace plot of L_{11} .



(d) Trace plot of ω_1 .

Figure 8.1: **TTMCMC for 3-dimensional case:** Trace plots of k , μ_{11} , L_{11} and ω_1 . Good mixing behavior of the TTMCMC chain is exhibited by the above panels.

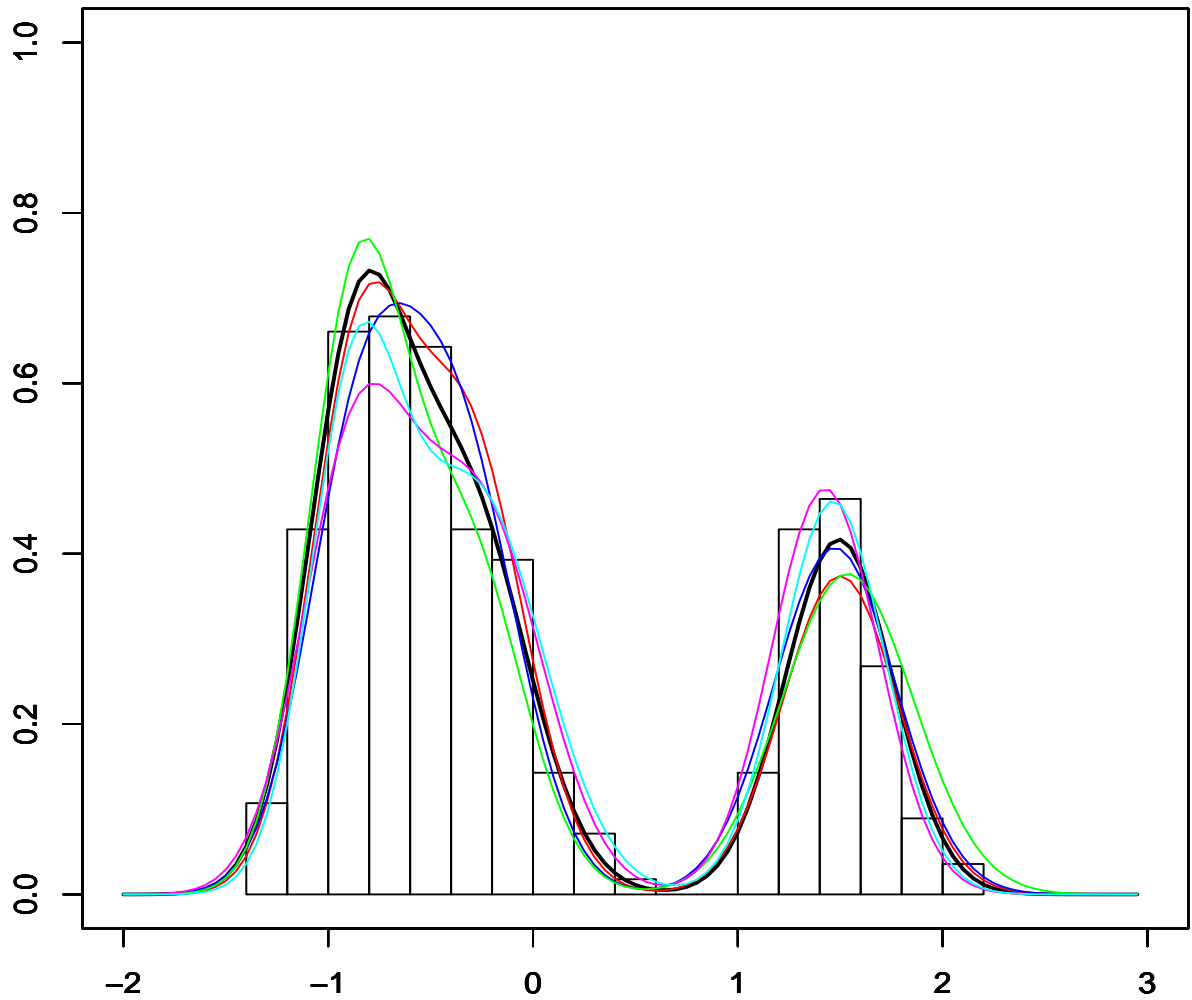


Figure 8.2: **TTMCMC for 3-dimensional case:** Goodness of fit of the posterior distribution of densities (coloured curves) to the histogram of the first component of the observed data $\{y_{i1}; i = 1, \dots, 285\}$. The thick black curve is the modal density and the other coloured curves are some densities contained in the 95% HPD.

where $\Theta^{(t)}$ denotes the stage of the parameters at iteration t , and \mathbf{a} denotes the vector of scaling constants for the additive transformation. We then calculated the acceptance probability of this proposal in the usual TMCMC set-up to either accept the new proposal $\Theta^{(t)} + \mathbf{a}r^{(t)}$ or to remain at $\Theta^{(t)}$. Such a strategy has also been employed by Mukhopadhyay & Bhattacharya (2013) to improve mixing in the context of palaeoclimate modeling. The strategy is akin to the so-called generalized Gibbs/MH methods in fixed-dimensional set-ups have the potential of improving mixing (see, for example, Liu et al. (2000), Liu (2001); see also Liu & Yu (1999)). Further details can be found in the supplement of Dutta & Bhattacharya (2014).

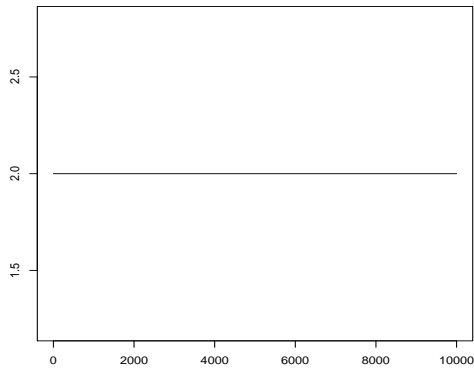
For our purpose, we chose the scales of the additive transformation associated with the original TTMCMC to be relatively large; 0.5 for the means, 0.05 for the Cholesky components and 1.5 for the weights, while for the mixing improvement step we chose the scales to be 1/10-th of the above scales. This ensures relatively small acceptance rate but large moves for the original TTMCMC steps but much higher acceptance rate at the mixing improvement step.

However, in spite of the above strategy, the mixing improvement was not dramatic in our case, and still a considerably long run was necessary. As such, we discarded the first 3×10^7 iterations, and stored one in 300 iterations out of the next 12×10^7 iterations to store 4×10^5 iterations. We applied further thinning of size 40 to the stored samples, finally storing 10,000 iterations. The entire procedure took about 68 hours on our VMWare. The overall acceptance rate, birth rate, death rate and the no-change rates in this implementation are 0.008173, 0.00014, 0.00037 and 0.023949, respectively.

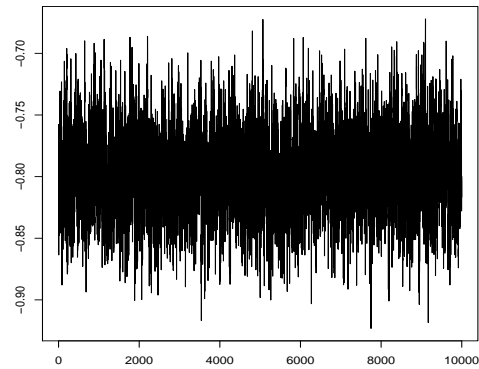
The trace plots and the goodness of fit (for the first co-ordinate of the 10-dimensional data) diagram shown in Figures 8.3 and 8.4 vindicate satisfactory performance of our method, in spite of high dimensionality. Importantly, the correct number of components, namely, $k = 2$ has been identified correctly.

8.5 Simulation experiment with $p = 20$

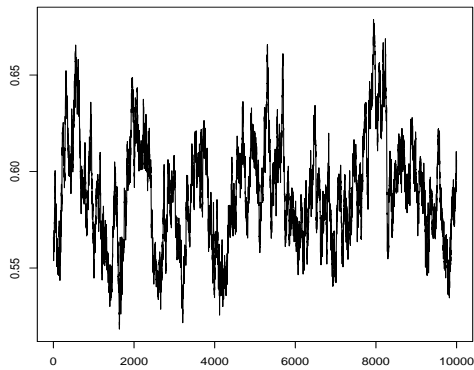
We conduct a further experiment, now with dimension $p = 20$. Our data generation mechanism remains the same as in Section 8.4, only the dimension is increased from $p = 10$ to $p = 20$. Our



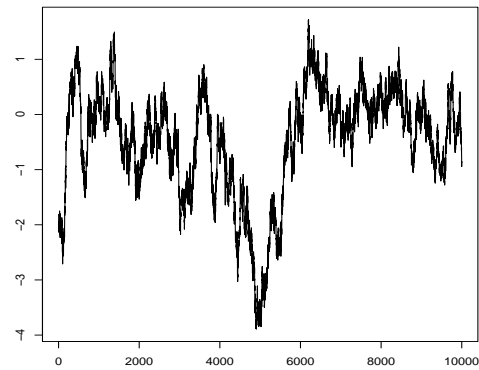
(a) Trace plot of k .



(b) Trace plot of μ_{11} .



(c) Trace plot of L_{11} .



(d) Trace plot of ω_1 .

Figure 8.3: **TTMCMC for 10-dimensional case:** Trace plots of k , μ_{11} , L_{11} and ω_1 . Adequate mixing behavior of the TTMCMC chain is exhibited by the above panels.

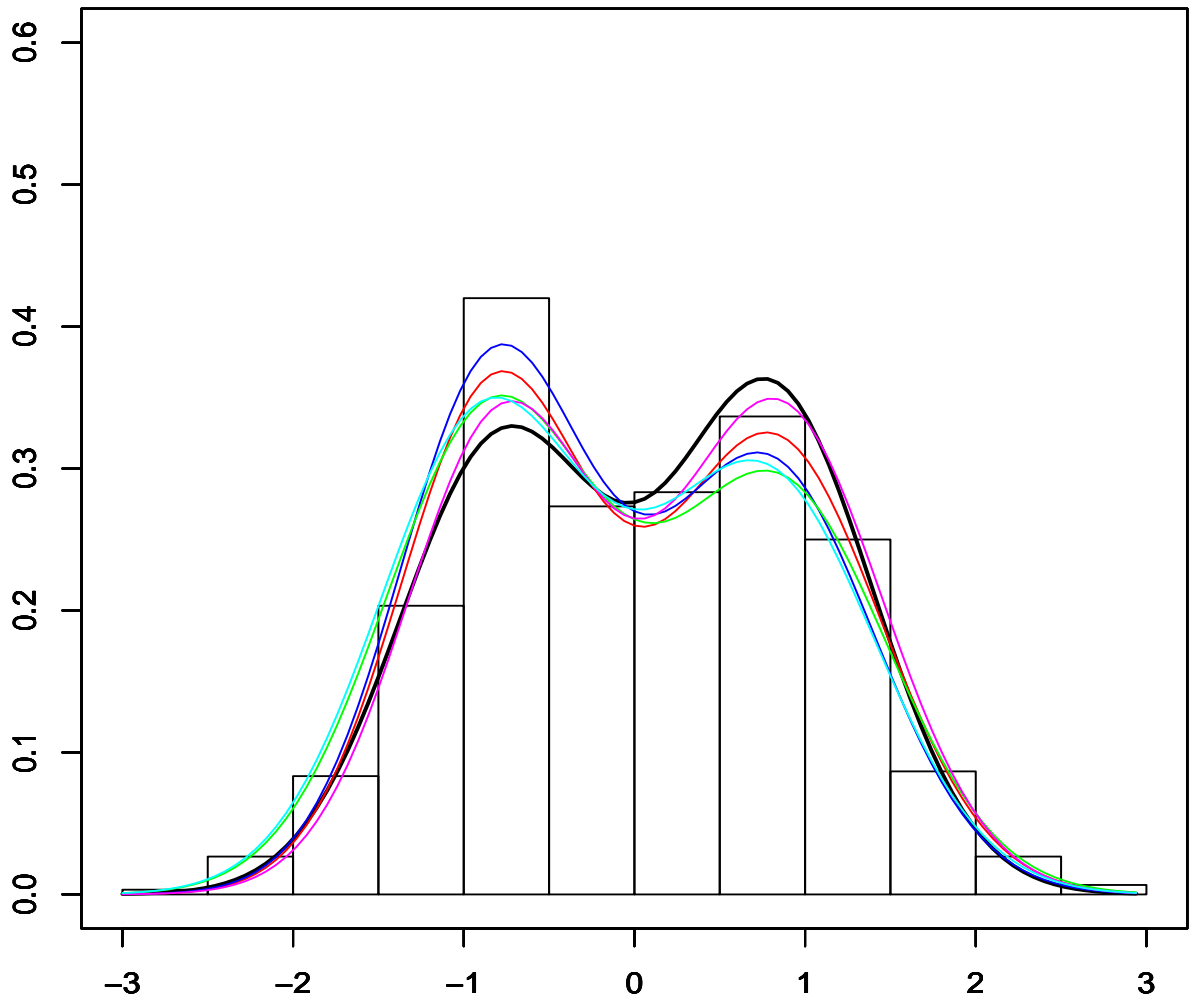


Figure 8.4: **TTMCMC for 10-dimensional case:** Goodness of fit of the posterior distribution of densities (coloured curves) to the histogram of the first component of the observed data $\{y_{i1}; i = 1, \dots, 600\}$. The thick black curve is the modal density and the other coloured curves are some densities contained in the 95% HPD.

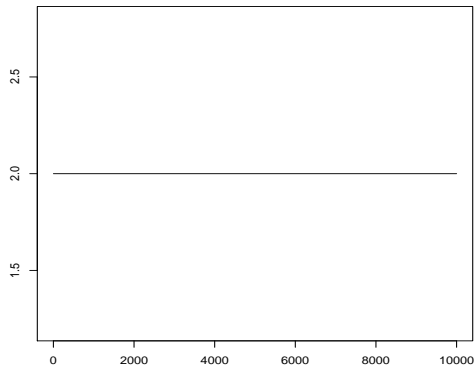
TTMCMC algorithm also remains almost the same, with the same mixing improvement strategy. We again obtain 10,000 samples by thinning from a total of 15×10^7 iterations. In this case, the overall acceptance rate, birth rate, death rate and the no-change rate are 0.00741, 0.00019, 0.000421 and 0.02163, respectively. The time taken is 136 hours and 44 minutes. The trace plots and the goodness-of-fit diagram depicted in Figures 8.5 and 8.6 once again speak in favour of our ideas, in particular, the great automation of our method, irrespective of dimensions.

9. CONCLUSION

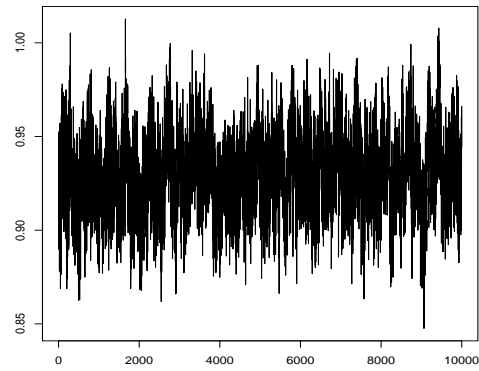
The transformation based concepts of TCMCMC in the fixed-dimensional set-up has led to the interesting variable-dimensional counterpart TTMCMC just as the traditional Metropolis-Hastings methodology has led to RJMCMC. Consequently, the advantages of TCMCMC over Metropolis-Hastings are expected to carry over to TTMCMC as compared to RJMCMC. Indeed, as we demonstrated in this paper, TTMCMC is simple to implement, can update all the (variable number of) parameters in a single block while maintaining reasonable acceptance rates thanks to drastic effective reduction of the dimensionality. In fact, TTMCMC effectively reduces the variable dimensional problem to a fixed dimensional problem involving a single ϵ or just a few, fixed number of ϵ 's, given any move type within the birth, death or no-change moves. The block updating strategy of TTMCMC using ϵ or a few ϵ 's also ensures huge computational savings. Furthermore, the mixture-type proposal distributions associated with TTMCMC ensures reasonable mixing properties.

There are three key features that manifested themselves in our comparative studies on TTMCMC and RJMCMC. First, TTMCMC yields reasonable acceptance rates, which are larger than those of RJMCMC for the same scales of the additive transformations. Importantly, in the gamma mixtures and the galaxy example, RJMCMC yields extremely poor acceptance rate, while that of TTMCMC is quite reasonable, for the same scales.

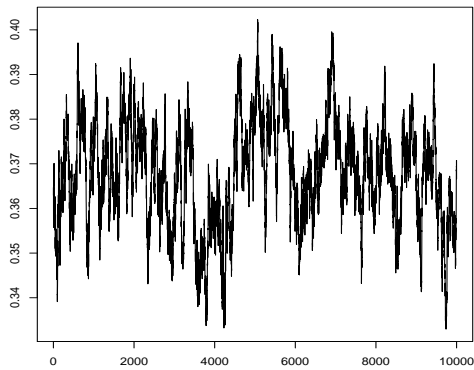
Second, ensuring reasonable mixing is a very challenging issue in variable dimensional problems. Here TTMCMC outperforms RJMCMC very significantly in all the cases, as vindicated by the autocorrelation plots shown in Figure S-4 of the supplement. In other words, even in univariate situations, the random walk RJMCMC completely fails to compete with TTMCMC.



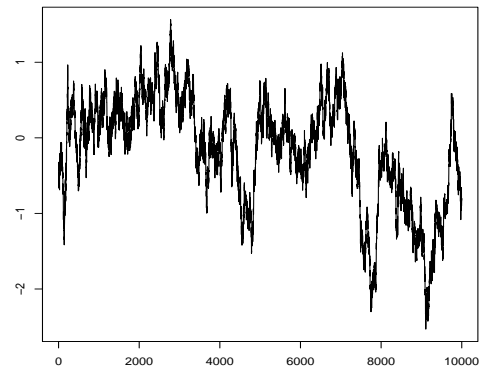
(a) Trace plot of k .



(b) Trace plot of μ_{11} .



(c) Trace plot of L_{11} .



(d) Trace plot of ω_1 .

Figure 8.5: **TTMCMC for 20-dimensional case:** Trace plots of k , μ_{11} , L_{11} and ω_1 . Adequate mixing behavior of the TTMCMC chain is exhibited by the above panels.

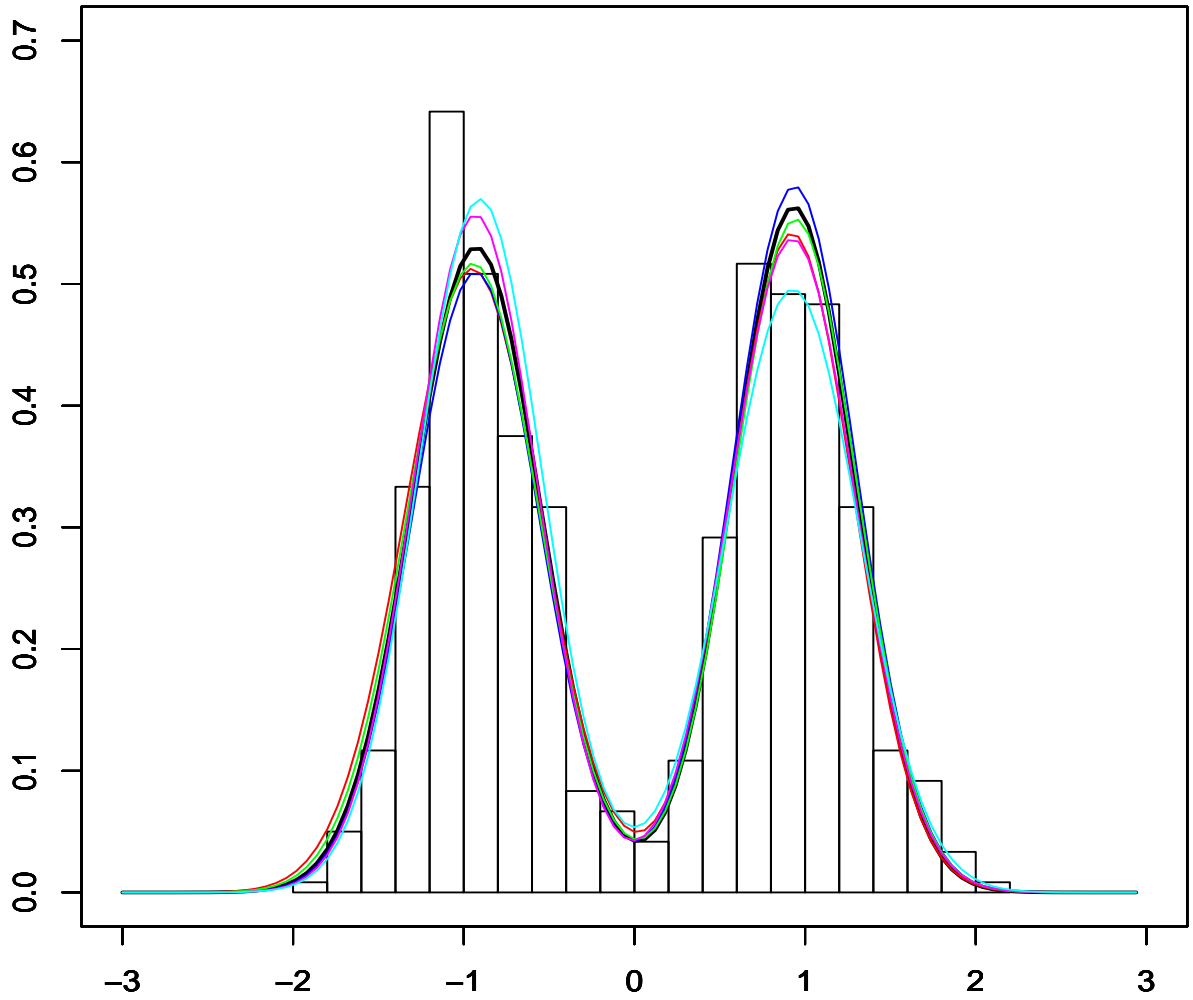


Figure 8.6: **TTMCMC for 20-dimensional case:** Goodness of fit of the posterior distribution of densities (coloured curves) to the histogram of the first component of the observed data $\{y_{i1}; i = 1, \dots, 600\}$. The thick black curve is the modal density and the other coloured curves are some densities contained in the 95% HPD.

Third, it seems to be infeasible to devise appropriate RJMCMC move types in high-dimensional contexts. Indeed, Dellaportas & Papageorgiou (2006) consider a maximum of only 5-dimensional example for RJMCMC application. On the other hand, we have demonstrated that our simple additive TTMCMC works even for dimensions as large as 20. In this regard it is useful to note that the split-merge proposals of Jain & Neal (2004) and Jain & Neal (2007) are perhaps better candidates compared to those of Richardson & Green (1997) and Dellaportas & Papageorgiou (2006) as they update all the allocation variables simultaneously, rather than Gibbs sampling. Since TTMCMC also generally updates all the variables in a single block, the general principles of their algorithm and TTMCMC match. But a key difference is that we do not introduce allocation variables for mixture updation, and hence have much less number of variables to update, which is expected to lead to better acceptance rate in our case. It is also to be noted that the algorithms of Jain & Neal (2004) and Jain & Neal (2007) are devised for mixtures only, not for general variable-dimensional problems. In contrast, our default additive TTMCMC that we used for mixtures can be applied to all variable dimensional problems.

A further issue with RJMCMC is that it tends to support more components than are expected. The main issue responsible for this possible non-convergence is the requirement of dimension-matching for RJMCMC implementation. This condition forces the acceptance ratio for the dimension-changing moves to depend upon the proposal density either via the denominator (birth move) or through the numerator (death move). Thus, unlike fixed-dimensional Metropolis-Hastings, the acceptance ratio is not balanced by the presence of the proposal density in both numerator and denominator. As already remarked in the discussion following Algorithm 3.1, this unbalanced nature of the RJMCMC acceptance ratio causes large number of birth moves if the proposal density is uniformly bounded by 1, as in our examples. Since TTMCMC does not require dimension-matching, it has been possible to free the corresponding acceptance ratio of the proposal density, which, in turn, completely solves the problem of bias towards large number of models in finite number of iterations.

The wisdom that emerges from the investigations and the subsequent analyses is that even the simplest version of TTMCMC, namely, additive TTMCMC, is capable enough of exploring

challenging variable-dimensional posteriors, providing ample support to our claim of automation inherent within TTMC MC. On the other hand, as our implementations show, the corresponding random walk RJMC MC do not measure up at all. In principle, there may exist RJMC MC algorithms which may perhaps perform reasonably in terms of convergence, but at the cost of being problem-specific, complicated, hard-to-implement, and computationally burdensome.

Also, very importantly, as we showed, our simple additive transformation exhibited very decent performance even in dimension as large as 20, thus providing a large boost to our claim of automation. To our knowledge, there exists no instance of RJMC MC that works in such high dimension.

Thus, as per our experiments and knowledge, TTMC MC is remarkably close to automation, while automation for RJMC MC is nowhere in sight.

Apart from developing TTMC MC, we have also proposed, in a separate supplementary material, a general methodology for summarizing the posterior distributions of densities. In particular, we have prescribed a procedure for obtaining the modes and desired HPD regions of the posterior distribution of density functions. Moreover, using these concepts as basis, we have proposed a convergence diagnostic criterion for the underlying TTMC MC algorithm, which is again very generally applicable. The convergence diagnostic method seems to be particularly useful in variable-dimensional contexts, where determining convergence is far more difficult than fixed-dimensional situations. Also, as we demonstrated with our applications, in the absence of optimal scaling theory in variable-dimensional situations, the criterion can provide guidance regarding choices of the scales of default additive TTMC MC.

Our results demonstrate that additive TTMC MC is promising enough to qualify as the default variable-dimensional algorithm. This is also vindicated by the excellent performances of TTMC MC in challenging spatio-temporal problems investigated by these authors and others. In this paper, we restricted ourselves to mixture models because of their high standing in statistics and challenging nature of the associated variable-dimensional problem. However, in a separate paper we shall present detailed comparisons of TTMC MC and RJMC MC with respect to various other variable-dimensional problems. Our investigations are on and we seek to establish TTMC MC as a

far superior alternative compared to RJMCMC.

ACKNOWLEDGMENTS

We are sincerely grateful to the two reviewers whose constructive comments have led to much improvement of this article.

Supplementary Material

Throughout, we refer to our main paper Das & Bhattacharya (2015b) as DB.

S-1. DETAILED BALANCE FOR ALGORITHM 3.1 OF DB

Before providing the proof of detailed balance in the general case, we first illustrate the proof with the example introduced in Section 3.1 of DB.

S-1.1 Detailed balance for the simple example illustrated in Section 3.1 of DB

We assume the additive transformation and set $w_b = w_d = w_{nc} = \frac{1}{3}$. Also, we let $P(z_i = 1) = P(z_i = -1) = p$ and the current state be $\mathbf{x} = (x_1, x_2) \in \mathbb{R}^2$.

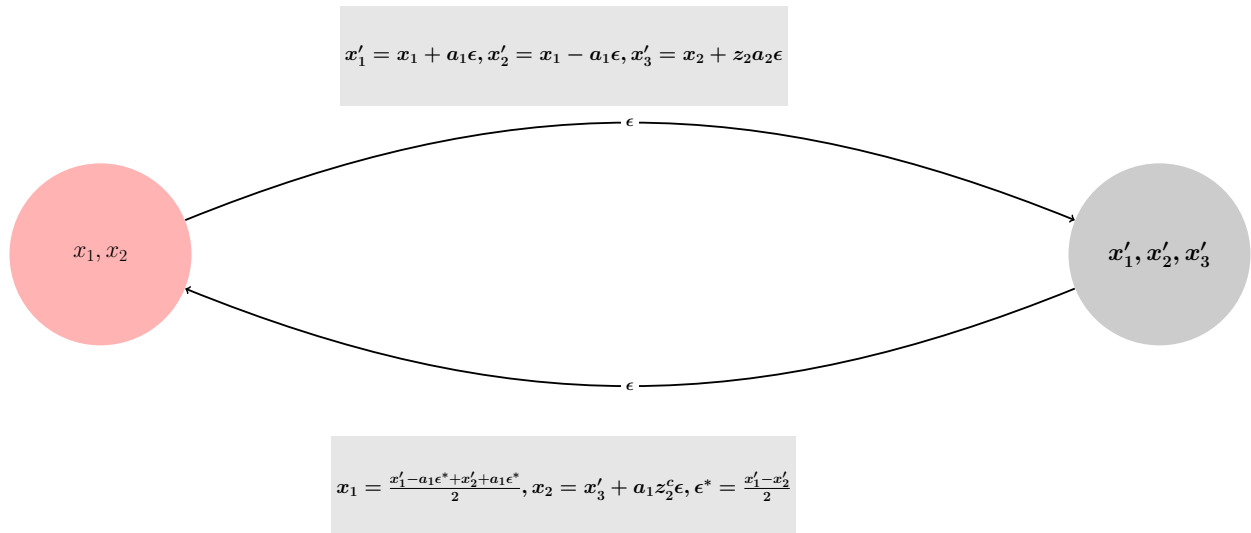


Figure S-1: Detailed balance condition.

Figure S-1 pictorially illustrates the detailed balance criterion. Specifically, according to our

algorithm, the probability of transition $(x_1, x_2) \mapsto (x'_1, x'_2, x'_3)$ is given by:

$$\begin{aligned}
& \pi(x_1, x_2) \times P(\text{birth move}) \times P(\text{selecting one random coordinate from } x_1, x_2) \times \varrho(\epsilon) \\
& \times P(z_2) \times a_b(\mathbf{x}, \epsilon) \\
& = \pi(x_1, x_2) \times \frac{1}{3} \times \frac{1}{2} \times \varrho(\epsilon) \times p \\
& \times \min \left\{ 1, \frac{1}{3} \times \frac{\pi(x'_1, x'_2, x'_3)}{\pi(x_1, x_2)} \times \left| \frac{\partial(x'_1, x'_2, x'_3)}{\partial(x_1, x_2)} \right| \right\} \\
& = \varrho(\epsilon) \min \left\{ \pi(x_1, x_2) \times p \times \frac{1}{6}, \pi(x'_1, x'_2, x'_3) \times p \times \frac{1}{18} \times 2a_1 \right\}. \tag{S-1.1}
\end{aligned}$$

For detailed balance to hold, we must be able to return from (x'_1, x'_2, x'_3) to (x_1, x_2) . The required transition, associated with the death move, has the following probability:

$$\begin{aligned}
& \pi(x'_1, x'_2, x'_3) \times P(\text{death move}) \times P(\text{selecting } x'_1, x'_2) \times \varrho(\epsilon) \\
& \times P(z_2^c) \times \left| \frac{\partial(x'_1, x'_2)}{\partial(x_1^*, \epsilon^*)} \right| \times a_d(\mathbf{x}', \epsilon, \epsilon^*) \\
& = \pi(x'_1, x'_2, x'_3) \times \frac{1}{3} \times \frac{1}{3 \times 2} \times \varrho(\epsilon) \times p \times 2a_1 \\
& \times \min \left\{ 1, 3 \times \frac{\pi(x_1, x_2)}{\pi(x'_1, x'_2, x'_3)} \times \left| \frac{\partial(x_1, x_2, \epsilon^*, \epsilon)}{\partial(x'_1, x'_2, x'_3, \epsilon)} \right| \right\} \\
& = \varrho(\epsilon) \min \left\{ \pi(x'_1, x'_2, x'_3) \times p \times \frac{1}{18} \times 2a_1, \pi(x_1, x_2) \times p \times \frac{1}{6} \right\}. \tag{S-1.2}
\end{aligned}$$

So, (S-1.1) = (S-1.2), implying that detailed balance holds for birth and death moves. We now prove detailed balance for the general TTMC algorithm.

S-1.2 Proof of detailed balance for the general TTMC algorithm

To see that detailed balance is satisfied for the birth and death moves, note that associated with the birth move, the probability of transition $\mathbf{x} (\in \mathbb{R}^k) \mapsto T_{b,z}(\mathbf{x}, \epsilon) (\in \mathbb{R}^{k+1})$ is given by:

$$\begin{aligned}
& \pi(\mathbf{x}) \times \frac{1}{k} \times w_{b,k} \times \varrho(\epsilon) \times \prod_{i \neq j=1}^k p_i^{I_{\{1\}}(z_i)} q_i^{I_{\{-1\}}(z_i)} \\
& \times \min \left\{ 1, \frac{1}{k+1} \times \frac{w_{d,k+1}}{w_{b,k}} \times \frac{\prod_{i \neq j=1}^k p_i^{I_{\{1\}}(z_i^c)} q_i^{I_{\{-1\}}(z_i^c)}}{\prod_{i \neq j=1}^k p_i^{I_{\{1\}}(z_i)} q_i^{I_{\{-1\}}(z_i)}} \times \frac{\pi(T_{b,z}(\mathbf{x}, \epsilon))}{\pi(\mathbf{x})} \times \left| \frac{\partial(T_{b,z}(\mathbf{x}, \epsilon))}{\partial(\mathbf{x}, \epsilon)} \right| \right\} \\
& = \varrho(\epsilon) \times \min \left\{ \pi(\mathbf{x}) \times \frac{1}{k} \times w_{b,k} \times \prod_{i \neq j=1}^k p_i^{I_{\{1\}}(z_i)} q_i^{I_{\{-1\}}(z_i)}, \right. \\
& \quad \left. \frac{1}{k(k+1)} \times w_{d,k+1} \times \prod_{i \neq j=1}^k p_i^{I_{\{1\}}(z_i^c)} q_i^{I_{\{-1\}}(z_i^c)} \pi(T_{b,z}(\mathbf{x}, \epsilon)) \times \left| \frac{\partial(T_{b,z}(\mathbf{x}, \epsilon))}{\partial(\mathbf{x}, \epsilon)} \right| \right\}. \quad (\text{S-1.3})
\end{aligned}$$

Here we assume that x_j was selected, and was split into $g_{j,z_j=1}(x_j, \epsilon)$ and $g_{j,z_j^c=-1}(x_j, \epsilon)$. Hence, it is not necessary to simulate z_j . For the remaining co-ordinates we need to simulate $z_i; i \neq j = 1, \dots, k$.

At the reverse death move we must be able to return to $\mathbf{x} (\in \mathbb{R}^k)$ from $T_{b,z}(\mathbf{x}, \epsilon) (\in \mathbb{R}^{k+1})$. We select $g_{j,z_j=1}(x_j, \epsilon)$ with probability $1/(k+1)$, then select $g_{j,z_j^c=-1}(x_j, \epsilon)$ without replacement with probability $1/k$, take their respective backward transformations after simulating $\epsilon \sim g$, and finally take the resultant average. Thus, although it is not necessary to simulate z_j here, we must simulate $z_i^c; i \neq j = 1, \dots, k$ for the co-ordinates after re-labelling them appropriately to correspond to the remaining $(k+1) - 2 = k - 1$ co-ordinates and $z_i; i \neq j = 1, \dots, k$, the latter simulated in the balancing birth move. The transition probability of the death move is hence given by:

$$\begin{aligned}
& \pi(T_{b,z}(\mathbf{x}, \epsilon)) \times w_{d,k+1} \times \varrho(\epsilon) \times \prod_{i \neq j=1}^k p_i^{I_{\{1\}}(z_i^c)} q_i^{I_{\{-1\}}(z_i^c)} \times \frac{1}{k+1} \times \frac{1}{k} \times \left| \frac{\partial(T_{d,z}^{-1}(\mathbf{x}, \epsilon), \epsilon^*)}{\partial(\mathbf{x}, \epsilon)} \right| \\
& \times \min \left\{ 1, (k+1) \times \frac{w_{b,k}}{w_{d,k+1}} \times \frac{\prod_{i \neq j=1}^k p_i^{I_{\{1\}}(z_i)} q_i^{I_{\{-1\}}(z_i)}}{\prod_{i \neq j=1}^k p_i^{I_{\{1\}}(z_i^c)} q_i^{I_{\{-1\}}(z_i^c)}} \times \frac{\pi(\mathbf{x})}{\pi(T_{b,z}(\mathbf{x}, \epsilon))} \times \left| \frac{\partial(T_{d,z}(\mathbf{x}, \epsilon), \epsilon^*)}{\partial(\mathbf{x}, \epsilon)} \right| \right\} \\
& = \varrho(\epsilon) \times \min \left\{ \pi(T_{b,z}(\mathbf{x}, \epsilon)) \times w_{d,k+1} \times \prod_{i \neq j=1}^k p_i^{I_{\{1\}}(z_i^c)} q_i^{I_{\{-1\}}(z_i^c)} \times \frac{1}{k(k+1)} \times \left| \frac{\partial(T_{d,z}^{-1}(\mathbf{x}, \epsilon), \epsilon^*)}{\partial(\mathbf{x}, \epsilon)} \right|, \right. \\
& \quad \left. \frac{1}{k} \times w_{b,k} \times \prod_{i \neq j=1}^k p_i^{I_{\{1\}}(z_i)} q_i^{I_{\{-1\}}(z_i)} \times \pi(\mathbf{x}) \right\}. \quad (\text{S-1.4})
\end{aligned}$$

Noting that $\left| \frac{\partial(T_{d,z}^{-1}(\mathbf{x}, \epsilon), \epsilon^*)}{\partial(\mathbf{x}, \epsilon)} \right| = \left| \frac{\partial(T_{b,z}(\mathbf{x}, \epsilon))}{\partial(\mathbf{x}, \epsilon)} \right|$, it follows that (S-1.3) = (S-1.4), showing that detailed balance holds for the birth and the death moves. The proof of detailed balance for the no-change move type where the dimension remains unchanged is the same as that of TMCMC, and has been proved in the supplement of Dutta & Bhattacharya (2014).

S-2. IRREDUCIBILITY AND APERIODICITY OF TTMCMC

It is easy to see that our TTMCMC algorithm is irreducible and aperiodic. Assume that $\mathbf{x} \in \mathbb{R}^k$, with $k \geq 1$. For $k' > 0$ with $k' \neq k$, let $(k', A_{k'})$ have positive probability under the target distribution, that is, $\pi(k', A_{k'}) > 0$; here $A_{k'}$ is a Borel set associated with $\mathbb{R}^{k'}$. Then $\mathbb{R}^{k'}$ can be reached from $\mathbf{x} \in \mathbb{R}^k$ in a finite number of steps using the birth and the death moves, accordingly as $k' > k$ or $k' < k$. Thus, if $k' > k$, $\mathbb{R}^{k'}$ can be reached in $(k' - k)$ steps by applying the birth move, and if $k' < k$, then $\mathbb{R}^{k'}$ can be reached in $(k - k')$ steps using the death move. Once $\mathbb{R}^{k'}$ is reached the no-change move-type and the transformations can be used to reach $A_{k'}$ in k' steps. For the proof of the latter see Dutta & Bhattacharya (2014) and Dey & Bhattacharya (2017c). Thus, $(k', A_{k'})$ can be reached from $\mathbf{x} \in \mathbb{R}^k$ in $(|k' - k| + k')$ steps with positive probability. Since the set $(k', A_{k'})$ is arbitrary, aperiodicity also follows.

S-3. GENERAL TTMCMC ALGORITHM FOR JUMPING M DIMENSIONS

Algorithm S-3.1 *General TTMCMC algorithm for jumping m dimensions.*

- Let the initial value be $\mathbf{x}^{(0)} \in \mathbb{R}^k$, where $k \geq m$.
- For $t = 0, 1, 2, \dots$
 1. Generate $u = (u_1, u_2, u_3) \sim \text{Multinomial}(1; w_{b,k}, w_{d,k}, w_{nc,k})$.
 2. If $u_1 = 1$ (increase dimension from k to $k + m$), then
 - (a) Randomly select m co-ordinates from $\mathbf{x}^{(t)} = (x_1^{(t)}, \dots, x_k^{(t)})$ without replacement. Let $\mathbf{j}_m = (j_1, \dots, j_m)$ denote the chosen co-ordinates.
 - (b) Generate $\boldsymbol{\epsilon}_m = (\epsilon_1, \dots, \epsilon_m) \stackrel{iid}{\sim} \varrho(\cdot)$ and for $i = 1, \dots, k$; $i \neq j_1, \dots, j_m$, simulate $z_i \sim \text{Multinomial}(1; p_i, q_i, 1 - p_i - q_i)$ independently.

(c) Propose the birth move as follows: apply the transformation $x_i^{(t)} \rightarrow g_{i,z_i}(x_i^{(t)}, \epsilon_1)$ for $i \in \{1, \dots, k\} \setminus \mathbf{j}_m$ and, for each $\ell \in \mathbf{j}_m$, split $x_\ell^{(t)}$ into $g_{\ell, z_\ell=1}(x_\ell^{(t)}, \epsilon_\ell)$ and $g_{\ell, z_\ell^c=-1}(x_\ell^{(t)}, \epsilon_\ell)$. In other words, the birth move is given by:

$$\begin{aligned} \mathbf{x}' = T_{b,z}(\mathbf{x}^{(t)}, \boldsymbol{\epsilon}_m) = & (g_{1,z_1}(x_1^{(t)}, \epsilon_1), \dots, g_{j_1-1, z_{j_1-1}}(x_{j_1-1}^{(t)}, \epsilon_1), \\ & g_{j_1, z_{j_1}=1}(x_{j_1}^{(t)}, \epsilon_1), g_{j_1, z_{j_1}^c=-1}(x_{j_1}^{(t)}, \epsilon_1), g_{j_1+1, z_{j_1+1}}(x_{j_1+1}^{(t)}, \epsilon_1), \dots, \\ & g_{j_2-1, z_{j_2-1}}(x_{j_2-1}^{(t)}, \epsilon_1), g_{j_2, z_{j_2}=1}(x_{j_2}^{(t)}, \epsilon_2), g_{j_2, z_{j_2}^c=-1}(x_{j_2}^{(t)}, \epsilon_2), \\ & g_{j_2+1, z_{j_2+1}}(x_{j_2+1}^{(t)}, \epsilon_1), \dots, g_{j_m-1, z_{j_m-1}}(x_{j_m-1}^{(t)}, \epsilon_1), g_{j_m, z_{j_m}=1}(x_{j_m}^{(t)}, \epsilon_m), \\ & g_{j_m, z_{j_m}^c=-1}(x_{j_m}^{(t)}, \epsilon_m), g_{j_m+1, z_{j_m+1}}(x_{j_m+1}^{(t)}, \epsilon_1), \dots, g_{k, z_k}(x_k^{(t)}, \epsilon_1)). \end{aligned}$$

Re-label the $k+m$ elements of \mathbf{x}' as $(x'_1, x'_2, \dots, x'_{k+m})$. Notice that except for the co-ordinates $x_{j_1}^{(t)}, x_{j_2}^{(t)}, \dots, x_{j_m}^{(t)}$, for which we use $\epsilon_1, \epsilon_2, \dots, \epsilon_m$ respectively for updating, for all the remaining co-ordinates we use only ϵ_1 .

(d) Calculate the acceptance probability of the birth move \mathbf{x}' :

$$a_b(\mathbf{x}^{(t)}, \boldsymbol{\epsilon}_m) = \min \left\{ 1, \frac{1}{(k+m)_m} \times \frac{w_{d,k+m}}{w_{b,k}} \times \frac{P_{(\mathbf{j}_m)}(\mathbf{z}^c)}{P_{(\mathbf{j}_m)}(\mathbf{z})} \frac{\pi(\mathbf{x}')}{\pi(\mathbf{x}^{(t)})} \left| \frac{\partial(T_{b,z}(\mathbf{x}^{(t)}, \boldsymbol{\epsilon}_m))}{\partial(\mathbf{x}^{(t)}, \boldsymbol{\epsilon}_m)} \right| \right\},$$

where for integers $a > 0$ and $r > 0$ with $a > (r-1)$, we define $(a)_r = a \times (a-1) \times (a-r+1)$. Also,

$$P_{(\mathbf{j}_m)}(\mathbf{z}) = \prod_{i \in \{1, \dots, k\} \setminus \mathbf{j}_m} p_i^{I_{\{1\}}(z_i)} q_i^{I_{\{-1\}}(z_i)},$$

and

$$P_{(\mathbf{j}_m)}(\mathbf{z}^c) = \prod_{i \in \{1, \dots, k\} \setminus \mathbf{j}_m} p_i^{I_{\{1\}}(z_i^c)} q_i^{I_{\{-1\}}(z_i^c)}.$$

(e) Set

$$\mathbf{x}^{(t+1)} = \begin{cases} \mathbf{x}' & \text{with probability } a_b(\mathbf{x}^{(t)}, \boldsymbol{\epsilon}) \\ \mathbf{x}^{(t)} & \text{with probability } 1 - a_b(\mathbf{x}^{(t)}, \boldsymbol{\epsilon}). \end{cases}$$

3. If $u_2 = 1$ (decrease dimension from k to $k - m$, for $k \geq 2m$), then

- (a) Generate $\boldsymbol{\epsilon}_m = (\epsilon_1, \dots, \epsilon_m) \stackrel{iid}{\sim} \varrho(\cdot)$.
- (b) Randomly, without replacement, select co-ordinates $\mathbf{j}_m = (j_1, \dots, j_m)$ and $\mathbf{j}'_m = (j'_1, \dots, j'_m)$ from $\mathbf{x} = (x_1, \dots, x_k)$. For $\ell = 1, \dots, m$, let $x_{j_\ell}^* = \left(g_{j_\ell, z_{j_\ell}^c = -1}(x_{j_\ell}, \epsilon_\ell) + g_{j'_\ell, z_{j'_\ell} = 1}(x_{j'_\ell}, \epsilon_\ell) \right) / 2$; replace the co-ordinate x_{j_ℓ} by the average $x_{j_\ell}^*$ and delete $x_{j'_\ell}$.
- (c) Simulate \mathbf{z} by generating independently, for $i \in \{1, \dots, k\} \setminus \mathbf{j}_m$, $z_i \sim \text{Multinomial}(1; p_i, q_i, 1 - p_i - q_i)$.
- (d) For $i \in \{1, \dots, k\} \setminus \mathbf{j}_m$, apply the transformation $x'_i = g_{i, z_i}(x_i^{(t)}, \epsilon_1)$.
- (e) Propose the following death move:

$$\begin{aligned} \mathbf{x}' &= T_{d, \mathbf{z}}(\mathbf{x}^{(t)}, \boldsymbol{\epsilon}_m) \\ &= (g_{1, z_1}(x_1^{(t)}, \epsilon_1), \dots, g_{j_1-1, z_{j_1-1}}(x_{j_1-1}^{(t)}, \epsilon_1), x_{j_1}^*, g_{j_1+1, z_{j_1+1}}(x_{j_1+1}^{(t)}, \epsilon_1), \\ &\quad \dots, g_{j_2-1, z_{j_2-1}}(x_{j_2-1}^{(t)}, \epsilon_1), x_{j_2}^*, g_{j_2+1, z_{j_2+1}}(x_{j_2+1}^{(t)}, \epsilon_1), \\ &\quad \dots, g_{j_m-1, z_{j_m-1}}(x_{j_m-1}^{(t)}, \epsilon_1), x_{j_m}^*, g_{j_m+1, z_{j_m+1}}(x_{j_m+1}^{(t)}, \epsilon_1), \dots, g_{k, z_k}(x_k^{(t)}, \epsilon_1)). \end{aligned}$$

Re-label the elements of \mathbf{x}' as $(x'_1, x'_2, \dots, x'_{k-m})$.

- (f) For $\ell = 1, \dots, m$, solve for ϵ_ℓ^* from the equations $g_{\ell, z_\ell = 1}(x_\ell^*, \epsilon_\ell^*) = x_{j_\ell}$ and $g_{\ell, z_{j_\ell}^c = -1}(x_{j_\ell}^*, \epsilon_\ell^*) = x_{j'_\ell}$ and express ϵ_ℓ^* in terms of x_{j_ℓ} and $x_{j'_\ell}$. Let $\boldsymbol{\epsilon}_m^* = (\epsilon_1^*, \dots, \epsilon_m^*)$.
- (g) Calculate the acceptance probability of the death move:

$$\begin{aligned} &a_d(\mathbf{x}^{(t)}, \boldsymbol{\epsilon}_m, \boldsymbol{\epsilon}_m^*) \\ &= \min \left\{ 1, (k)_m \times \frac{w_{b, k-m}}{w_{d, k}} \times \frac{P_{(\mathbf{j}_m, \mathbf{j}'_m)}(\mathbf{z}^c)}{P_{(\mathbf{j}, \mathbf{j}'_m)}(\mathbf{z})} \frac{\pi(\mathbf{x}')}{\pi(\mathbf{x}^{(t)})} \left| \frac{\partial(T_{d, \mathbf{z}}(\mathbf{x}^{(t)}, \boldsymbol{\epsilon}_m), \boldsymbol{\epsilon}_m^*, \boldsymbol{\epsilon}_m)}{\partial(\mathbf{x}^{(t)}, \boldsymbol{\epsilon}_m)} \right| \right\}, \end{aligned}$$

where

$$P_{(\mathbf{j}_m, \mathbf{j}'_m)}(\mathbf{z}) = \prod_{i \in \{1, \dots, k\} \setminus \{\mathbf{j}_m, \mathbf{j}'_m\}} p_i^{I_{\{1\}}(z_i)} q_i^{I_{\{-1\}}(z_i)},$$

and

$$P_{(\mathbf{j}_m, \mathbf{j}'_m)}(\mathbf{z}^c) = \prod_{i \in \{1, \dots, k\} \setminus \{\mathbf{j}_m, \mathbf{j}'_m\}} p_i^{I_{\{1\}}(z_i^c)} q_i^{I_{\{-1\}}(z_i^c)}.$$

(h) Set

$$\mathbf{x}^{(t+1)} = \begin{cases} \mathbf{x}' & \text{with probability } a_d(\mathbf{x}^{(t)}, \boldsymbol{\epsilon}_m, \boldsymbol{\epsilon}_m^*) \\ \mathbf{x}^{(t)} & \text{with probability } 1 - a_d(\mathbf{x}^{(t)}, \boldsymbol{\epsilon}_m, \boldsymbol{\epsilon}_m^*). \end{cases}$$

4. If $u_3 = 1$ (dimension remains unchanged), then implement steps (1), (2), (3) of Algorithm 3.1 of Dutta & Bhattacharya (2014).

• End for

S-4. PROOF OF DETAILED BALANCE FOR GENERAL TTMCMC ALGORITHM FOR JUMPING M DIMENSIONS

To see that detailed balance is satisfied for the birth and death moves, note that associated with the birth move, the probability of transition $\mathbf{x} \in \mathbb{R}^k \mapsto T_{b,z}(\mathbf{x}, \boldsymbol{\epsilon}_m) \in \mathbb{R}^{k+m}$, with $k \geq m$, is given by:

$$\begin{aligned} & \pi(\mathbf{x}) \times \frac{1}{(k)_m} \times w_{b,k} \times \prod_{i=1}^m \varrho(\epsilon_i) \times \prod_{i \in \{1, \dots, k\} \setminus \mathbf{j}_m} p_i^{I_{\{1\}}(z_i)} q_i^{I_{\{-1\}}(z_i)} \\ & \times \min \left\{ 1, \frac{1}{(k+m)_m} \times \frac{w_{d,k+m}}{w_{b,k}} \times \frac{\prod_{i \in \{1, \dots, k\} \setminus \mathbf{j}_m} p_i^{I_{\{1\}}(z_i^c)} q_i^{I_{\{-1\}}(z_i^c)}}{\prod_{i \in \{1, \dots, k\} \setminus \mathbf{j}_m} p_i^{I_{\{1\}}(z_i)} q_i^{I_{\{-1\}}(z_i)}} \right. \\ & \quad \left. \times \frac{\pi(T_{b,z}(\mathbf{x}, \boldsymbol{\epsilon}_m))}{\pi(\mathbf{x})} \times \left| \frac{\partial(T_{b,z}(\mathbf{x}^{(t)}, \boldsymbol{\epsilon}_m))}{\partial(\mathbf{x}^{(t)}, \boldsymbol{\epsilon}_m)} \right| \right\} \\ & = \prod_{i=1}^m \varrho(\epsilon_i) \times \min \left\{ \pi(\mathbf{x}) \times w_{b,k} \times \frac{1}{(k)_m} \times \prod_{i \in \{1, \dots, k\} \setminus \mathbf{j}_m} p_i^{I_{\{1\}}(z_i)} q_i^{I_{\{-1\}}(z_i)}, \frac{1}{(k)_m} \times \frac{1}{(k+m)_m} \right. \\ & \quad \left. \times w_{d,k+m} \times \prod_{i \in \{1, \dots, k\} \setminus \mathbf{j}_m} p_i^{I_{\{1\}}(z_i^c)} q_i^{I_{\{-1\}}(z_i^c)} \pi(T_{b,z}(\mathbf{x}, \boldsymbol{\epsilon}_m)) \times \left| \frac{\partial(T_{b,z}(\mathbf{x}^{(t)}, \boldsymbol{\epsilon}_m))}{\partial(\mathbf{x}^{(t)}, \boldsymbol{\epsilon}_m)} \right| \right\}. \quad (\text{S-4.1}) \end{aligned}$$

The transition probability of the reverse death move is given by:

$$\begin{aligned}
& \pi(\mathbf{x}) \times w_{d,k+m} \times \prod_{i=1}^m \varrho(\epsilon_i) \times \prod_{i \in \{1, \dots, k\} \setminus \mathbf{j}_m} p_i^{I_{\{1\}}(z_i^c)} q_i^{I_{\{-1\}}(z_i^c)} \\
& \quad \times \frac{1}{(k+m)_m} \times \frac{1}{(k)_m} \times \left| \frac{\partial(T_{d,z}^{-1}(\mathbf{x}^{(t)}, \epsilon_m), \epsilon_m^*, \epsilon_m)}{\partial(\mathbf{x}^{(t)}, \epsilon_m)} \right| \\
& \times \min \left\{ 1, (k+m)_m \times \frac{w_{b,k}}{w_{d,k+m}} \times \frac{\prod_{i \in \{1, \dots, k\} \setminus \mathbf{j}_m} p_i^{I_{\{1\}}(z_i)} q_i^{I_{\{-1\}}(z_i)}}{\prod_{i \in \{1, \dots, k\} \setminus \mathbf{j}_m} p_i^{I_{\{1\}}(z_i^c)} q_i^{I_{\{-1\}}(z_i^c)}} \right. \\
& \quad \left. \times \frac{\pi(\mathbf{x})}{\pi(T_{b,z}(\mathbf{x}, \epsilon_m))} \times \left| \frac{\partial(T_{d,z}(\mathbf{x}^{(t)}, \epsilon_m), \epsilon_m^*, \epsilon_m)}{\partial(\mathbf{x}^{(t)}, \epsilon_m)} \right| \right\} \\
& = \prod_{i=1}^m \varrho(\epsilon_i) \times \min \left\{ \pi(T_{b,z}(\mathbf{x}, \epsilon_m)) \times w_{d,k+m} \times \prod_{i \in \{1, \dots, k\} \setminus \mathbf{j}_m} p_i^{I_{\{1\}}(z_i^c)} q_i^{I_{\{-1\}}(z_i^c)} \right. \\
& \quad \times \frac{1}{(k)_m} \times \frac{1}{(k+m)_m} \times \left| \frac{\partial(T_{d,z}^{-1}(\mathbf{x}^{(t)}, \epsilon_m), \epsilon_m^*, \epsilon_m)}{\partial(\mathbf{x}^{(t)}, \epsilon_m)} \right|, \\
& \quad \left. \frac{1}{(k)_m} \times w_{b,k} \times \prod_{i \in \{1, \dots, k\} \setminus \mathbf{j}_m} p_i^{I_{\{1\}}(z_i)} q_i^{I_{\{-1\}}(z_i)} \times \pi(\mathbf{x}) \right\}. \quad (\text{S-4.2})
\end{aligned}$$

Noting that $\left| \frac{\partial(T_{d,z}^{-1}(\mathbf{x}^{(t)}, \epsilon_m), \epsilon_m^*, \epsilon_m)}{\partial(\mathbf{x}^{(t)}, \epsilon_m^*, \epsilon_m)} \right| = \left| \frac{\partial(T_{b,z}(\mathbf{x}^{(t)}, \epsilon_m))}{\partial(\mathbf{x}^{(t)}, \epsilon_m)} \right|$, it follows that (S-4.1) = (S-4.2), showing that detailed balance holds for the birth and the death moves.

S-5. JUMPING MORE THAN ONE DIMENSIONS AT A TIME WHEN THERE SEVERAL SETS OF PARAMETERS ARE RELATED

It is often the case that changing dimension of one set of parameters forces changing dimension of the other sets of parameters accordingly. For instance, in a mixture problem with unknown number of components, where the i -th component is characterized by the mean and standard deviation (μ_i, σ_i) , when the dimension of the current k -dimensional mean vector (μ_1, \dots, μ_k) is increased by one, then one must simultaneously increase the dimension of the current k -dimensional vector of standard deviations $(\sigma_1, \dots, \sigma_k)$ by one. In this section we extend TTMC to general situations of this kind.

For an illustrative example, assume that the TTMC chain is currently at the state

$$\{(\mu_1, \log(\sigma_1)), (\mu_2, \log(\sigma_2))\} = (\mu_1, \mu_2, \log(\sigma_1), \log(\sigma_2)) \in \mathbb{R}^2 \times \mathbb{R}^2.$$

Let $\mathbf{x} = (x_1, x_2, x_3, x_4) = (\mu_1, \mu_2, \log(\sigma_1), \log(\sigma_2))$. Suppose that it is required to increase the dimension to $\mathbb{R}^3 \times \mathbb{R}^3$ using the additive transformation.

To achieve consistency with respect to dimensions such that the Jacobian is well-defined, we need to simulate two ϵ 's from $\varrho(\cdot)$: ϵ_1 for splitting x_1 into $x_1 + a_1\epsilon_1$ and $x_1 - a_1\epsilon_1$, and ϵ_2 for splitting x_3 into $x_3 + a_3\epsilon_2$ and $x_3 - a_3\epsilon_2$. With the same ϵ_1 we can also update x_2 to $x_2 + z_2a_2\epsilon_1$, and x_4 to $x_4 + z_4a_4\epsilon_1$. Note that it is possible to use ϵ_2 to split x_3 into $x_3 + a_3\epsilon_2$ and $x_3 - a_3\epsilon_2$, and to update x_4 to $x_4 + z_4a_4\epsilon_2$, instead of using ϵ_1 to update x_4 to $x_4 + z_4a_4\epsilon_1$. That is, we can use ϵ_1 and ϵ_2 for updating the sub-blocks (μ_1, μ_2) and $(\log(\sigma_1), \log(\sigma_2))$, respectively. However, using ϵ_1 for both the sub-blocks induces dependence between the updates through the common ϵ_1 and hence may be desirable since we are updating all the sub-blocks in a single block. Hence, in this article, we confine ourselves to using a common ϵ_1 across the sub-blocks.

Hence, in this example, the birth move takes the form $\mathbf{x}' = T_{b,z_2,z_4}(\mathbf{x}, \epsilon_1, \epsilon_2) = (x_1 + a_1\epsilon_1, x_1 - a_1\epsilon_1, x_2 + z_2a_2\epsilon_1, x_3 + a_3\epsilon_2, x_3 - a_3\epsilon_2, x_4 + z_4a_4\epsilon_1) = (x'_1, x'_2, x'_3, x'_4, x'_5, x'_6)$. Now the dimensions of both $\mathbf{x}' = (x'_1, x'_2, x'_3, x'_4, x'_5, x'_6)$ and $(\mathbf{x}, \epsilon_1, \epsilon_2) = (x_1, x_2, x_3, x_4, \epsilon_1, \epsilon_2)$ is 6, and so the Jacobian

$$\left| \frac{\partial(T_{b,z_2,z_4}(\mathbf{x}, \epsilon_1, \epsilon_2))}{\partial(\mathbf{x}, \epsilon_1, \epsilon_2)} \right| = \left| \frac{\partial(x_1 + a_1\epsilon_1, x_1 - a_1\epsilon_1, x_2 + z_2a_2\epsilon_1, x_3 + a_3\epsilon_2, x_3 - a_3\epsilon_2, x_4 + z_4a_4\epsilon_1)}{\partial(x_1, x_2, x_3, x_4, \epsilon_1, \epsilon_2)} \right| = 4a_1a_3,$$

is well-defined. The acceptance probability of the birth move in this example is given by

$$\begin{aligned} a_b(\mathbf{x}, \epsilon_1, \epsilon_2) &= \min \left\{ 1, \frac{1}{3} \times \frac{w_{d,6}}{w_{b,4}} \times \prod_{i=2,4} \frac{p_3^{I_{\{1\}}(z_i^c)} q_i^{I_{\{-1\}}(z_i^c)}}{p_i^{I_{\{1\}}(z_i)} q_i^{I_{\{-1\}}(z_i)}} \times \frac{\pi(\mathbf{x}')}{\pi(\mathbf{x})} \times \left| \frac{\partial(T_{b,z}(\mathbf{x}, \epsilon_1, \epsilon_2))}{\partial(\mathbf{x}, \epsilon_1, \epsilon_2)} \right| \right\} \\ &= \min \left\{ 1, \frac{1}{3} \times \frac{w_{d,6}}{w_{b,4}} \times \prod_{i=2,4} \frac{p_i^{I_{\{1\}}(z_i^c)} q_i^{I_{\{-1\}}(z_i^c)}}{p_i^{I_{\{1\}}(z_i)} q_i^{I_{\{-1\}}(z_i)}} \frac{\pi(\mathbf{x}')}{\pi(\mathbf{x})} \times 4a_1a_3 \right\}. \end{aligned} \tag{S-5.1}$$

For the corresponding death move, that is, for moving from $\mathbf{x}' = (x'_1, x'_2, x'_3, x'_4, x'_5, x'_6)$ to $\mathbf{x}'' = T_{d,z}(\mathbf{x}', \epsilon_1) = (\frac{x'_1+x'_2}{2}, x'_3 + z_2^c a_2 \epsilon_1, \frac{x'_4+x'_5}{2}, x'_6 + z_4^c a_4 \epsilon_1) = (x''_1, x''_2, x''_3, x''_4)$, we must have, for the reverse of this death move, $x''_1 + a_1\epsilon_1^* = x'_1$, $x''_1 - a_1\epsilon_1^* = x'_2$, $x''_3 + a_3\epsilon_2^* = x'_4$, $x''_3 - a_3\epsilon_2^* = x'_5$. The first two equations yield $\epsilon_1^* = \frac{x'_1 - x'_2}{2a_1}$ and the last two equations yield $\epsilon_2^* = \frac{x'_4 - x'_5}{2a_3}$. The Jacobian

is given by

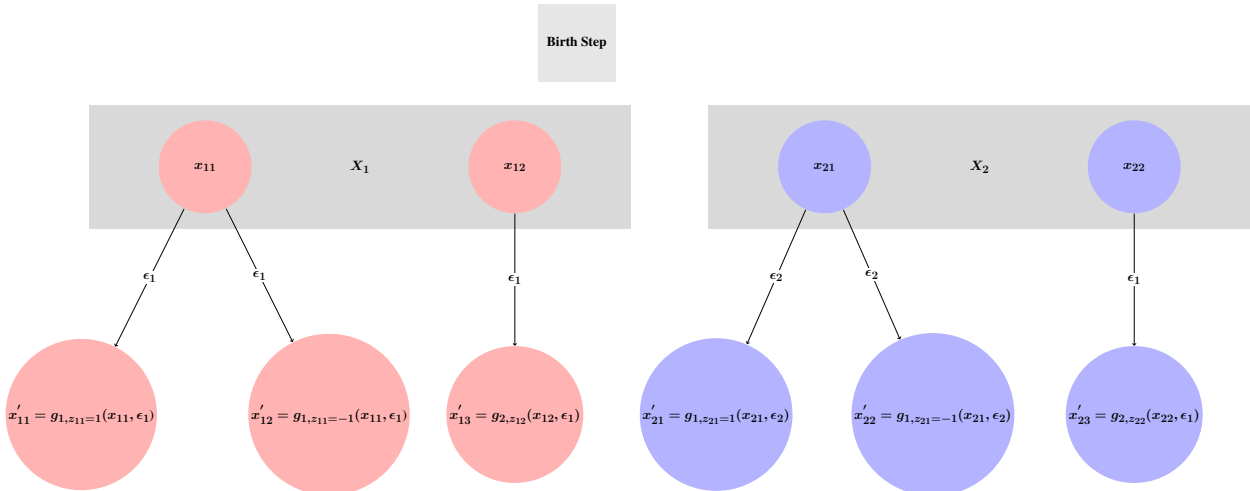
$$\left| \frac{\partial(T_{d,z_2,z_4}(\mathbf{x}', \epsilon_1); \epsilon_1^*, \epsilon_2^*, \epsilon_1)}{\partial(\mathbf{x}', \epsilon_1)} \right| = \left| \frac{\partial\left(\frac{x'_1+x'_2}{2}, x'_3 + z_2^c a_2 \epsilon_1, \frac{x'_4+x'_5}{2}, x'_6 + z_4^c a_4 \epsilon_1, \frac{x'_1-x'_2}{2a_1}, \frac{x'_4-x'_5}{2a_3}, \epsilon_1\right)}{\partial(x'_1, x'_2, x'_3, x'_4, x'_5, x'_6, \epsilon_1)} \right| = \frac{1}{4a_1 a_3}. \quad (\text{S-5.2})$$

We accept this death move with probability

$$\begin{aligned} a_d(\mathbf{x}'', \epsilon_1, \epsilon_1^*, \epsilon_2^*) &= \min \left\{ 1, 3 \times \frac{w_{b,4}}{w_{d,6}} \times \frac{P(\mathbf{z}^c)}{P(\mathbf{z})} \frac{\pi(\mathbf{x}'')}{\pi(\mathbf{x}')} \left| \frac{\partial(T_{d,z}(\mathbf{x}', \epsilon_1); \epsilon_1^*, \epsilon_2^*, \epsilon_1)}{\partial(\mathbf{x}', \epsilon_1)} \right| \right\} \\ &= \min \left\{ 1, 3 \times \frac{w_{b,4}}{w_{d,6}} \times \prod_{i=2,4} \frac{p_i^{I_{\{1\}}(z_i)} q_i^{I_{\{-1\}}(z_i)}}{I_{\{1\}}(z_i^c) q_i^{I_{\{-1\}}(z_i^c)}} \times \frac{\pi(\mathbf{x}'')}{\pi(\mathbf{x}')} \times \frac{1}{4a_1 a_3} \right\}. \quad (\text{S-5.3}) \end{aligned}$$

The key idea of the algorithm is described schematically in Figure S-1.

Note that for given k , in general mixture problems we would need to update $((\mu_1, \mu_2, \dots, \mu_k), (\log(\sigma_1), \log(\sigma_2), \dots, \log(\sigma_k)), (\omega_1, \omega_2, \dots, \omega_k))$, where, for $j = 1, \dots, k$, ω_j correspond to the mixing proportion π_j , where $\sum_{j=1}^k \pi_j = 1$, as $\pi_j = \exp(\omega_j) / \sum_{\ell=1}^k \exp(\omega_\ell)$. If $(a_{\mu_1}, \dots, a_{\mu_k})$, $(a_{\sigma_1}, \dots, a_{\sigma_k})$, and $(a_{\omega_1}, \dots, a_{\omega_k})$ are the scales associated with the three sub-blocks, then the Jacobian for the birth move, if the j -th component is selected, is given by $8a_{\mu_j} a_{\sigma_j} a_{\omega_j}$, and that for the death move is $(8a_{\mu_j} a_{\sigma_j} a_{\omega_j})^{-1}$.



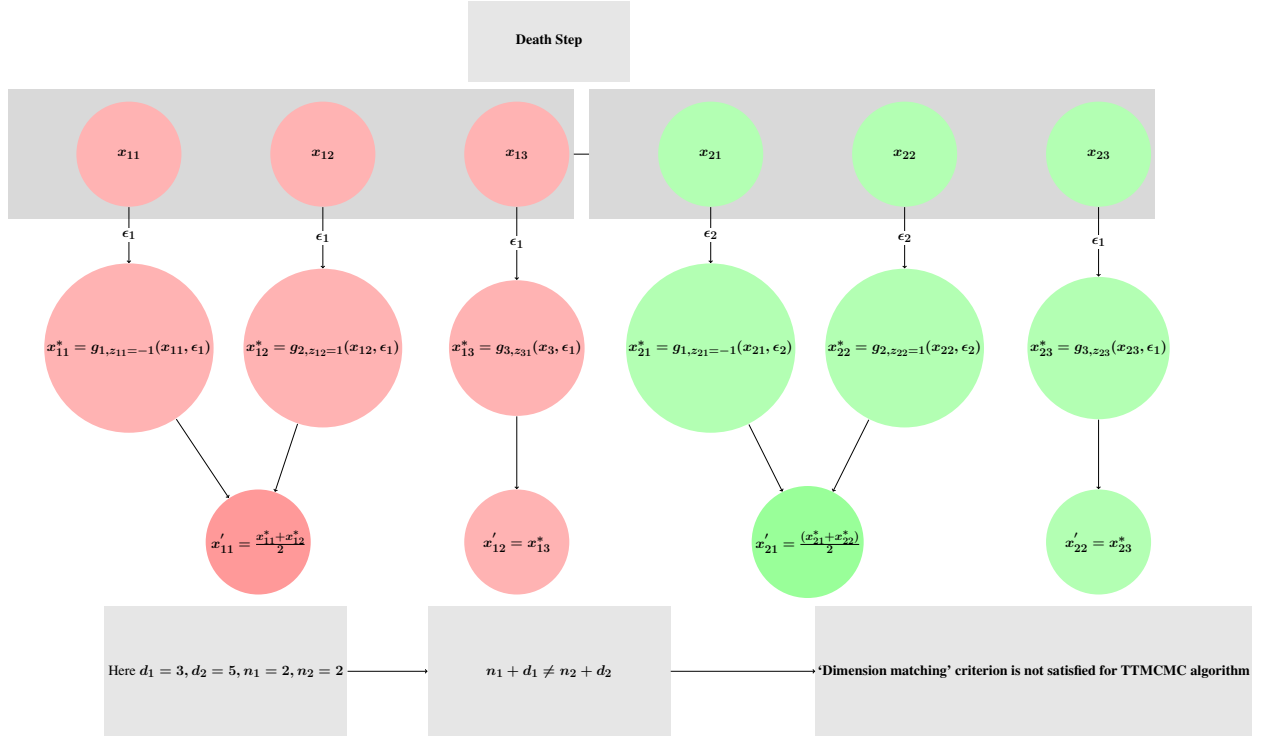


Figure S-1: **Illustration of TTMCMC algorithm for jumping more than one dimension when several sets of parameters are related.**

In general, $\mathbf{x} \in \mathbb{R}^{mk}$ may be of the form $(\mathbf{x}_1, \mathbf{x}_2, \dots, \mathbf{x}_m)$, where $\mathbf{x}_\ell = (x_{\ell,1}, x_{\ell,2}, \dots, x_{\ell,k})$ for $\ell = 1, 2, \dots, m$, where $m \geq 1$ is an integer. If the dimension of any one \mathbf{x}_ℓ is changed, then the dimensions of all other $\mathbf{x}_{\ell'}$; $\ell' \neq \ell$ must also change accordingly, as in the above example. We provide the general TTMCMC algorithm as Algorithm S-5.1 below. It can be easily checked that detailed balance is satisfied for this algorithm.

Algorithm S-5.1 *General TTMCMC algorithm for jumping m dimensions with m related sets of co-ordinates.*

- Let the initial value be $\mathbf{x}^{(0)} \in \mathbb{R}^{mk}$, where $k \geq m$.
- For $t = 0, 1, 2, \dots$
 1. Generate $u = (u_1, u_2, u_3) \sim \text{Multinomial}(1; w_{b,k}, w_{d,k}, w_{nc,k})$.
 2. If $u_1 = 1$ (increase dimension from mk to $m(k+1)$), then

- (a) Randomly select one co-ordinate from $\mathbf{x}_1^{(t)} = (x_{11}^{(t)}, \dots, x_{1k}^{(t)})$ without replacement. Let j denote the chosen co-ordinate.
- (b) Generate $\boldsymbol{\epsilon}_m = (\epsilon_1, \dots, \epsilon_m) \stackrel{iid}{\sim} \varrho(\cdot)$ and for $i \in \{1, \dots, k\} \setminus \{j\}$ simulate $z_{\ell,i} \sim \text{Multinomial}(1; p_{\ell,i}, q_{\ell,i}, 1-p_{\ell,i}-q_{\ell,i})$ independently, for every $\ell = 1, \dots, m$.
- (c) Propose the birth move as follows: for each $\ell = 1, \dots, m$, apply the transformation $x_{\ell,i}^{(t)} \rightarrow g_{i,z_{\ell,i}}(x_{\ell,i}^{(t)}, \epsilon_1)$ for $i \in \{1, \dots, k\} \setminus \{j\}$ and, for each $\ell \in \{1, \dots, m\}$, split $x_{\ell,j}^{(t)}$ into $g_{\ell,z_{\ell,j}=1}(x_{\ell,j}^{(t)}, \epsilon_\ell)$ and $g_{\ell,z_{\ell,j}^c=-1}(x_{\ell,j}^{(t)}, \epsilon_\ell)$. In other words, let $\mathbf{x}' = T_{b,z}(\mathbf{x}^{(t)}, \boldsymbol{\epsilon}_m) = (\mathbf{x}'_1, \dots, \mathbf{x}'_m)$ denote the complete birth move, where, for $\ell = 1, \dots, m$, \mathbf{x}'_ℓ is given by

$$\begin{aligned} \mathbf{x}'_\ell = & (g_{\ell,z_{\ell,1}}(x_{\ell,1}^{(t)}, \epsilon_1), \dots, g_{j-1,z_{\ell,j-1}}(x_{\ell,j-1}^{(t)}, \epsilon_1), \\ & g_{j,z_{\ell,j}=1}(x_{\ell,j}^{(t)}, \epsilon_\ell), g_{j,z_{\ell,j}^c=-1}(x_{\ell,j}^{(t)}, \epsilon_\ell), g_{j+1,z_{\ell,j+1}}(x_{\ell,j+1}^{(t)}, \epsilon_1), \dots, \\ & \dots, g_{k,z_{\ell,k}}(x_{\ell,k}^{(t)}, \epsilon_1)). \end{aligned}$$

Re-label the $k+1$ elements of \mathbf{x}'_ℓ as $(x'_{\ell,1}, x'_{\ell,2}, \dots, x'_{\ell,k+1})$. Notice that, following the discussion presented in the illustrative example in the beginning of this section, we use ϵ_ℓ only for splitting $x_{\ell,j}^{(t)}$ into $g_{j,z_{\ell,j}=1}(x_{\ell,j}^{(t)}, \epsilon_\ell)$ and $g_{j,z_{\ell,j}^c=-1}(x_{\ell,j}^{(t)}, \epsilon_\ell)$. To update the remaining co-ordinates, we use ϵ_1 for all the blocks.

- (d) Calculate the acceptance probability of the birth move \mathbf{x}' :

$$a_b(\mathbf{x}^{(t)}, \boldsymbol{\epsilon}_m) = \min \left\{ 1, \frac{1}{k+1} \times \frac{w_{d,k+1}}{w_{b,k}} \times \frac{P_{(j)}(\mathbf{z}^c)}{P_{(j)}(\mathbf{z})} \frac{\pi(\mathbf{x}')}{\pi(\mathbf{x}^{(t)})} \left| \frac{\partial(T_{b,z}(\mathbf{x}^{(t)}, \boldsymbol{\epsilon}_m))}{\partial(\mathbf{x}^{(t)}, \boldsymbol{\epsilon}_m)} \right| \right\},$$

where

$$P_{(j)}(\mathbf{z}) = \prod_{\ell=1}^m \prod_{i \in \{1, \dots, k\} \setminus \{j\}} p_{\ell,i}^{I_{\{1\}}(z_{\ell,i})} q_{\ell,i}^{I_{\{-1\}}(z_{\ell,i})},$$

and

$$P_{(j)}(\mathbf{z}^c) = \prod_{\ell=1}^m \prod_{i \in \{1, \dots, k\} \setminus \{j\}} p_{\ell,i}^{I_{\{1\}}(z_{\ell,i}^c)} q_{\ell,i}^{I_{\{-1\}}(z_{\ell,i}^c)}.$$

(e) Set

$$\mathbf{x}^{(t+1)} = \begin{cases} \mathbf{x}' & \text{with probability } a_b(\mathbf{x}^{(t)}, \boldsymbol{\epsilon}_m) \\ \mathbf{x}^{(t)} & \text{with probability } 1 - a_b(\mathbf{x}^{(t)}, \boldsymbol{\epsilon}_m). \end{cases}$$

3. If $u_2 = 1$ (decrease dimension from k to $k - m$, for $k \geq 2m$), then

(a) Generate $\boldsymbol{\epsilon}_m = (\epsilon_1, \dots, \epsilon_m) \stackrel{iid}{\sim} \varrho(\cdot)$.

(b) Randomly, without replacement, select co-ordinates j and j' from $\mathbf{x}_1 = (x_{1,1}, \dots, x_{1,k})$. For $\ell = 1, \dots, m$, let

$$x_{\ell,j}^* = \left(g_{j, z_{\ell,j}^c = -1}(x_{\ell,j}, \epsilon_\ell) + g_{j', z_{\ell,j'} = 1}(x_{\ell,j'}, \epsilon_\ell) \right) / 2;$$

replace the co-ordinate $x_{\ell,j}$ by the average $x_{\ell,j}^*$ and delete $x_{\ell,j'}$.

(c) Simulate \mathbf{z} by generating independently, for $\ell = 1, \dots, m$ and for $i \in \{1, \dots, k\} \setminus \{j, j'\}$, $z_{\ell,i} \sim \text{Multinomial}(1; p_{\ell,i}, q_{\ell,i}, 1 - p_{\ell,i} - q_{\ell,i})$.

(d) For $\ell = 1, \dots, m$ and for $i \in \{1, \dots, k\} \setminus \{j, j'\}$, apply the transformation $x'_{\ell,i} = g_{i, z_{\ell,i}}(x_{\ell,i}^{(t)}, \epsilon_1)$.

(e) Propose the following death move $\mathbf{x}' = T_{d,\mathbf{z}}(\mathbf{x}^{(t)}, \boldsymbol{\epsilon}_m) = (\mathbf{x}'_1, \dots, \mathbf{x}'_m)$ where for $\ell = 1, \dots, m$, \mathbf{x}_ℓ is given by

$$\begin{aligned} \mathbf{x}'_\ell = & (g_{1, z_{\ell,1}}(x_{\ell,1}^{(t)}, \epsilon_1), \dots, g_{j-1, z_{\ell,j-1}}(x_{\ell,j-1}^{(t)}, \epsilon_1), x_{\ell,j}^*, g_{j+1, z_{\ell,j+1}}(x_{\ell,j+1}^{(t)}, \epsilon_1), \\ & \dots, g_{k, z_{\ell,k}}(x_{\ell,k}^{(t)}, \epsilon_1)). \end{aligned}$$

Re-label the elements of \mathbf{x}'_ℓ as $(x'_{\ell,1}, x'_{\ell,2}, \dots, x'_{\ell,k-1})$.

(f) For $\ell = 1, \dots, m$, solve for ϵ_ℓ^* from the equations $g_{\ell, z_{\ell,j} = 1}(x_{\ell,j}^*, \epsilon_\ell^*) = x_{\ell,j}$ and $g_{\ell, z_{\ell,j}^c = -1}(x_{\ell,j}^*, \epsilon_\ell^*) = x_{\ell,j'}$ and express ϵ_ℓ^* in terms of $x_{\ell,j}$ and $x_{\ell,j'}$. Let $\boldsymbol{\epsilon}_m^* = (\epsilon_1^*, \dots, \epsilon_m^*)$.

(g) Calculate the acceptance probability of the death move:

$$a_d(\mathbf{x}^{(t)}, \boldsymbol{\epsilon}_m, \boldsymbol{\epsilon}_m^*) = \min \left\{ 1, k \times \frac{w_{b,k-m}}{w_{d,k}} \times \frac{P_{(j,j')}(\mathbf{z}^c)}{P_{(j,j')}(\mathbf{z})} \frac{\pi(\mathbf{x}')}{\pi(\mathbf{x}^{(t)})} \left| \frac{\partial(T_{d,\mathbf{z}}(\mathbf{x}^{(t)}, \boldsymbol{\epsilon}_m), \boldsymbol{\epsilon}_m^*, \boldsymbol{\epsilon}_m)}{\partial(\mathbf{x}^{(t)}, \boldsymbol{\epsilon}_m)} \right| \right\},$$

where

$$P_{(j,j')}(\mathbf{z}) = \prod_{\ell=1}^m \prod_{i \in \{1, \dots, k\} \setminus \{j, j'\}} p_{\ell, i}^{I_{\{1\}}(z_{\ell, i})} q_{\ell, i}^{I_{\{-1\}}(z_{\ell, i})},$$

and

$$P_{(j,j')}(\mathbf{z}^c) = \prod_{\ell=1}^m \prod_{i \in \{1, \dots, k\} \setminus \{j, j'\}} p_{\ell, i}^{I_{\{1\}}(z_{\ell, i}^c)} q_{\ell, i}^{I_{\{-1\}}(z_{\ell, i}^c)}.$$

(h) Set

$$\mathbf{x}^{(t+1)} = \begin{cases} \mathbf{x}' & \text{with probability } a_d(\mathbf{x}^{(t)}, \boldsymbol{\epsilon}_m, \boldsymbol{\epsilon}_m^*) \\ \mathbf{x}^{(t)} & \text{with probability } 1 - a_d(\mathbf{x}^{(t)}, \boldsymbol{\epsilon}_m, \boldsymbol{\epsilon}_m^*). \end{cases}$$

4. If $u_3 = 1$ (dimension remains unchanged), then implement steps (1), (2), (3) of Algorithm 3.1 of Dutta & Bhattacharya (2014).

- End for

S-6. BRIEF DISCUSSION ON LABEL SWITCHING

It is well-known that the mixture likelihood is invariant to permutations (labels) of the component parameters; hence, the mixture parameters are not identifiable. This problem is often referred to as label-switching. So, if inference on the parameters is of interest, then proper labeling of the components is necessary. Richardson & Green (1997) considered ordering the mean parameters; see also Stephens (2000) for other methods for tackling label switching. However, Lee, Marin, Mengersen & Robert (2009) argue and demonstrate that putting constraints on the prior parameter space can have severe ill effects on both inference and computation. Moreover, there seems to be a subtle question if identifiability is at all desirable when inference regarding clustering of the data is of interest. To consider a simple example, suppose that clustering the dataset $\{y_1, y_2, y_3, y_4\}$ using a two-component normal mixture model is of interest. Assume that $\{y_1, y_3\}$ are associated with ν_1 and $\{y_2, y_4\}$ are associated with ν_2 , where $\nu_1 < \nu_2$. But because of this imposed constraint, the clusterings $\{\{y_1, y_3\}, \{y_2, y_4\}\}$ and $\{\{y_2, y_4\}, \{y_1, y_3\}\}$ can not be regarded as identical.

S-7. SUMMARIZATION OF THE POSTERIOR DISTRIBUTION OF MIXTURE DENSITIES

Note that the mixture setup induces a posterior distribution on mixture densities of the form

$$f(y_i | \boldsymbol{\nu}_k, \boldsymbol{\tau}_k, \boldsymbol{\pi}_k, k) = \sum_{j=1}^k \pi_j \sqrt{\frac{\tau_j}{2\pi}} \exp \left\{ -\frac{\tau_j}{2} (y_i - \nu_j)^2 \right\}. \quad (\text{S-7.1})$$

In other words, the set-up provides a way to make Bayesian inference regarding the unknown density of the observed data y_1, \dots, y_n . An obvious candidate of such density estimate is the unconditional posterior expectation of the function

$$f(x | k, \boldsymbol{\nu}_k, \boldsymbol{\tau}_k, \boldsymbol{\pi}_k) = \sum_{j=1}^k \pi_j \sqrt{\frac{\tau_j}{2\pi}} \exp \left\{ -\frac{\tau_j}{2} (x - \nu_j)^2 \right\}; \quad -\infty < x < \infty, \quad (\text{S-7.2})$$

with respect to the posterior of $k, \boldsymbol{\nu}, \boldsymbol{\tau}_k, \boldsymbol{\pi}_k$. For empirical purposes, one can just average $f(x | k, \boldsymbol{\nu}_k, \boldsymbol{\tau}_k, \boldsymbol{\pi}_k)$ over TTMC MC samples of $k, \boldsymbol{\nu}, \boldsymbol{\tau}_k, \boldsymbol{\pi}_k$.

Note, however, that the posterior expectation (or the corresponding empirical average) fails to retain the finite mixture form of the resultant density estimate (see also Richardson & Green (1997)). More importantly, although this averaging yields a point density estimate, hitherto there does not seem to be any attempt to quantify the uncertainty of the posterior distribution of the densities having the mixture form with unknown number of components.

Motivated by Mukhopadhyay, Bhattacharya & Dihidar (2011) who propose a methodology for obtaining the modes and any desired highest posterior density credible regions associated with the posterior distribution of clusterings, here we attempt the same for the posterior distribution of densities having form (S-7.1). Following Mukhopadhyay et al. (2011) here we propose a definition of ‘‘central density’’:

Definition 1 A density f_0 is ‘‘central’’ which, for any $\epsilon > 0$ satisfies the following equation:

$$P(\{f : d(f_0, f) < \epsilon\}) = \sup_g P(\{f : d(g, f) < \epsilon\}), \quad (\text{S-7.3})$$

for some suitable metric d .

In this article, we consider the sup-norm metric between any two density functions f and h , given by $d(f, h) = \sup_{-\infty < x < \infty} |f(x) - h(x)|$. For empirical purpose we evaluate this metric at discrete equidistant points x_0, x_1, \dots, x_m covering the effective support of the densities in question.

Observe that f_0 is the global mode of the posterior distribution of densities as $\epsilon \rightarrow 0$. If the distribution of f is unimodal, then the central density remains the same for all $\epsilon > 0$. However, for multimodal distributions, the central density varies with ϵ , signifying existence of local modes, which we define as follows.

Definition 2 We define f_{loc} to be a local mode if

$$\lim_{\epsilon \downarrow 0} \frac{\sup_{h \in \mathcal{N}(f_{loc}, \eta)} P(\{f \in \mathcal{N}(f_{loc}, \eta) : d(f, h) < \epsilon\})}{P(\{f \in \mathcal{N}(f_{loc}, \eta) : d(f, f_{loc}) < \epsilon\})} = 1, \quad (\text{S-7.4})$$

where $\mathcal{N}(f_{loc}, \eta) = \{f : f(f_{loc}, f) < \eta\}$ for some $\eta > 0$.

Note that unlike the distribution of clusterings considered by Mukhopadhyay et al. (2011), which is discrete, the distribution of the mixture densities of the form (S-7.2) is continuous; this is clear since although k , the number of mixture components is at most countable, the parameters ν , τ and π are continuous. Hence, although obtaining the global mode in the case of clusterings is an arduous task, here our problem is relatively easier.

It is nevertheless clear that without the aid of empirical methods the central density function defined in (S-7.3) can not be obtained. Using available TTMC samples $\{f^{(j)}; j = 1, \dots, N\}$ of length N , the latter sufficiently large, useful empirical methods can be devised, as we demonstrate in the next section.

S-7.1 Empirical definition of central density function

We define that density $f^{(j)}$ as ‘‘approximately central,’’ which, for a given small $\epsilon > 0$, satisfies the following equation:

$$f^{(j)} = \arg \max_{1 \leq i \leq N} \frac{1}{N} \# \{f^{(\ell)}; 1 \leq \ell \leq N : d(f^{(i)}, f^{(\ell)}) < \epsilon\}. \quad (\text{S-7.5})$$

The central density $f^{(j)}$ is easily computable and the ergodic theorem ensures convergence of $f^{(j)}$ almost surely to the true central density f_0 .

S-7.2 Construction of desired credible regions of densities

Given a central density $f^{(j)}$, an approximate 95% posterior density credible region is given by the set $\{f^{(\ell)}; 1 \leq \ell \leq N : d(f^{(\ell)}, f^{(j)}) < \epsilon^*\}$, where ϵ^* is such that

$$\frac{1}{N} \# \{f^{(\ell)}; 1 \leq \ell \leq N : d(f^{(\ell)}, f^{(j)}) < \epsilon^*\} \approx 0.95. \quad (\text{S-7.6})$$

In (S-7.6) ϵ^* can be chosen adaptively by starting with $\epsilon^* = 0$ and then slightly increasing ϵ^* by a quantity ζ until (S-7.6) is satisfied. In our applications, we chose $\zeta = 10^{-5}$. Approximate highest posterior density (HPD) regions can be constructed by taking the union of the highest density regions. Following Mukhopadhyay et al. (2011) we next discuss an adaptive methodology for constructing HPD regions.

S-7.3 Construction of desired HPD regions of densities

Assume that there are ℓ modes, $\{f_1^*, \dots, f_\ell^*\}$, obtained by varying ϵ of the neighborhoods $\{f : d(f, f^{(i)}) < \epsilon\}; i = 1, \dots, N$. Consider the regions $S_j = \{f : d(f_j^*, f) < \epsilon_j^*\}; j = 1, \dots, \ell$. Set, initially, $\epsilon_1^* = \epsilon_2^* = \dots = \epsilon_\ell^* = 0$.

- (i) For $i = 1, \dots, N$, if the i -th TTMC MC realization $f^{(i)}$ does not fall in S_j for some j , then increase ϵ_j^* by a small quantity, say, ζ .
- (ii) Calculate the probability of $\cup_{j=1}^{\ell} S_j$ as $P = \#\{\cup_{j=1}^{\ell} S_j\}/N$.
- (iii) Repeat steps (i) and (ii) until $P \approx 0.95$ or any desired probability.

In step (i) we implicitly assume that, since $f^{(i)} \notin S_j$, S_j must be a region with low probability, so its expansion is necessary to increase the probability. We achieve this expansion by increasing ϵ_j^* by ζ . Thus the sets S_j are selected adaptively, by adaptively increasing ϵ_j^* . The desired approximate HPD region is then the final union of the S_j 's.

S-8. TTMC MC CONVERGENCE DIAGNOSTICS FOR THE MIXTURE PROBLEM

S-8.1 Difficulties of convergence assessment in variable dimensional problems

A particularly problematic area in variable dimensional problems is ascertaining whether or not the underlying MCMC algorithm has converged to the stationary distribution. The reason that

the convergence assessment problem in transdimensional set-ups is more difficult in comparison with the fixed-dimensional counterpart is that the dimensionality of the parameters, as well as their interpretations, can vary with the iterations. The difficulty of the problem did motivate researchers to devise appropriate measures of convergence diagnostics; however, to date, the developments are relatively few. Sisson (2005) provide a comprehensive review of such developments, along with their shortcomings. The shortcomings generally pertain to marginal, rather than joint convergence assessment, computational burden that comes with implementing many independent runs of the sampler, and of course, various assumptions which may be difficult to validate in practice.

S-8.2 A new convergence diagnostic method for mixtures with known or unknown number of components

Armed with our metric-based methodology we now provide a convergence diagnostic method for the challenging variable dimensional mixture problem. Following the same principle as Mukhopadhyay et al. (2011), we divide our TTMC sample of size N into m equal parts, each part having the same size N/m , assuming divisibility of N by m . For each such subsample of size N/m , we compute a central density function and the corresponding approximate 95% credible region. If the m credible regions thus obtained are close to each other, one can safely infer that the m subsamples arose from the same stationary distribution.

Analogous to the convergence diagnostic method Mukhopadhyay et al. (2011), our method can assess if two credible regions corresponding to two separate subsamples are close to each other. Let $(CR_{\epsilon_1}, \epsilon_1)$ and $(CR_{\epsilon_2}, \epsilon_2)$ denote the 95% credible regions and the corresponding radii obtained from any two subsamples. Suppose that $\eta_1 > 0$ is the *least positive value* such that $CR_{\epsilon_1 + \eta_1} \supseteq CR_{\epsilon_2}$, and also suppose that $\eta_2 > 0$ is the *least positive value* such that $CR_{\epsilon_2 + \eta_2} \supseteq CR_{\epsilon_1}$. Then, if both the increments η_1, η_2 are sufficiently small, then the 95% credible regions CR_{ϵ_1} and CR_{ϵ_2} can be said to be “close”.

Currently in this paper we restrict ourselves to mixture problems only. But from the construction it is clear that our proposed diagnostics is readily applicable to function estimation context. These developments, in our opinion, can play important roles in various applications involving

random basis function expansions, for instance, in nonparametric regression and functional data analysis. Since basis function expansions typically involve unknown number of summands, TTMCMC based inference along with our procedure for summarizing posterior distribution of functions, are expected to constitute a very interesting and important combination for such challenging data analysis. Indeed, the functions may also be the modeled density (either discrete or continuous) associated with the likelihood, indicating that our methods are very generally applicable. Since convergence in variable dimensional problems is particularly difficult to assess, our methodology, which seems to provide a reliable convergence assessment criterion, perhaps provides a significant advance.

S-9. FURTHER SIMULATION STUDIES WITH THE GAMMA MIXTURES WITH DIFFERENT DATA SIZES

In our simulation studies so far, we considered data sets of size 400. We now experiment by varying the data sizes for the four mixtures and note the changes for the TTMCMC based posteriors of k .

S-9.1 1-component mixture

For a data set of size 60, the posterior distribution of k was concentrated on $k = 1, 2, 3, 4$ with probabilities 0.9308, 0.0647, 0.0041 and 0.0004, respectively, hence not differing too significantly from our reported results when the data size was 400. In this case, the overall acceptance rate turned out to be 0.089759, the birth rate was 0.016024, the death rate was 0.357057, and 0.151372 was the no-change rate. Further experiments with data sets larger than 60 revealed that the posterior distribution of k increasingly concentrated around $k = 1$. For instance, with data size 1000, the posterior of k assigned probabilities 0.9798, 0.02 and 0.0002 to $k = 1, 2, 3$, respectively. In this case, the overall acceptance rate was 0.022835, and the birth, death, no change rates were 0.00188, 0.03401 and 0.043119, respectively. For data sizes smaller than 60, the information seemed to be insufficient to precisely capture $k = 1$.

S-9.2 2-component mixture

Since this is perhaps the most challenging example in that it is hard to distinguish two mixture components, it is easy to anticipate that a somewhat large data set is necessary to capture the true information. As such, we find that data sets of size 300 or more produces good results. Indeed, for a dataset of size 300, we obtain the posterior probabilities of $k = 1, 2, 3$ to be 0.1917, 0.8037 and 0.0046. The overall acceptance rate, birth, death and the no-change rates are given by 0.064524, 0.001132, 0.002295 and 0.158743, respectively. Thus, unlike the data of size 400, we no longer obtain point posterior mass at $k = 2$, although the truth (namely, 2 components) has clearly been identified.

S-9.3 3-component mixture

In this example, we consider a consistency check by considering a dataset of size 1000 and expecting our TTMC MC to give close to point posterior mass to 3 components, given that it has given point posterior mass to 3 components for the data of size 400. On implementation of TTMC MC, we find that consistency is indeed attained. The posterior probabilities for $k = 3$ and $k = 4$ are 0.9987 and 0.0013, respectively, while all other values of k received zero posterior mass. The overall acceptance rate is 0.034308, the overall birth and death rates are 0.000028 and 0.000035, respectively, while the no-change rate is 0.102759.

S-9.4 4-component mixture

Since the 4-component mixture seems to be somewhat easy to identify, we investigate if TTMC MC can identify the true number of components even for much smaller datasets. With our implementation Indeed, for a dataset of size 170, we find that $k = 4, 5, 6, 7$ receive posterior probabilities 0.7006, 0.2932, 0.0057 and 0.0005, respectively, while the other values of k receive zero posterior probability. In this case, the overall acceptance, birth, death and the no-change rates are 0.026976, 0.000284, 0.000289 and 0.080268, respectively.

S-10. COMPARISON BETWEEN ADDITIVE TTMC MC AND RANDOM WALK RJMCMC IN NORMAL MIXTURES WITH RESPECT TO THE THREE REAL DATA SETS

S-10.1 Comparison in enzyme data

The implementation of random walk RJMCMC took 38 minutes and 29 seconds to yield 10,000 realizations following a burn-in of 375,000 iterations, after storing one in 150 iterations out of further 15,00,000 iterations after the burn-in period.

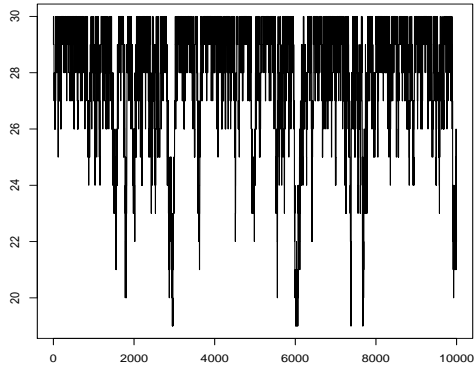
The RJMCMC algorithm yielded an overall acceptance rate 0.05605344, which is slightly larger than that of TTMC MC. The birth, death and no-change rates turned out to be 0.007919, 0.005228 and 0.138663, respectively. The birth and death rates are significantly larger than in TTMC MC, while the no-change rate is smaller.

However, we obtained $\eta_1 = 0.11463$ and $\eta_2 = 0.10610$, which are significantly larger than in TTMC MC, indicating better convergence of TTMC MC. Moreover, the trace plots of k displayed in Figure S-1 show that very large number of components are favored by RJMCMC, showing that the chain is far from convergence. The main issue here seems to be the dependence of the acceptance rate on the proposal density $\prod_{i=1}^3 \varrho(u_i)$. Since, $\prod_{i=1}^3 \varrho(u_i)$, the product of left truncated standard normal densities, is less than one, it follows that the acceptance probability of the birth move is higher than that of the death move. This explains the large number of components favored by random walk RJMCMC, clearly impeding convergence.

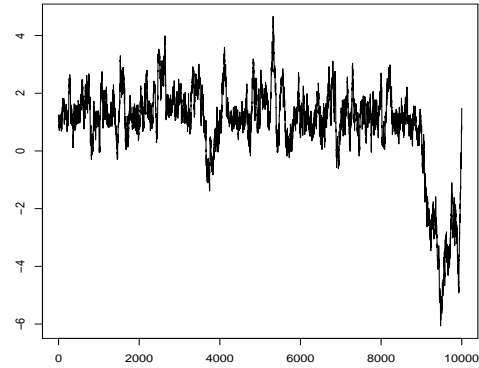
S-10.2 Comparison in acidity data

With RJMCMC based on random walk, the time for implementation is 11 minutes and 25 seconds, much larger than that of TTMC MC. The overall acceptance rate turned out to be 0.196064, smaller than that of TTMC MC. The birth, death and no-change rates are 0.012153, 0.012177 and 0.56334, respectively, that is, the birth and death rates are significantly larger than in TTMC MC while the no-change rate is smaller.

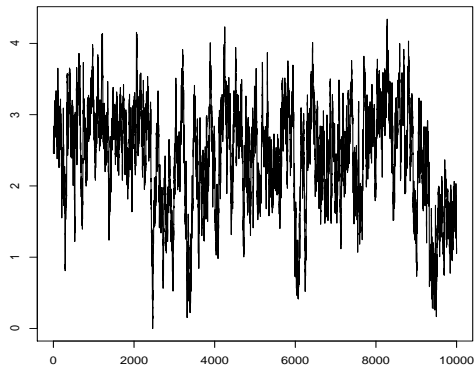
As before, however, for this RJMCMC implementation, $\eta_1 = 0.03616$ and $\eta_2 = 0.03522$, showing that the convergence is much inferior compared to TTMC MC. Here, k assigned positive



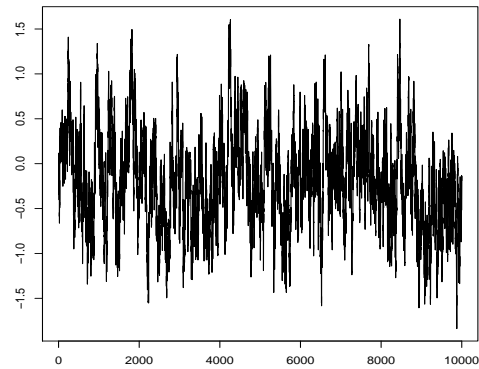
(a) Trace plot of k .



(b) Trace plot of ν_1 .

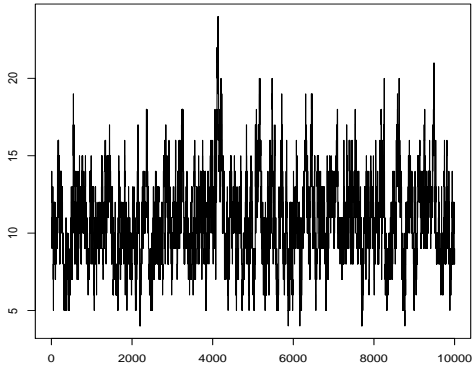


(c) Trace plot of τ_1 .

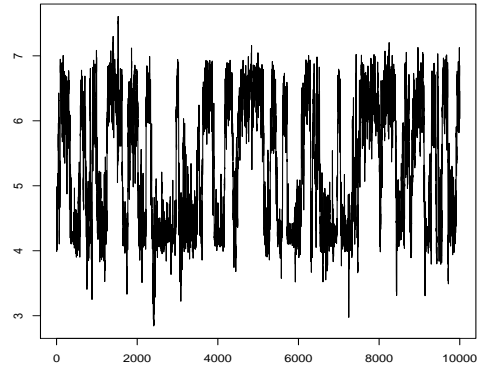


(d) Trace plot of ω_1 .

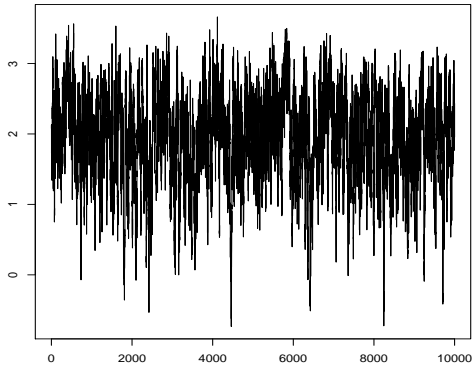
Figure S-1: **RJMCMC for the enzyme data:** Trace plots of k , ν_1^* , τ_1^* and ω_1 .



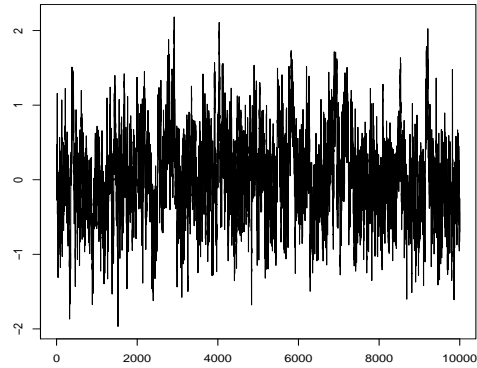
(a) Trace plot of k .



(b) Trace plot of ν_1^* .



(c) Trace plot of τ_1^* .



(d) Trace plot of ω_1 .

Figure S-2: **RJMCMC for the acidity data:** Trace plots of k , ν_1^* , τ_1^* and ω_1 .

posterior probabilities to large values and gave zero mass to $k = 2$ and $k = 3$, which received full posterior mass from TTMCMC implementation, again showing that in comparison with TMCMC, RJMCMC tends to assign larger posterior mass to larger number of components.

S-10.3 Comparison in galaxy data

In this case, RJMCMC took 11 minutes and 3 seconds for implementation, which is significantly higher than the computing time of TTMCMC. Here the acceptance rate of RJMCMC turned out to be as low as 0.000008, and the birth, death, no-change rates are 0.000007, 0.000008 and 0.00001,

respectively. Consequently, as the trace plots of Figure S-3 show, Bayesian inference based on RJMCMC would be absolutely hopeless! The reason for such miserable performance of RJMCMC particularly in this example is that here the local modes are well-separated from one another and are concentrated on much smaller regions compared to the previous examples, which, in accordance with high-dimensionality, render the jump size of the proposal too large for RJMCMC for adequate performance. Low dimensionality on the other hand ensures excellent performance of TTMCMC.

S-10.4 Comparison of the autocorrelations associated with additive TTMCMC and random walk RJMCMC in the three real data examples

The comparisons of TTMCMC and RJMCMC with respect to the autocorrelations of k , associated with the three real data sets, are provided in Figure S-4. TTMCMC outperforms RJMCMC very significantly.

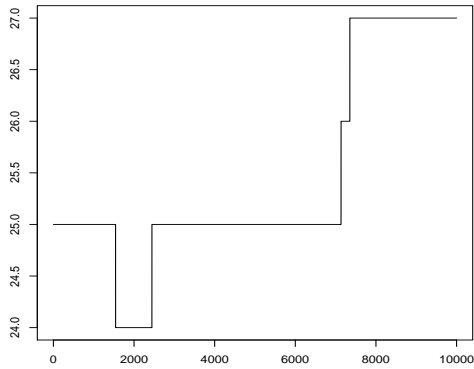
S-11. COMPARISONS BETWEEN ADDITIVE TTMCMC AND RJMCMC WITH RESPECT TO THE PRIOR STRUCTURE AND THE ALGORITHM OF RICHARDSON AND GREEN (1997) IN THE GALAXY DATA CONTEXT

In our main manuscript we have shown that for the galaxy data set, additive RJMCMC exhibits poor performance with respect to the prior we have chosen. We now consider the prior structure of Richardson & Green (1997) (henceforth, RG) and compare the results of our additive TTMCMC with the results reported in RG obtained by their RJMCMC algorithm.

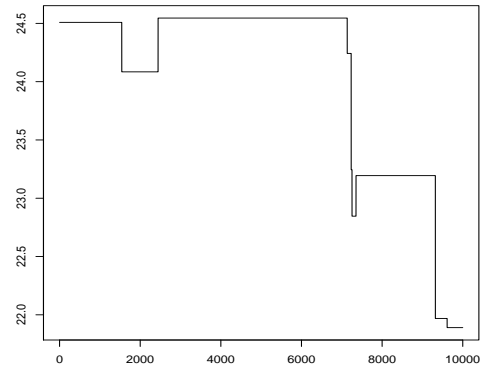
Recall from Section 8.1 of DB that the data points y_1, \dots, y_n are assumed to be *iid* as the normal mixture of the following form: for $i = 1, \dots, n$

$$f(y_i | \boldsymbol{\nu}_k, \boldsymbol{\tau}_k, \boldsymbol{\pi}_k, k) = \sum_{j=1}^k \pi_j \sqrt{\frac{\tau_j}{2\pi}} \exp \left\{ -\frac{\tau_j}{2} (y_i - \nu_j)^2 \right\},$$

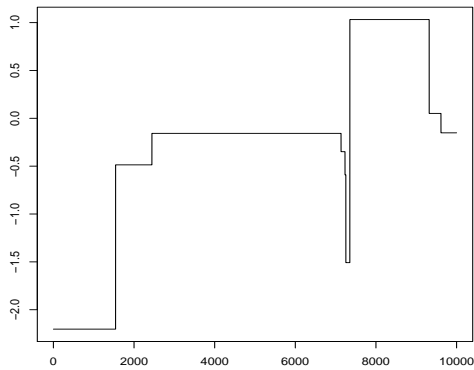
where $\boldsymbol{\nu}_k = (\nu_1, \dots, \nu_k)$, $\boldsymbol{\tau}_k = (\tau_1, \dots, \tau_k)$, and $\boldsymbol{\pi}_k = (\pi_1, \dots, \pi_k)$. Given $k > 0$, for each j , $-\infty < \nu_j < \infty$, $\tau_j > 0$, $0 < \pi_j < 1$ such that $\sum_{j=1}^k \pi_j = 1$.



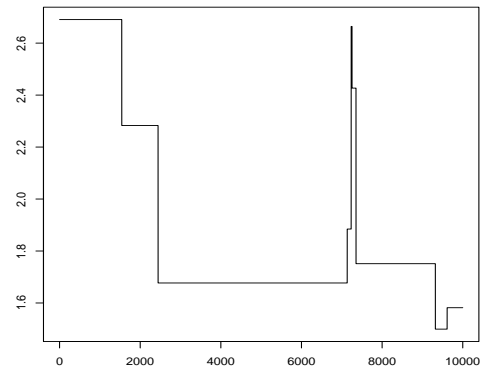
(a) Trace plot of k .



(b) Trace plot of ν_1^* .

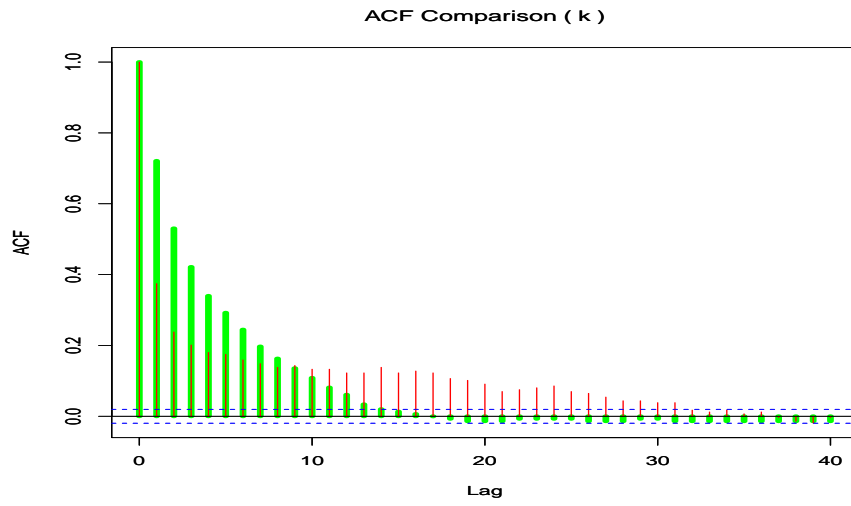


(c) Trace plot of τ_1^* .

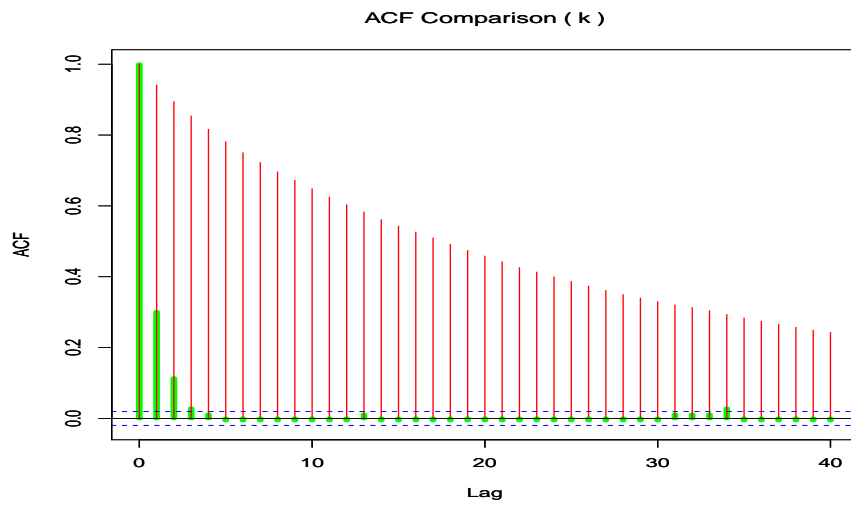


(d) Trace plot of ω_1 .

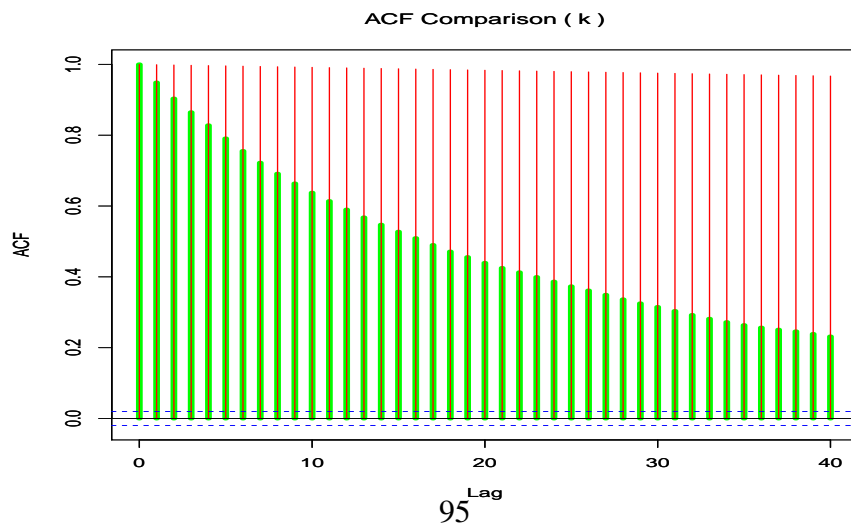
Figure S-3: **RJMCMC for the galaxy data:** Trace plots of k , ν_1^* , τ_1^* and ω_1 . Poor performance of the RJMCMC chain is exhibited by the above panels.



(a) Enzyme.



(b) Acidity.



(c) Galaxy.

Figure S-4: Autocorrelation comparisons between RIMCMC and TTMCMC for enzyme.

S-11.1 Prior structure

Following RG, we assume that

$$\beta \sim \mathcal{G}(g, h); \quad (\text{S-11.1})$$

$$[\tau_j] \sim \mathcal{G}(\alpha, \beta); \quad (\text{S-11.2})$$

$$[\nu_j] \sim N(\xi, \kappa^{-1}); \quad (\text{S-11.3})$$

$$[\pi_1, \dots, \pi_k | k] \sim \mathcal{D}(\delta, \dots, \delta); \quad (\text{S-11.4})$$

$$[k] \sim \text{Discrete Uniform} \{1, 2, \dots, k_{\max}\}. \quad (\text{S-11.5})$$

Furthermore, in order to somehow enforce identifiability, RG assume that $-\infty < \nu_1 < \nu_2 < \dots < \nu_k < \infty$, for all $k = 1, \dots, k_{\max}$. RG consider $\alpha > 1 > g$ to express the belief that $\sigma_j^2 = \tau_j^{-1}$ are similar, without being informative about their absolute size. Specifically for the galaxy data, RG set $g = 0.2$, $h = 0.016$, $\alpha = 2$, $\kappa = 0.0016$, $\xi = 21.73$, $\delta = 1$ and $k_{\max} = 30$.

We consider two implementations of additive TTMC MC when the above prior structure is considered; in one implementation we consider the above prior as it is and simulate β in an additive TMC MC set-up simultaneously with the joint additive TTMC MC step, and in the other case, we keep β fixed as in Cappé et al. (2003). When β is simulated, we reparameterize as $\exp(\beta^*)$, where $\beta^* \sim \log(\mathcal{G}(g, h))$.

S-11.2 Results of additive TTMC MC with RG's prior when β is updated using additive TMC MC

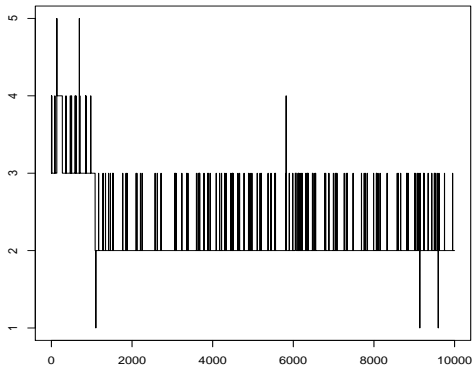
For all the variables including β , we found the optimum scale for the additive transformation to be 0.5. As in our main manuscript, here also we assume a burn-in of 300,000 iterations, and a further 1,500,000 iterations, storing one in 150 iterations, thus obtaining a total of 10,000 realizations from the posterior distribution. It took 1 minute and 20 seconds in our laptop and yielded an acceptance rate 0.089363. The birth, death and no-change rates are 0.002298, 0.002336 and 0.262948, respectively. The resulting trace plots and the goodness-of-fit diagram are provided in Figures S-1 and S-2, respectively. In this case, k takes the values 1, 2, 3, 4, 5 with probabilities 0.0003, 0.8766, 0.1079, 0.015 and 0.0002, respectively, which are quite different from the posterior distribution of k obtained by RG. Indeed, RG obtained much larger values of k , with significant posterior proba-

bilities. As we argued before, the inherent bias of RJMCMC methods for larger values of k in finite samples seems to be responsible for this. The reason that we think that k should not be large in this case is the following. The prior on the τ 's is set so that they are similar, and this does not seem to be a good strategy for exploring relatively large number of modal regions with highly different local variabilities. Thus, the prior seems to be too smooth for the purpose, which is reflected in the results that we obtained.

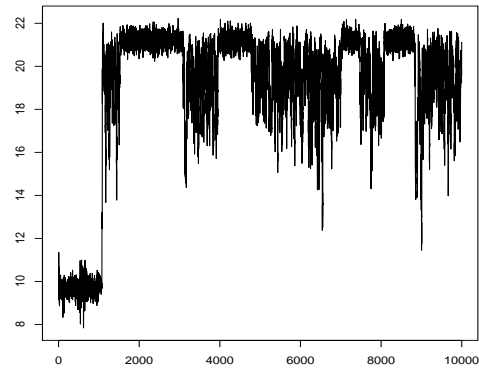
However, note that the trace plots visually indicate that the chain perhaps did not stabilize in the initial stages, and so, to ensure proper convergence, we doubled the burn-in period from 300,000 to 600,000. In this case, the time taken is 1 minute 28 seconds and the overall acceptance rate turned out to be 0.09077, while the birth, death and no-change rates are 0.002361, 0.002394 and 0.267125, respectively. The modified diagrams are provided in Figures S-3 and S-4. The current as well as the previous trace plots clearly indicate that the posteriors of ν 's and τ 's are bi-modal; even the trace plots of the weights are suggestive of mild bi-modality. Importantly, the trace plots now indicate proper convergence and now k takes the values 1, 2, 3, 4 with posterior probabilities 0.0002, 0.9842, 0.0155, 0.0001 respectively. However, Figure S-4 shows that the minor modes of the histogram are much ill-captured compared to that in Figure S-2. In fact, the current posterior predictive densities are unimodal. Thus larger values of k in Figure S-1 are not indicative of better exploration, but non-convergence of the chain, even after a large number of iterations. Since larger number of mixture components can often *illusively* result in good fit of the minor modes of the histogram, our exposition shows that one needs to exercise caution while analysing larger values of k .

The above exposition and arguments are applicable to RJMCMC as well. In fact, RG use $\mathcal{B}(2, 2)$, the Beta distribution with both parameters 2, as a proposal for their dimension changing move. Since with probability approximately 0.21 any realized value of $\mathcal{B}(2, 2)$ has density less than one, it follows from the discussion in the third point following Algorithm 3.1 of our main manuscript that the RJMCMC algorithm of RG is influenced by its bias towards larger values of k for finite samples, where the actual posterior does not support more than 4 components.

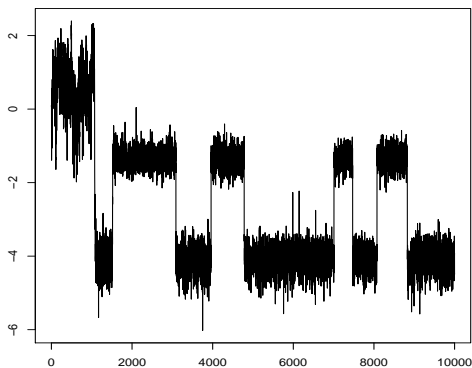
In other words, it seems that the algorithm of RG needed much longer run to even attain conver-



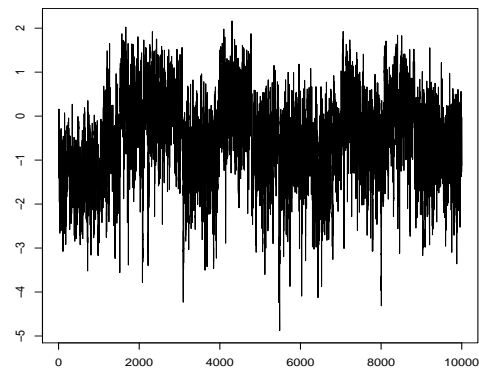
(a) Trace plot of k .



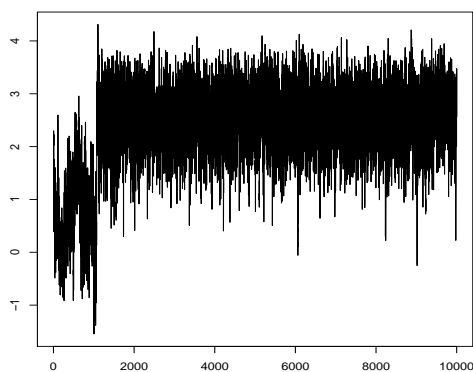
(b) Trace plot of ν_1^* .



(c) Trace plot of τ_1^* .



(d) Trace plot of ω_1 .



(e) Trace plot of β^* .

Figure S-1: **TTMCMC for the galaxy data with RG prior when β is random and burn-in = 300,000:** Trace plots of k , ν_1^* , τ_1^* , ω_1 and β^* . 98

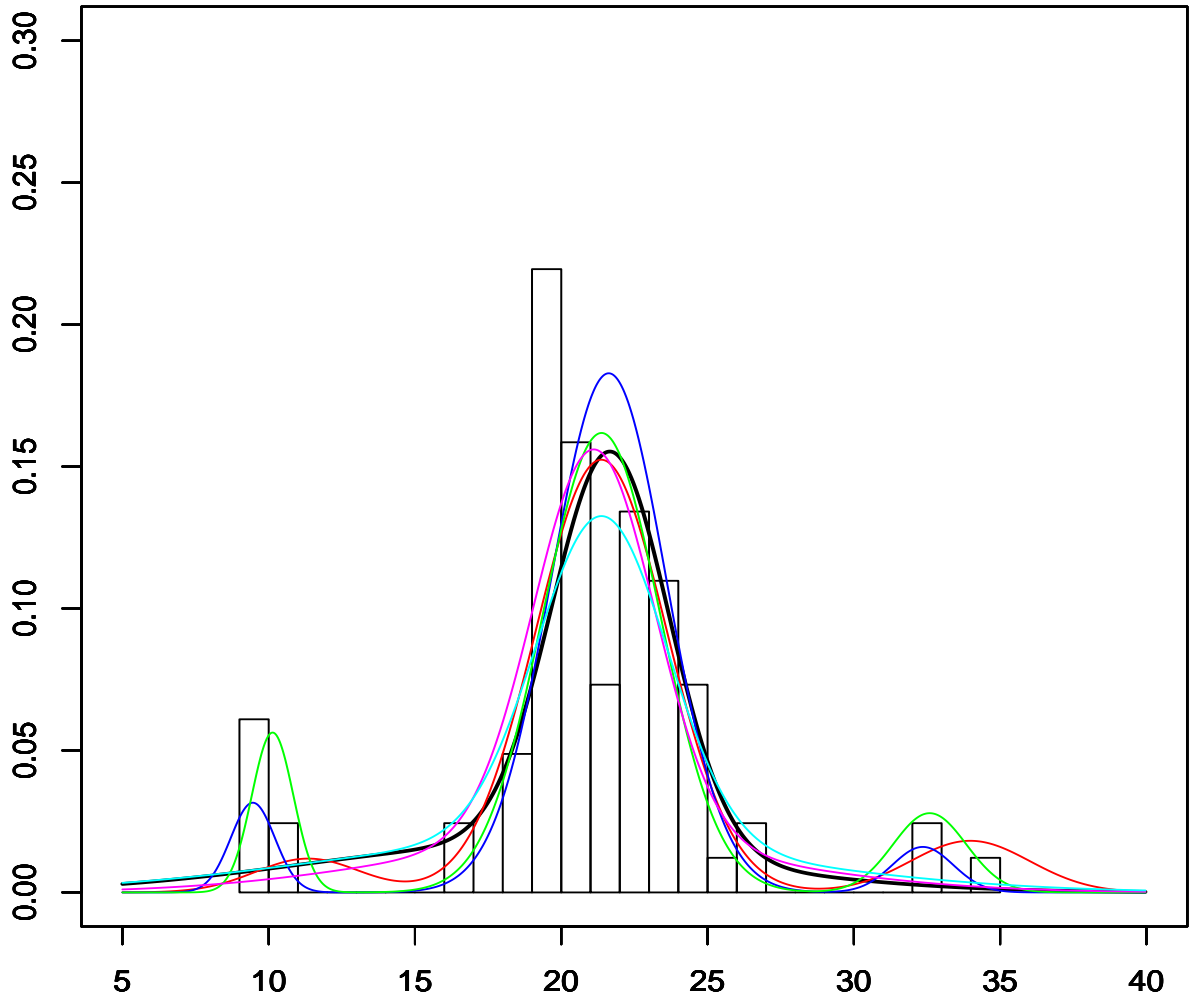


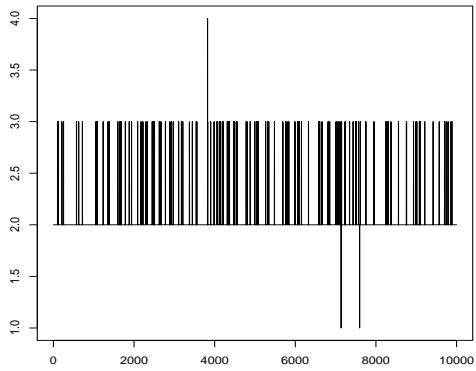
Figure S-2: **TTMCMC for the galaxy data when β is random and burn-in = 300,000:** Goodness of fit of the posterior distribution of densities (colored curves) to the observed data (histogram). The thick black curve is the modal density and the other colored curves are some densities contained in the 95% HPD.

gence, and that the burn-in period of just 100,000 that RG considered (see page 742) seems to be too small given that even with 300,000 as burn-in, Figure S-1 clearly showed lack of convergence of our TTMC MC algorithm.

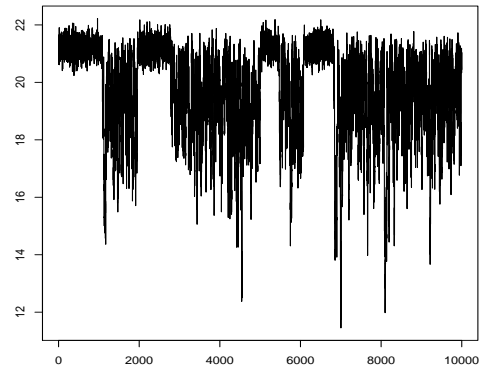
S-11.3 Results of additive TTMC MC with RG's prior when β is fixed

We now consider another experiment with β fixed. This is motivated by Cappé et al. (2003) who set $\alpha = 0.5$ and $\beta = 0.001$. In this experiment we consider these values, keeping the remaining prior structure the same as RG for the galaxy data. With this prior and our TTMC MC algorithm with all the scales of the additive transformations fixed at 0.5 we consider a burn-in of 15,00,000 iterations. Indeed, our chain did not converge even in 600,000 iterations, however, the burn-in we chose turned out to be many more than sufficient for convergence. We thus implemented our TTMC MC algorithm for 30,00,000 iterations, storing one in 150 iterations after the burn-in period. We obtained an overall acceptance rate 0.054212. The birth, death and the no-change rates turned out to be 0.004234, 0.004259 and 0.154383, respectively. The time taken for the implementation is about 4 minutes.

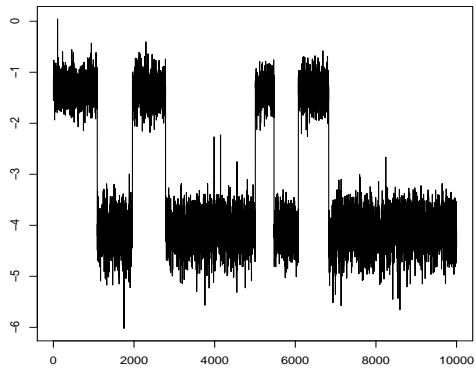
The relevant plots are shown in Figures S-5 and S-6. Now, k takes as large values as required, with significant posterior probabilities. Indeed, k takes the values 2 to 8 with posterior probabilities 0.0002, 0.4998, 0.3249, 0.1281, 0.0385, 0.0073 and 0.0012. Expectedly, as shown in Figure S-6, the posterior predictive distribution provides reasonably good fit to the histogram, capturing the minor modes much better than with the RG prior. The reason for much improved performance in this case with fixed β is that the τ 's are now *a priori* independent and lets the data speak for itself, enabling the posterior to adequately learn about the modal regions from the data.



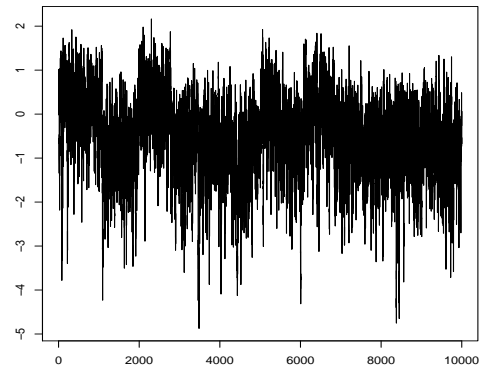
(a) Trace plot of k .



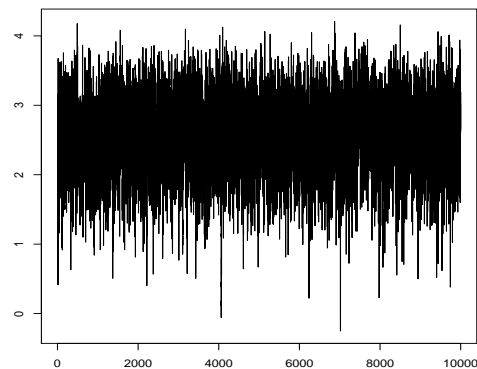
(b) Trace plot of ν_1^* .



(c) Trace plot of τ_1^* .



(d) Trace plot of ω_1 .



(e) Trace plot of β^* .

Figure S-3: TTMC for the galaxy data with RG prior when β^* is random and burn-in = 600,000: Trace plots of k , ν_1^* , τ_1^* , ω_1 and β^* . 101

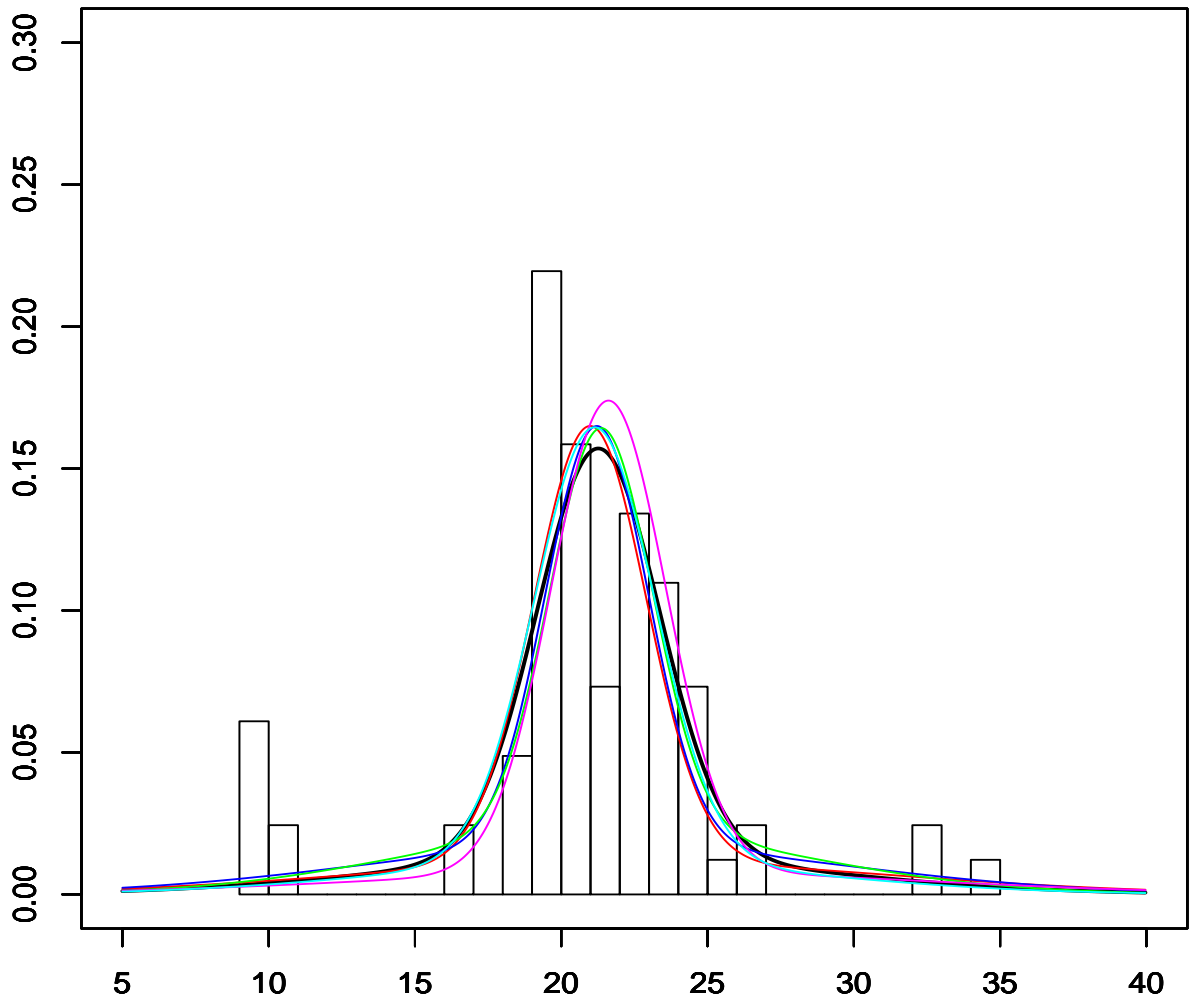
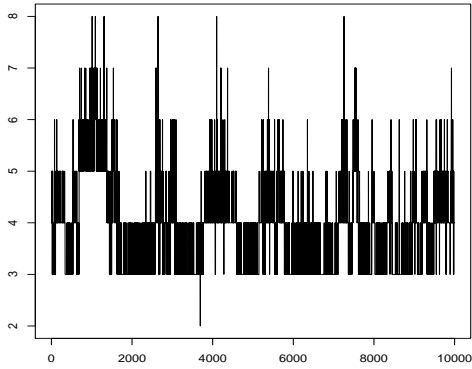
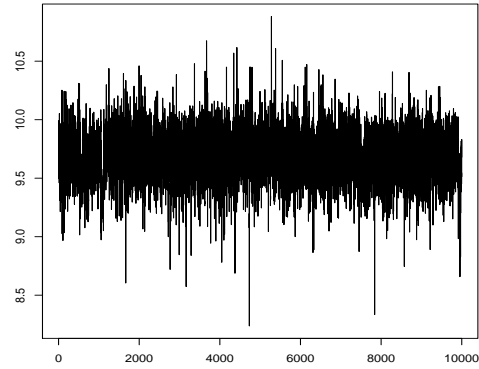


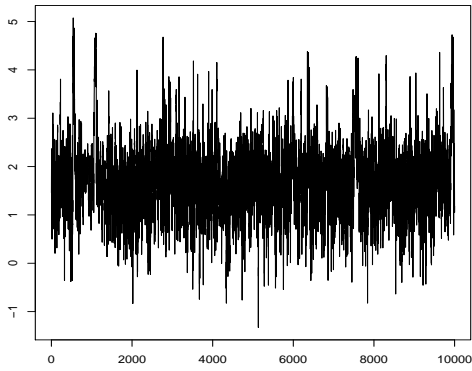
Figure S-4: **TTMCMC for the galaxy data when β is random and burn-in = 600,000:** Goodness of fit of the posterior distribution of densities (colored curves) to the observed data (histogram). The thick black curve is the modal density and the other colored curves are some densities contained in the 95% HPD.



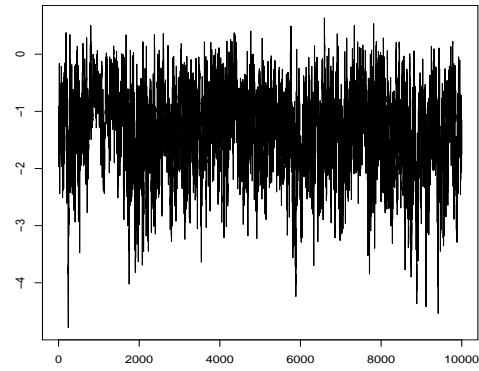
(a) Trace plot of k .



(b) Trace plot of ν_1^* .



(c) Trace plot of τ_1^* .



(d) Trace plot of ω_1 .

Figure S-5: **TTMCMC for the galaxy data with RG prior for fixed β** : Trace plots of k , ν_1^* , τ_1^* and ω_1 when β is fixed.

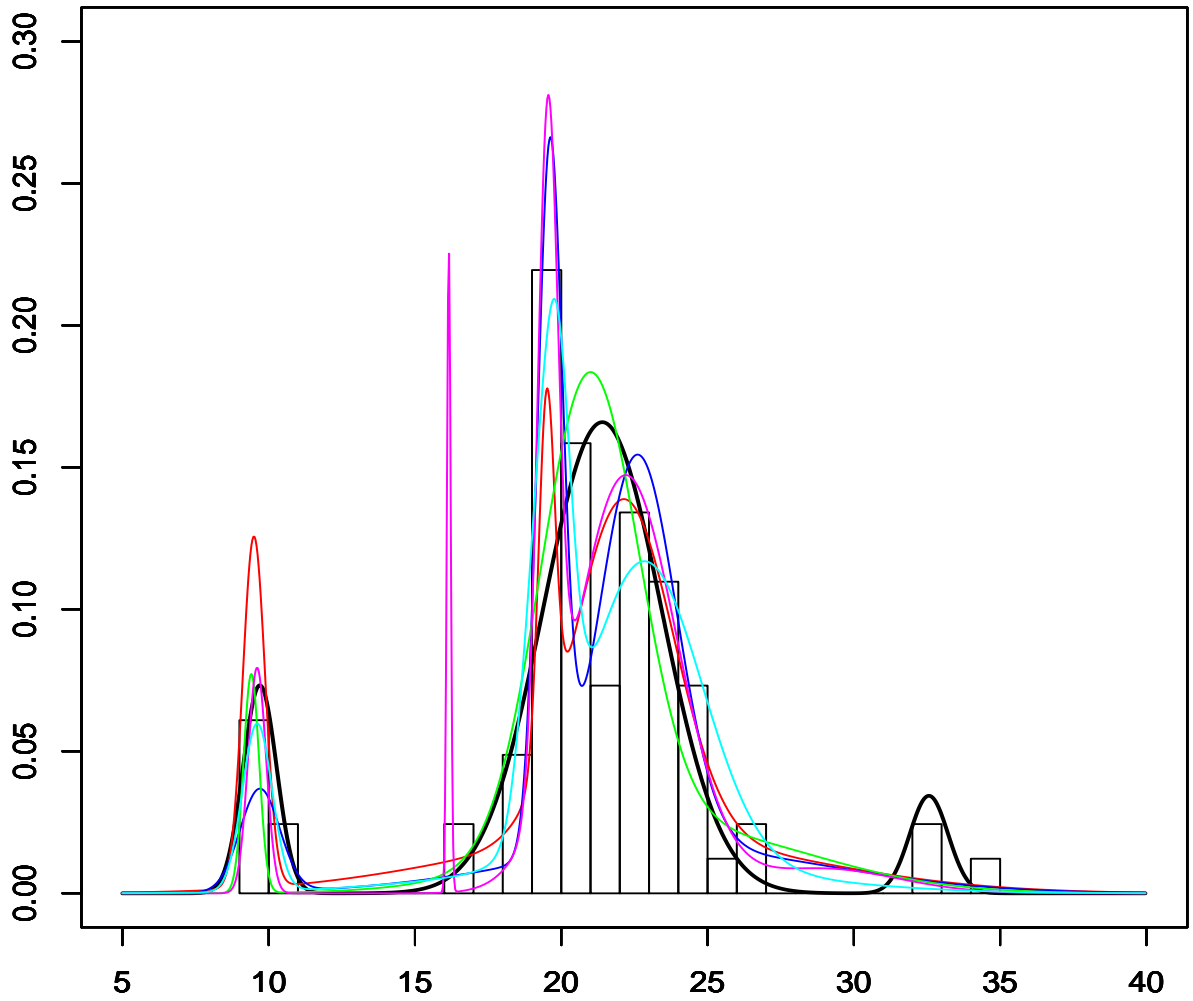


Figure S-6: **TTMCMC for the galaxy data for fixed β** : Goodness of fit of the posterior distribution of densities (colored curves) to the observed data (histogram). The thick black curve is the modal density and the other colored curves are some densities contained in the 95% HPD.

REFERENCES

- Al-Awadhi, F., & Jennison, C. (2004), "Improving the Acceptance Rate of Reversible-Jump MCMC Proposals," *Statistics and Probability Letters*, 69, 189–198.
- Bhattacharya, S. (2008), "Gibbs Sampling Based Bayesian Analysis of Mixtures with Unknown Number of Components," *Sankhya. Series B*, 70, 133–155.
- Brooks, S. P., Giudici, P., & Roberts, G. O. (2003), "Efficient Construction of Reversible-Jump Markov Chain Monte Carlo Proposal Distributions (with discussion)," *Journal of the Royal Statistical Society. Series B*, 65, 3–39.
- Cappé, O., Robert, C. P., & Rydén, T. (2003), "Reversible Jump, Birth-and-Death and More General Continuous Time Markov Chain Monte Carlo Samplers," *Journal of the Royal Statistical Society. Series B*, 65, 679–700.
- Chu, J. H., Clyde, M. A., & Liang, F. (2009), "Bayesian Function Estimation Using Continuous Wavelet Dictionaries," *Statistica Sinica*, 19, 1419–1438.
- Das, M., & Bhattacharya, S. (2015a), "Supplement to "Transdimensional Transformation based Markov Chain Monte Carlo: with Mixture Illustrations",". Supplementary Document.
- Das, M., & Bhattacharya, S. (2015b), "Transdimensional Transformation based Markov Chain Monte Carlo: with Mixture Illustrations, ". Submitted.
- Das, M., & Bhattacharya, S. (2016), "Nonstationary Nonparametric Bayesian Spatio-Temporal Modeling Using Kernel Convolution of Order Based Dependent Dirichlet Process, ". Submitted. Available at "<http://arxiv.org/pdf/1405.4955>".
- Dellaportas, P., & Forster, J. J. (1999), "Markov Chain Monte Carlo Model Determination for Hierarchical and Graphical Log-Linear Models," *Biometrika*, 86, 615–633.
- Dellaportas, P., Forster, J. J., & Ntzoufras, I. (2002), "On Bayesian Model and Variable Selection Using MCMC," *Statistics and Computing*, 12, 27–36.
- Dellaportas, P., & Papageorgiou, I. (2006), "Multivariate Mixtures of Normals With Unknown Number of Components," *Statistics and Computing*, 17, 57–68.
- Denison, D. G. T., Mallick, B. K., & Smith, A. F. M. (1998), "Automatic Bayesian Curve Fitting," *Journal of the Royal Statistical Society. Series B*, 60, 333–350.

- Dey, K. K., & Bhattacharya, S. (2017a), “A Brief Review of Optimal Scaling of the Main MCMC Approaches and Optimal Scaling of Additive TMCMC Under Non-Regular Cases,”. Submitted. Available at “<http://arxiv.org/pdf/1405.0913>”.
- Dey, K. K., & Bhattacharya, S. (2017b), “A Brief Tutorial on Transformation Based Markov Chain Monte Carlo and Optimal Scaling of the Additive Transformation,” *Brazilian Journal of Probability and Statistics*, . To appear. Available at “<http://arxiv.org/abs/1307.1446>”.
- Dey, K. K., & Bhattacharya, S. (2017c), “On Geometric Ergodicity of Additive and Multiplicative Transformation based Markov Chain Monte Carlo in High Dimensions,” *Brazilian Journal of Probability and Statistics*, . To appear. Also available at “Available at <http://arxiv.org/pdf/1312.0915v2.pdf>”.
- Dutta, S., & Bhattacharya, S. (2014), “Markov Chain Monte Carlo Based on Deterministic Transformations,” *Statistical Methodology*, 16, 100–116. Also available at <http://arxiv.org/abs/1106.5850>. Supplement available at <http://arxiv.org/abs/1306.6684>.
- Escobar, M. D., & West, M. (1995), “Bayesian Density Estimation and Inference Using Mixtures,” *Journal of the American Statistical Association*, 90(430), 577–588.
- Fan, Y., & Sisson, S. A. (2011), Reversible Jump MCMC., in *Handbook of Markov Chain Monte Carlo*, eds. S. Brooks, A. Gelman, G. L. Jones, & X.-L. Meng, Chapman & Hall/CRC, New York, pp. 67–87.
- Gilks, W. R., Roberts, G. O., & George, E. I. (1994), “Adaptive Direction Sampling,” *Journal of the Royal Statistical Society. Series D (The Statistician)*, 43, 179–189.
- Godsill, S. J. (2003), Discussion of “Trans-Dimensional Markov Chain Monte Carlo”, in *Highly Structured Stochastic Systems*, eds. P. J. Green, N. L. Hjort, & S. Richardson, Oxford University Press, Oxford, UK, pp. 199–203.
- Green, P. J. (1995), “Reversible jump Markov chain Monte Carlo computation and Bayesian model determination,” *Biometrika*, 82, 711–732.
- Green, P. J. (2003), Trans-dimensional Markov Chain Monte Carlo., in *Highly Structured Stochastic Systems*, eds. P. J. Green, N. L. Hjort, & S. Richardson, Oxford University Press, Oxford, UK, pp. 179–198.

- Guan, Y., & Krone, S. M. (2007), “Small-World MCMC and Convergence to Multi-Modal Distributions: From Slow Mixing to Fast Mixing,” *The Annals of Applied Probability*, 17, 284–304.
- Jain, S., & Neal, R. M. (2004), “A Split-Merge Markov Chain Monte Carlo Procedure for the Dirichlet Process Mixture Model,” *Journal of Computational and Graphical Statistics*, 13, 158–182.
- Jain, S., & Neal, R. M. (2007), “Splitting and Merging Components of a Nonconjugate Dirichlet Process Mixture Model,” *Bayesian Analysis*, 2, 445–472.
- Lee, K., Marin, J.-M., Mengersen, K., & Robert, C. P. (2009), Bayesian Inference on Mixtures of Distributions., in *Perspectives in Mathematical Sciences I, Probability and Statistics*, World Scientific, New York, pp. 165–202. Available at “<http://arxiv.org/pdf/0804.2413.pdf>”.
- Liu, J. (2001), *Monte Carlo Strategies in Scientific Computing*, New York: Springer-Verlag.
- Liu, J. S., Liang, F., & Wong, W. H. (2000), “The Multiple-Try Method and Local Optimization in Metropolis Sampling,” *Journal of the American Statistical Association*, 95, 121–134.
- Liu, J. S., & Yu, Y. N. (1999), “Parameter Expansion for Data Augmentation,” *Journal of the American Statistical Association*, 94, 1264–1274.
- Lopes, H. F., & West, M. (2004), “Bayesian Model Assessment in Factor Analysis,” *Statistica Sinica*, 14, 41–67.
- Martino, L., Elvira, V., Luengo, D., Corander, J., & Louzada, F. (2016), “Orthogonal Parallel MCMC Methods for Sampling and Optimization,” *Digital Signal Processing*, 58, 64–84.
- Møller, J., & Waagepetersen, R. P. (2004), *Statistical Inference and Simulation for Spatial Point Processes*, Boca Raton, Florida: Chapman & Hall/CRC.
- Mukhopadhyay, S., & Bhattacharya, S. (2013), “Cross-Validation Based Assessment of a New Bayesian Palaeoclimate Model,” *Environmetrics*, 24, 550–568.
- Mukhopadhyay, S., Bhattacharya, S., & Dihidar, K. (2011), “On Bayesian “Central Clustering””: Application to Landscape Classification of Western Ghats,” *Annals of Applied Statistics*, 5, 1948–1977.
- Richardson, S., & Green, P. J. (1997), “On Bayesian Analysis of Mixtures with an Unknown Number of Components (with discussion),” *Journal of the Royal Statistical Society. Series B*, 59, 731–792.

- Robert, C. P. (2003), Advances in MCMC: A Discussion,, in *Highly Structured Stochastic Systems*, eds. P. J. Green, N. L. Hjort, & S. Richardson, Oxford University Press, Oxford, UK, pp. 167–171.
- Robert, C. P., & Casella, G. (2004), *Monte Carlo Statistical Methods*, New York: Springer-Verlag.
- Sisson, S. A. (2005), “Transdimensional Markov Chains: A Decade of Progress and Future Perspectives,” *Journal of the American Statistical Association*, 100, 1077–1089.
- Stephens, M. (2000), “Dealing with Label Switching in Mixture Models,” *Journal of the Royal Statistical Society. Series B*, 62, 795–809.
- Storvik, G. (2011), “On the Flexibility of Metropolis-Hastings Acceptance Probabilities in Auxiliary Variable Proposal Generation,” *Scandinavian Journal of Statistics*, 38, 342–358.
- Vermaak, J., Andrieu, C., Doucet, A., & Godsill, S. J. (2004), “Reversible Jump Markov Chain Monte Carlo Strategies for Bayesian Model Selection in Autoregressive Processes,” *Journal of Time Series Analysis*, 25, 785–809.
- Wiper, M., Insua, D. R., & Ruggeri, F. (2001), “Mixtures of Gamma Distributions With Applications,” *Journal of Computational and Graphical Statistics*, 10, 440–454.